APPENDIX A

(CLEAN VERSION OF SUBSTITUTE SPECIFICATION EXCLUDING CLAIMS)

(Serial No. 10/750,411)

PATENT
Attorney Docket 2183-6265US

NOTICE OF EXPRESS MAILING

Express Mail Mailing Label Number: _____

Date of Deposit with USPS: _____

Person making Deposit: _____

APPLICATION FOR LETTERS PATENT

for

CORONAVIRUS-LIKE PARTICLES COMPRISING FUNCTIONALLY DELETED GENOMES

Inventors:
Petrus J. M. Rottier
Cornelis A. M. de Haan
Bert J. Haijema
Berend J. Bosch

Attorney:
Allen C. Turner
Registration No. 33,041
TraskBritt, P.C.
P.O. Box 2550
Salt Lake City, Utah 84110
(801) 532-1922

TITLE OF THE INVENTION

CORONAVIRUS-LIKE PARTICLES COMPRISING FUNCTIONALLY DELETED GENOMES

CROSS-REFERENCE TO RELATED APPLICATIONS

This application is a continuation-in-part of co-pending application, serial no. 10/714,534, filed November 14, 2003, and a continuation-in-part of co-pending application serial no. 10/414,256, filed April 14, 2003, which are both continuations of PCT International Patent Application No. PCT/NL/02/00318, filed May 17, 2002, designating the United States of America, and published, in English, as PCT International Publication No. WO 02/092827 A2 on November 21, 2002, the contents of the entirety of all of which are incorporated herein by this reference.

TECHNICAL FIELD

The invention relates generally to biotechnology, and more specifically to the field of coronaviruses and diagnosis, therapeutic use and associated vaccines.

BACKGROUND

Coronavirions have a rather simple structure. They consist of a nucleocapsid surrounded by a lipid membrane. The helical nucleocapsid is composed of the RNA genome packaged by one type of protein, the nucleocapsid protein N. The viral envelope generally contains 3 membrane proteins: the spike protein (S), the membrane protein (M) and the envelope protein (E). Some coronaviruses have a fourth protein in their membrane, the hemaglutinin-esterase protein (HE). Like all viruses, coronaviruses encode a wide variety of different gene products and proteins. Most important among these are obviously the proteins responsible for functions related to viral replication and virion structure. But besides these elementary functions, viruses generally specify a diverse collection of proteins, the function of which is often still unknown but which are known or assumed to be in some way beneficial to the virus. These proteins may either be essential - operationally defined as being required for virus replication in cell culture - or dispensable. Coronaviruses constitute a family of large, positive-sense RNA viruses that usually cause respiratory and intestinal infections in many

different species. Based on antigenic, genetic and structural protein criteria they have been divided into three distinct groups: group I, II and III. Actually, in view of the great differences between the groups, their classification into three different genera is presently being discussed by the responsible ICTV Study Group. The features that all these viruses have in common are a characteristic set of essential genes encoding replication and structural functions. Interspersed between and flanking these genes, sequences occur that differ profoundly among the groups and that are, more or less, specific for each group.

To successfully initiate an infection, viruses need to overcome the cell membrane barrier. Enveloped viruses achieve this by membrane fusion, a process mediated by specialized viral fusion proteins. Most viral fusion proteins are expressed as precursor proteins, which are endoproteolytically cleaved by cellular proteases giving rise to a metastable complex of a receptor binding and a membrane fusion subunit.

SUMMARY OF THE INVENTION

The present invention provides methods and means to interfere with fusion of coronaviruses. According to the invention, after receptor binding at the cell membrane, the fusion proteins undergo a dramatic conformational transition. A hydrophobic fusion peptide becomes exposed and inserts into the target membrane. The free energy released upon subsequent refolding of the fusion protein to its most stable conformation is believed not only to facilitate the close apposition of viral and cellular membranes but also to effect the actual membrane merger (1, 46, 54).The present invention further provides methods and means to use the biochemical and functional characteristics of the heptad repeat (HR) regions of the coronavirus spike proteins. The inventors show herein that peptides corresponding to the HR regions assemble into a thermostable, oligomeric, alpha-helical rod-like complex, with the HR1 and HR2 helices oriented in an anti-parallel manner.

Furthermore, we have found that HR2 of the coronavirus spike protein such as MHV-A59 spike protein is a strong inhibitor of both virus-cell and cell-cell fusion.

The invention also provides the amino acid sequences of the HR regions of a coronavirus belonging to another group such as Feline infectious peritonitis virus (FIPV) spike protein, and of the inhibition of cell-to-cell fusion in FIPV infected cells by administration

of HR2 of viruses such as FIPV. We demonstrate that the same mechanism is valid in different groups of coronaviruses.

The present invention also provides the amino acid sequences of the HR regions of the spike protein of a coronavirus, which causes a severe acute respiratory syndrome (SARS) in humans and which has been designated provisionally as SARS coronavirus (SARS-CoV). The inhibitory effect of SARS-CoV HR derived peptides on infection of cells by SARS-CoV is also disclosed, and peptides have been identified that can be used as a vaccine against SARS-CoV infections or for the preparation of a medicine against a SARS-CoV caused disease. In addition, this invention discloses the amino acid sequence of the fusion peptide of SARS-CoV. The fusion peptide can also be used as a vaccine against SARS-CoV infections or for the preparation of a medicament against a SARS-CoV caused disease.

The invention makes use of the discovery that in coronaviruses the energy necessary for the membrane fusion process is at least partly provided by the formation of an anti-parallel coiled coil structure by folding of the spike protein and interaction of the HR1 and HR2 repeat region. Decreasing the contact of the heptad repeat regions in the spike protein results in a less optimal fit of the coiled coil and thus in less energy for the fusion of membranes. Therefore, this invention teaches a method for at least in part inhibiting anti-parallel coiled coil formation of a coronavirus spike protein comprising decreasing the contact between heptad repeat regions of the protein. Of course, blocking the coiled coil formation by occupying the sequence of either HR1 or HR2 is a good way of decreasing, or even preventing coiled coil formation.

The contact of the heptad repeat regions can be disturbed by a molecule or compound that binds to HR1 or HR2 and by binding to these regions, or in close proximity, the compound blocks the site for binding to another HR site. This will result in decreasing, or inhibiting, the ability of the coronavirus to fuse with a membrane and enter a cell. Of course, if binding of a compound occurs in the vicinity of these regions, contact of the heptad repeat regions may also be decreased and/or inhibited. Such a compound may for example, be a peptide and/or a functional fragment and/or an equivalent thereof with an amino acid sequence as shown in FIG. 1.

A functional fragment of a protein or peptide is defined as a part which has the same kind of biological properties in kind, not necessarily in amount. A "functional equivalent" of a peptide is defined as a compound, be it a peptide or proteinaceous or nonproteinaceous molecule with essentially the same functional properties in kind, not necessarily in amount. A functional equivalent can be provided in many ways, for instance, through conservative amino acid substitution.

A person skilled in the art is well able to generate analogous equivalents of a protein. This can, for instance, be done through screening of a peptide library. Such an equivalent has essentially the same biological properties of the protein or peptide in kind, not necessarily in amount.

Therefore, this invention teaches a method for at least in part inhibiting anti-parallel coiled coil formation of a coronavirus spike protein comprising decreasing the contact between heptad repeat regions of the protein, wherein the decreasing is provided by a peptide and/or a functional fragment and/or an equivalent thereof.

Decreasing the contact between heptad regions may also be provided by a peptide comprising a heptad repeat region of a coronaviral spike protein and/or a functional fragment and/or an equivalent thereof. Therefore, this invention provides a method to decrease and/or inhibit contact between heptad regions wherein the decreasing and/or inhibiting is provided by a peptide comprising a heptad repeat region of a coronaviral spike protein and/or a functional fragment and/or an equivalent thereof. The disclosure of the amino acid sequence of HR2 of SARS-CoV enables the production and/or selection of peptides comprising SARS-CoV HR2 of spike protein and/or a functional fragment and/or an equivalent thereof.

In another embodiment, such decreasing can be achieved by providing an antibody directed against a part of HR1 or HR2. The antibody will inhibit the binding of a heptad repeat region to another heptad repeat region, thus preventing, at least in part, the formation of an anti-parallel coiled coil. Of course, binding of an antibody to a region in close proximity to the heptad region may also disturb the correct fit of the heptad repeat regions in a coiled coil. Therefore, the present invention teaches a method for at least in part inhibiting anti-parallel coiled coil formation of a coronavirus spike protein comprising decreasing the contact

between heptad repeat regions of the protein, wherein the decreasing is provided by an antibody and/or a functional fragment and/or an equivalent thereof.

The present invention shows comparative data on the amino acid sequences of the HR1and HR2 region of a number of coronaviruses and of SARS coronavirus (FIG. 1). The human coronavirus HCV-229E and the feline infectious peritonitis virus (FIPV), which both belong to the group 1 coronaviruses, show an insertion of 14 amino acids in the HR1 and in the HR2 region, which the other coronaviruses, like mouse hepatitis virus and another human coronavirus (HCV-OC43) (group 2), and infectious bronchitis virus of poultry (group 3) and SARS-CoV, do not have. This insertion of 14 amino acids in each heptad region may generate more electrostatic power for the fusion of a membrane, once the coiled coil is formed, because the total length of each heptad alpha helix is elongated by 2 coils. The fact that FIPV and HCV-229E have these extra 2 coils per heptad repeat region may indicate that these viruses need extra energy to fuse their membrane with that of their host cell. Decreasing this energy by inhibiting, at least in part, the formation of a coiled coil will effectively decrease the penetrating power of the viruses. Therefore, the invention teaches a method for, at least in part, inhibiting anti-parallel coiled coil formation of a coronavirus spike protein comprising decreasing the contact between heptad repeat regions of the protein, wherein the coronavirus comprises a feline coronavirus and/or a human coronavirus, and/or a mouse hepatitis virus MHV and/or a SARS virus.

After infection of a cell by a coronavirus, the infected cell exhibits coronaviral spike protein on its surface. Coronaviral spike protein present on the cell membrane surface mediates the fusion of cell membranes of other cells, thus allowing cell-to-cell fusion and allowing the virus to passage from the infected cell to a neighboring cell without the need to leave the cell. An important step in decreasing viral infection of cells is preventing the cell-to-cell fusion. By providing a compound such as a peptide or an antibody that decreases and/or inhibits the contact of heptad regions, cell-to-cell fusion will be decreased and/or inhibited. The present invention teaches a method for inhibiting coronavirus spike protein mediated cell-to-cell fusion, comprising decreasing and/or inhibiting the contact between heptad repeat regions of the spike protein.

The present invention also provides methods for selecting further inhibitors of coiled coil formation in coronaviruses. For example, the HR1 and HR2 peptides may be used *in vitro* to select binding compounds from libraries of molecules. Any compound that binds to at least part of an HR1 or HR2 peptide is selected and is used as an inhibitor of the formation of an anti-parallel coiled coil in a spike protein of coronavirus. Therefore, this invention teaches a method to select a compound binding to a heptad repeat region of a coronavirus spike protein, comprising contacting *in vitro* at least one heptad region of a coronavirus spike protein with a collection of compounds and measuring the formation of an anti-parallel coiled coil in the protein.

The present invention also teaches a compound selected by contacting *in vitro* at least one heptad region of a coronavirus spike protein with a collection of compounds and measuring the formation of an anti-parallel coiled coil in the protein. With this method, non-proteinaceous compounds, proteinaceous compounds and antibodies are selected for their capacity to bind to the heptad repeat regions. Of course, a functional fragment and/or derivative of an antibody may also bind to heptad repeat regions. Therefore, this invention also teaches an antibody or a functional fragment and/or derivative thereof, capable of decreasing and/or inhibiting the contact between heptad repeat regions of a coronavirus spike protein. The above-mentioned compounds and/or antibodies may be incorporated into a pharmaceutical composition with a suitable diluent and/or or carrier compound. Therefore, the invention teaches a pharmaceutical composition comprising the compound and/or the antibody or a functional fragment and/or derivative thereof, and a suitable diluent and/ or carrier. Administration of the pharmaceutical composition to a cell or a subject with a coronaviral infection will inhibit the infection of cells and at least in part decrease the coronaviral infection. Therefore, the invention teaches a method of treatment of coronavirus infections comprising providing to a subject the pharmaceutical composition.

In another embodiment, the compounds and/or antibodies may be used to detect the presence of coronavirus in a cell or in a subject by contacting a sample of the cells or of the subject to the compound or the antibody and visualizing any binding of the coronavirus to the compound and/or the antibody. The visualizing may be performed by any method known in the art, for example by ELISA techniques or by fluorescence or histochemistry. Therefore,

the present invention also teaches a diagnostic kit for detecting coronavirus infection in a sample of a subject comprising the compound or the antibody, further comprising a means of detecting binding of the compound or antibody to the coronavirus. In yet another embodiment, the compound may be used to measure antibody titers of a subject. This may be done to diagnose whether a subject is undergoing a coronaviral infection, or has undergone a coronaviral infection in the past. This may be useful, not only for diagnostic purposes, but also for assessing the possible risk of a subject for a coronaviral infection, and for evaluating vaccination efficiency and strategy. Therefore, the present invention also teaches a diagnostic kit for detecting coronavirus antibodies in a sample of a subject comprising the compound, further comprising a means of detecting binding of the compound to the antibodies.

In another embodiment, the amino acid sequence of the heptad repeat regions is manipulated by recombination, insertion, or deletion techniques that are known in the art. Such a manipulation of the coronaviral genome in or around the heptad repeat regions will result in decreased and/or inhibited contact of the heptad repeat regions; it will result in attenuation of the coronavirus. Therefore, the invention teaches a method to attenuate a coronavirus comprising decreasing and/or inhibiting the contact between heptad repeat regions of the spike protein of the coronavirus. The method enables the production of an attenuated coronavirus with a decreased contact between the heptad repeat regions. Therefore, the invention teaches an attenuated coronavirus characterized in that the contact between heptad repeat regions of the spike protein of the coronavirus is decreased and/or inhibited.

The invention also discloses a number of peptides derived from SARS-C0V HR2 region that inhibited infection of cells by SARS-CoV. Therefore, the present invention discloses a method for at least in part inhibiting anti-parallel coiled coil formation of a coronavirus spike protein comprising decreasing the contact between heptad repeat regions of the protein, wherein the peptide comprises an amino acid sequence according to peptide sHR2-1, (SEQ ID NO: 1) and/or sHR2-2, (SEQ ID NO: 2) and/or sHR2-8 (SEQ ID NO: 3), and/or sHR2-9 (SEQ ID NO: 4) as described in FIG. 11B, and/or a functional fragment and/or an equivalent thereof.

In another embodiment, the invention discloses amino acid sequences of the fusion peptide of SARS-CoV. Therefore, the present invention discloses a method for at least in part

inhibiting anti-parallel coiled coil formation of a coronavirus spike protein comprising decreasing the contact between heptad repeat regions of the protein, for at least in part inhibiting a fusion of a coronavirus with a cell membrane comprising decreasing binding of a fusion peptide with the cell membrane. Furthermore, the present invention discloses the above-described method, wherein the fusion peptide comprises the amino acid sequence of SARS-CoV as described in FIG. 17 (SEQ ID NO: 5).

Because the fusion peptide of SARS-CoV is disclosed, inhibition of fusion may be used to find and select molecules that specifically bind to the fusion protein. Therefore, the present invention discloses the above-described method, wherein the decreased binding is provided by a specific binding molecule for the fusion peptide. The disclosed fusion peptide is used to select antibodies and/or a functional fragment and/or a derivative thereof that specifically bind to the fusion peptide, according to well known techniques in the art, such as, for example, phage display. Therefore, the present invention also discloses a method for at least in part inhibiting anti-parallel coiled coil formation of a coronavirus spike protein comprising decreasing the contact between heptad repeat regions of the protein, for at least in part inhibiting a fusion of a coronavirus with a cell membrane comprising decreasing binding of a fusion peptide with the cell membrane, wherein the specific binding molecule is an antibody and/or a functional fragment and/or a derivative thereof.

BRIEF DESCRIPTION OF THE FIGURES

FIG. 1. (A) Schematic representation of the coronavirus spike protein structure. The glycoprotein has an N-terminal signal sequence (SS) and a transmembrane domain (TM) close to the C-terminus. Group 2 and 3 coronavirus spike proteins are proteolytically cleaved (arrow) into an S1 and an S2 subunit, which are non-covalently linked. S2 contains two heptad repeat regions (shaded bars), HR1 and HR2, as indicated. (B) Sequence alignment of HR1 and HR2 domains of the newly identified SARS-CoV (strain TOR2) (SEQ ID NOS: 6 and 7, respectively) with those of the group 1 coronaviruses FIPV (feline infectious peritonitis virus strain 79-1146) (SEQ ID NOS: 8 and 9, respectively) and HCoV-229E (human coronavirus strain 229E) (SEQ ID NOS: 10 and 11, respectively), the group 2 coronaviruses MHV-A59 (mouse hepatitis virus strain A59) (SEQ ID NOS: 12 and 13,

respectively) and HCoV-OC43 (human coronavirus strain OC43) (SEQ ID NOS: 14 and 15, respectively), and the group 3 coronavirus IBV (infectious bronchitis virus strain Beaudette) (SEQ ID NOS: 16 and 17, respectively) (GenBank accession nos. P59594, VGIH79, VGIHHC, P11224, CAA83661 and P11223, respectively). Dark shading marks sequence identity while lighter shading represents sequence similarity. The alignment shows a remarkable insertion of exactly two heptad repeats (14 a.a.) in both HR1 and HR2 of HCoV-229E (SEQ ID NOS: 10 and 11, respectively), and FIPV (SEQ ID NOS. 8 and 9, respectively), a characteristic of all group 1 viruses. The predicted hydrophobic heptad repeat "a" and "d" residues are indicated above the sequence. Asterisks denote conserved residues, dots represent similar residues. The amino acid sequences of the HR1 derived peptides HR1 (SEQ ID NO: 18), HR1a (SEQ ID NO: 9), HR1b (SEQ ID NO: 20), HR1c (SEQ ID NO: 21), and a FLAG-tagged HR1 (Fl.HR1) (SEQ NO: 22) and of the HR2 derived peptides HR2 (SEQ ID NO: 23), HR2-1 (SEQ ID NO: 24), and a FLAG-tagged HR2 (Fl-HR2) (SEQ ID NO: 25) of SARS-CoV used in this study are presented in italics below the alignments. N-terminal glycine and serine residues derived from the thrombin proteolytic cleavage site of the GST fusion protein are in parentheses.

FIG. 2. Hetero-oligomeric complex formation of HR1 and HR1a with HR2. (A) HR1 and HR2 on their own or as a preincubated equimolar (80 μM) mix were subjected to 15% tricine SDS-PAGE. Before gel loading, samples were either heated at 100°C or left at room temperature. Positions of HR1, HR2 and HR1-HR2 complex are indicated on the left, while the positions of molecular mass markers are indicated at the right. (B) Same as (A) but with peptide HR1a instead of HR1.

FIG. 3. Temperature stability of HR1-HR2 complex. An equimolar mix of HR1 and HR2 (80 μM) was incubated at room temperature for 1 hour. Samples were subsequently heated for 5 minutes at the indicated temperatures in 1x tricine sample buffer and analyzed by SDS-PAGE in a 15% tricine gel, together with HR1 and HR2 alone. Positions of HR1, HR2 and HR1-HR2 complex are indicated on the left, while the molecular mass markers are indicated at the right.

FIG. 4. Circular dichroism spectra (mean residue ellipticity of the HR1 (25 μM; open square) peptide, the HR2 (25 μM; filled triangle) peptide, and of the HR1-HR2 complex (25

μM; filled square) in water at room temperature. Note that the HR1 and HR2 spectra virtually coincide.

FIG. 5. Electron micrographs of HR1-HR2 complex.

FIG. 6. Proteinase K treatment of HR peptides. The peptides HR2, HR1, HR1a, HR1b and HR1c were subjected to Proteinase K either individually in solution or after mixing of the different HR1 peptides with HR2 at equimolar concentration followed by 1 hour of incubation at 37°C. Proteolytic fragments were separated and purified by HPLC and characterized by mass spectrometry. Peptides are schematically indicated by bars. Hatched bars indicate the protease sensitive part(s) of the peptide. N- and C-terminal position of the peptide and the amino acid numbering are indicated.

FIG. 7. Inhibition of virus-cell and cell-cell fusion by HR peptides. (A) Virus-cell inhibition by HR peptides using a luciferase gene expressing MHV. LR7 cells were inoculated with virus at an MOI of 5 in the presence of varying concentrations of peptide ranging from 0.4 - 50 μM. At 5 hours post infection cells were lysed and luciferase activity was measured. (B) Inhibition of spike mediated cell-cell fusion by HR peptides. BSR T7/5 effector cells - BHK cells constitutively expressing T7 RNA polymerase (3), were infected with vaccinia virus for 1 hour and subsequently transfected with a plasmid containing the S gene under a T7 promoter. Three hours post transfection, LR7 target cells transfected with a plasmid carrying the luciferase gene behind a T7 promoter, were added to the effector cells. Cells were incubated for another 4 hours in the presence or absence of HR peptide. Cells were lysed and luciferase activity was measured.

FIG. 8. Schematic representation (approximately to scale) of the viral fusion proteins of six different virus families; MHV-A59 S (*Coronaviridae*), Influenza HA (*Orthomyxoviridae*), HIV-1 gp160 (*Retroviridae*), SV5 F, (*Paramyxoviridae*), Ebola Gp2 (*Filoviridae*) and Se*M*NPV F (*Baculoviridae*). Cleavage sites are indicated by triangles; the black bars represent the (putative) fusion peptides, the vertically hatched bars represent the HR1 domains and the horizontally hatched bars represent the HR2 domains. Transmembrane domains are indicated by the vertical, dashed lines. For each polypeptide, the total length is given at the right.

FIG. 9. GST-FIPV fusion protein sequences of GST-HR1 (SEQ ID NO: 26) and GST-HR2 (SEQ ID NO: 27).

FIG. 10. SARS nucleotide and deduced protein sequence as derived from the RT-PCR fragment (SEQ ID NO: 28).

FIG. 11. Inhibition of SARS-CoV infection by HR peptides. (A) VERO cells were mock infected or infected with SARS-CoV (MOI = 0.5) in the presence of the HR2-1 peptide (sHR2-1) at concentrations of 0, 5, or 25 μM and incubated in medium containing the same concentration of peptide. An infection in the presence of peptide (25 μM) corresponding to the HR2 domain of MHV (mHR2) was taken along as a negative control. At 16 hours post infection, cells were fixed and SARS-CoV positive cells were visualized by immunofluorescence staining. The Table (panel B) shows amino acid sequences of HR2 (B1) (sHR2-1 through sHR2-10 and mHR2 (SEQ ID NOs: 1, 2, 29-33, 3, 4, 34, and 35, respectively) and HR1 (B2) (sHR1, sHR1a, sHR1b, and sHR1c (SEQ ID NOs: 36 through 39, respectively) derived peptides of SARS-CoV (SCV) and MHV and their EC_{50} values as determined in a 96 wells format infection inhibition assay. (EC_{50}: 50% inhibitory concentration; SD: standard deviation).

FIG. 12. Complex formation of SARS-CoV HR1 and HR2 peptides. (A). Comparison of SARS-CoV and MHV. HR1 and HR2 peptides on their own or as a preincubated equimolar (100 μM) mixture were subjected to 15% Tricine SDS-PAGE. Just before loading onto the gel, some samples were heated at 100°C. (B) HR1-HR2 complex formation using FLAG-tagged and nontagged SARS-CoV HR peptides. Samples of the individual peptides HR1 (1), HR2 (2), FLAG-tagged HR1 (F1) and FLAG-tagged HR2 (F2), and of preincubated mixtures of these peptides (1+2, F1+2, 1+F2 and F1+F2) were subjected to 15% Tricine SDS-PAGE. The positions of molecular mass markers are indicated at the left.

FIG. 13. Stoichiometry of peptides in HR1-HR2 complexes. (A) FLAG-tagged HR2 and nontagged HR2 were mixed in different ratios and incubated with an equimolar amount of HR1 to allow complex formation for 3 hours followed by analysis in a 10% Tricine SDS-PAGE. (B) FLAG-tagged HR1, nontagged HR1 and a 1:1 mixture of the two peptides were incubated with an equimolar amount of HR2 for 3 hours and subsequently analyzed in a 10% Tricine SDS-PAGE. (C) Acetonitrile was added to a concentration of 50% (v/v) to

solutions of FLAG-tagged HR1 (100 μM), nontagged HR1 (100 μM) or to a 1:1 mixture of these two solutions. After mixing and incubation for 5 minutes, the acetonitrile was evaporated and an equimolar amount of HR2 was added to allow complex formation. After 3 hours samples were analyzed in a 10% Tricine SDS-PAGE. Only the part of the gel containing the complexes is shown. The positions of molecular mass markers are indicated at the left.

FIG. 14. Comparative temperature stabilities of HR1-HR2 complexes of SARS-CoV and MHV. Equal amounts of SARS-CoV and MHV HR1-HR2 complexes were pooled, subsequently incubated for 5 minutes at the indicated temperatures in 1x Tricine sample buffer and analyzed directly by SDS-PAGE in a 15% Tricine gel. Positions of the HR1-HR2 complex of SARS-CoV and MHV are indicated on the right, while the molecular mass markers are indicated at the left.

FIG. 15. Circular dichroism spectra (mean residue ellipticity Φ) of the HR1 (20 μM; filled square) peptide, the HR2 (20 μM; open square) peptide, and of the HR1-HR2 complex (20 μM; filled triangle) in water at room temperature. Note that the three spectra virtually coincide.

FIG. 16. Proteolytic analysis of the HR1-HR2 complex. The peptides HR2 (SEQ ID NO: 40), HR1a (SEQ ID NO: 41) or preincubated equimolar mixtures of HR2 (SEQ ID NO: 40) with HR1a (SEQ ID NO: 41) or HR1c (SEQ ID NO: 42) were subjected to Proteinase K (pK) digestion and analyzed by RP HPLC (upper part). The peaks representing the protected fragments were purified by RP HPLC. The molecular masses of the protected fragments were determined by mass spectrometry (lower part), allowing the identification of the protease-resistant cores of the peptides. The molecular masses of the protected fragments determined by mass spectrometry (Ms Mw) matched their predicted masses (Pred. Mw) within 1 Da.

FIG. 17. Hydrophobic domains in coronavirus spike proteins. The TMAP program was applied on a Clustal W alignment of nine coronavirus spike sequences (see Methods section). In the hydrophobicity plot obtained, the three predicted transmembrane domains are indicated by black bars (middle part). Arrows point to the corresponding hydrophobic regions in the schematic drawing of the spike protein (upper part), which represent the N-terminal

signal sequence (SS), the C-terminal transmembrane anchor (TM) downstream of the HR2 domain, and the putative fusion peptide (FP) immediately upstream of the HR1 domain. In the bottom part of the figure the Clustal W multiple sequence alignment of this latter domain is shown for the nine coronavirus spike proteins (SEQ ID NOs: 43-49, 5, and 50, respectively).

DETAILED DESCRIPTION OF THE INVENTION

With a positive stranded RNA genome of 28-32 kb, the *Coronaviridae* are the largest enveloped RNA viruses. Coronaviruses exhibit a broad host range, infecting mammalian and avian species. They are responsible for a variety of acute and chronic diseases of the respiratory, hepatic, gastrointestinal and neurological systems (56).

Recently, coronavirus induced pneumonia (Severe Acute Respiratory Syndrome, SARS) has spread rapidly from China via Hong Kong to the rest of the world. The spike (S) protein is the sole viral membrane protein responsible for cell entry. It binds to the receptor on the target cell and mediates subsequent virus-cell fusion (6). Spikes can be seen under the electron microscope as clear, 20 nm large, bulbous surface projections on the virion membrane (14). The spike protein of mouse hepatitis virus (MHV-A59) is a 180 kDa heavily N-glycosylated type I membrane protein which occurs in a homodimeric (37, 66) or homotrimeric (16) complex. In most murine hepatitis strains, the S protein is cleaved intracellularly into an N-terminal subunit (S1) and a membrane anchored subunit (S2) of similar size, which are noncovalently linked and have distinct functions. Binding to the MHV receptor (MHVR) (74) has been mapped to the N-terminal 330 amino acids (a.a.) of the S1 subunit (62), whereas the membrane fusion function resides in the S2 subunit (78). It has been suggested that the S1 subunit forms the globular head while the S2 subunit constitutes the stalk-like region of the spike (15). Binding of S1 to soluble MHVR, or exposure to 37°C and an elevated pH (pH 8.0) induces a conformational change which is accompanied by the separation of S1 and S2 and which might be involved in triggering membrane fusion (21, 27, 60). Cleavage of the S protein into S1 and S2 has been shown to enhance fusogenicity (25, 61) but cleavage is not absolutely required for fusion (2, 26, 59, 61).

The ectodomain of the S2 subunit contains two regions with a 4,3 hydrophobic (heptad) repeat (15), a sequence motif characteristic of coiled coils. These two heptad repeat (HR) regions, designated here as HR1 and HR2, are conserved in position and sequence among the members of the three coronavirus antigenic clusters (FIG. 1). A number of studies have shown that the HR1 and HR2 regions are involved in viral fusion. First, a putative internal fusion peptide has been proposed to occur close to (7) or within (40) the HR1 region. Second, viruses with mutations in the membrane-proximal HR2 region exhibited defects in spike oligomerization and in fusion ability (39). Third, it has been suggested that the MHV-4 (JHM) strain can utilize both endosomal and nonendosomal pathways for cell entry but does not require acidification of endosomes for fusion activation (48). However, mutations found in murine hepatitis viruses which do require a low pH for fusion, appeared to map to the HR1 region (23).

HR regions appear to be a common motif in many viral fusion proteins (57). There are usually two of them; one N-terminal HR region (HR1) adjacent to the fusion peptide and a C-terminal HR region (HR2) close to the transmembrane anchor. Structural studies on viral fusion proteins reveal that the HR regions form a six-helix bundle structure implicated in viral entry (reviewed in (18)). The structure consists of a homotrimeric coiled coil of HR1 domains in the exposed hydrophobic grooves of which the HR2 regions are packed in an anti-parallel manner. This conformation brings the N-terminal fusion peptide in close proximity to the transmembrane anchor. Because the fusion peptide inserts into the cell membrane during the fusion event, such a conformation facilitates a close apposition of the cellular and viral membrane (reviewed in (18)). Recent evidence suggests that the actual six-helix bundle formation is directly coupled to the merging of the membranes (46, 54). The similarities in the structures of the six-helix bundle complexes elucidated for influenza virus HA (4, 11), human and simian immunodeficiency virus (HIV-1, SIV) gp41 (5, 8, 41, 63, 69, 76), Moloney murine leukemia virus type1 (MoMLV) gp21 (19), Ebola virus GP2 (42, 68), human T-cell leukemia virus type I (HTLV-1) gp21 (32), Visna virus TM, (43), simian parainfluenza virus (SV5) F1 (1), and human respiratory syncytial virus (HRSV) F1 (80), all point to a common fusion mechanism for these viruses.

Based on structural similarities, two classes of viral fusion proteins have been distinguished (36). Proteins containing HR regions and an N-terminal or N-proximal fusion peptide are classified as class I viral fusion proteins. Class II viral fusion proteins (e.g., the alphavirus E1 and the flavivirus E fusion protein) lack HR regions and have an internal fusion peptide. Their fusion protein is folded in tight association with a second protein as a heterodimer. Here, fusion activation takes place upon cleavage of the second protein.

The coronavirus fusion protein (S) shares several features with class I virus fusion proteins. It is a type I membrane protein, synthesized in the ER, and is transported to the plasma membrane. It contains two heptad repeat sequences, one located downstream of the fusion peptide and one in close proximity to the transmembrane region.

However, despite its similarity to class I fusion proteins, there are several characteristics that make the coronavirus S protein exceptional. One is the absence of an N-terminal or even N-proximal fusion peptide in the membrane-anchored subunit. Another peculiarity is the relatively large sizes of the HR regions (~100 and ~40 a.a.). Third, cleavage of the S protein is not required for membrane fusion; rather, it does not occur at all in the group 1 coronaviruses. For these reasons, it is not likely to assume that coronavirus fusion protein is a class 1 fusion protein.

Heptad repeat regions play an important role in viral membrane fusion. Fusion proteins from widely disparate virus families have been shown to contain two such regions, one located close to the fusion peptide, the other generally in the vicinity of the viral membrane ((7); summarized in FIG. 8). Distances between the HR regions vary greatly, from some 50 a.a. as in HIV-1 to about 300 residues in *Spodoptera exigua* multicapsid nucleopolyhedrosis virus (71). The crystal structures resolved for influenza HA (4, 10, 75) HIV-1 and SIV gp41 (5, 8, 41, 63, 69, 76), MuMLV gp21 (19), Ebola virus GP2 (42, 68), HTLV-1 gp21 (32), Visna virus TM, (43), SV5 F1 (1), HRSV F1 (80) and NDV F (13) all show a central trimeric coiled coil constituted by three HR1 regions. In some of these structures (e.g., HIV-1 and SIV gp41, SV5 F1, Ebola virus gp2, Visna virus TM and HRSV F1) a second layer of helices or elongated peptide chains was observed contributed by HR2 domains which were packed in an anti-parallel manner into the hydrophobic grooves of the HR1 coiled coil, forming a six-helix bundle. In the full-length protein, such a

conformation brings the fusion peptide present at the N-terminus of HR1 close to the transmembrane region that occurs at the C-terminal of HR2. With the fusion peptide inserted in the cellular membrane and the transmembrane region anchored in the viral membrane, such a hairpin-like structure facilitates the close apposition of cellular and viral membrane and enables subsequent membrane fusion (reviewed in (18)). Combined with the findings that peptides derived from these HR domains can act as potent inhibitors of fusion (reviewed in (18)), the biological relevance of the heptad repeat regions in the viral life cycle is obvious. Our studies of the heptad repeat motifs in coronavirus spike protein presented here show that coronaviruses use coiled coil formation for membrane fusion and cell entry mechanisms comparable to some other viruses, probably allowing coronavirus spike proteins to be classified as class I viral fusion proteins (36).

The coronavirus (MHV-A59) derived HR peptides exhibited a number of typical class I characteristics. First of all, the purified HR1 and HR2 peptides assembled spontaneously into unique, homogeneous multimeric complexes. These complexes were highly stable surviving, for instance, high concentrations (2%) of SDS and high temperatures (70-80°C). The peptides apparently associate with great specificity into an energetically very favorable structure. Another typical feature was the observed secondary structure in the peptides. The CD spectra of both the individual and the complexed HR1 and HR2 peptides showed patterns characteristic of alpha-helical structure. Alpha-helix contents were calculated to be about 89% for the separate peptides and about 82% for their equimolar mixture. Consistent with these observations, the HR complex revealed a rod-like structure when examined by electron microscopy. The length of this structure (~14.5 nm) correlates well with the length predicted for an alpha-helix the size of HR1 (96 a.a.). Similar rod-like structures have been observed for other class I virus fusion proteins such as the influenza virus HA protein (12, 53), portions of the HIV-1 gp41 protein (70), and the Ebola virus GP2 protein (67) but the length of the MHV-A59 derived structures is substantially larger. This is presumably even more so for type I coronaviruses which have an insertion of two heptad repeats (14 a.a.; see FIG. 1) in both HR regions. These insertions into otherwise conserved areas suggest these additional sequences to associate with each other in the HR1-HR2 complex thereby extending the alpha-helical complex by exactly four turns. The

significance of the exceptional lengths of coronavirus HR complexes may be that the higher energy gain of their formation corresponds with higher energy requirements for membrane fusion by these viruses.

Another important characteristic of class I viral fusion proteins is the formation of a heterotrimeric six-helix bundle during the membrane fusion process, resulting in a close allocation of the fusion peptide and the transmembrane domain. Consistently, protein dissection studies using proteinase K demonstrated an anti-parallel organization of the HR1 and HR2 alpha-helical peptides in the MHV-A59 HR complex. So far, no fusion peptides have been identified in any coronavirus spike protein but predictions for MHV S have located such fusion sequences at (7) or in (40) the N-terminus of HR1. In both cases, an anti-parallel orientation of the HR1 and HR2 alpha helices ensures that the fusion peptide is brought into close proximity to the transmembrane region. Sequence analysis reveals that the "e" and "g" positions in the HR1 regions of all coronaviruses are primarily occupied by hydrophobic residues, unlike the "e" and "g" positions in the HR2 regions, which are mostly polar (see FIG. 1). The HR2 region also contains a strictly conserved N-linked glycosylation sequence, indicating its surface accessibility. Preliminary X-ray data on the HR1-HR2 complex show a six-helix bundle structure in the electron dense region (Bosch, B.J., Rottier, P.J.M, and Rey F.A., unpublished results). The combined observations suggest a packing analogous to the fusion proteins of other class I viruses (e.g., HIV, SV5), where the HR1 and HR2 peptides can form a six-helix bundle with the long HR1 peptide centered in the middle as a three-stranded coiled coil with the hydrophobic "a" and "d" residues in its inner core. The shorter HR2 peptide packs with its apolar interface in the hydrophobic grooves of the HR1 coiled coil, which expose the mostly hydrophobic residues on 'e' and 'g' positions.

Peptides derived from the heptad repeat regions of retrovirus (28, 30, 38, 47, 49, 58, 72, 73) and paramyxovirus (29, 35, 51, 77, 79) fusion proteins have been shown to strongly interfere with the fusion activity of these proteins. We observed the same effect when we tested the HR2 peptide of the MHV-A59 spike protein. Using a recombinant luciferase-expressing MHV-A59, the peptide acted as an effective inhibitor of virus entry at micromolar concentrations. Cell-cell fusion inhibition was even more efficiently blocked by the peptide as tested in a cell fusion luciferase assay system. However, peptides derived from

the HR1 region had no or only a minor effect on virus entry and syncytia formation. HIV-1 gp41 derived HR peptides that inhibit membrane fusion have been shown not to bind to the native protein or to the six-helix bundle. They can only bind to an intermediate stage of gp41 occurring during the fusion process (9, 20, 31). Repeated passage of HIV in the presence of the inhibitory peptide DP178, which is derived from the C-terminal gp41 HR region, resulted in resistant viruses containing mutations in the N-terminal HR region (52). Inhibition of membrane fusion by the MHV HR2 peptide most likely takes place during an intermediate stage of the fusion process by binding of the peptide to the HR1 region in the spike protein. This binding, which may occur before, during or after the association of the HR1 regions into the inner trimeric coiled coil, presumably inhibits the subsequent interaction with native HR2 and, consequently, membrane fusion. For the HIV-1 gp41 and SV5 F protein also peptides corresponding to the HR1 region show membrane fusion inhibition, supposedly by binding to the native HR2 region (29, 72). It has been reported previously for HIV-1 that the HR1 peptide aggregates in solution (38) and that its inhibitory activity could be enhanced by fusing it to a designed soluble trimeric coiled coil, making the HR1 peptide more soluble (17). The MHV-A59 HR1 peptide is soluble in water but appeared to precipitate in salt solutions (data not shown). This solubility feature may have obscured the inhibitory potency of our HR1 derived peptides and accounts for the negative results with these peptides in our fusion assays. The HR2 peptide (as well as soluble forms of HR1) provides powerful antivirals for the therapy of coronavirus induced diseases both in animals and man.

Membrane fusion mediated by class I fusion proteins is accompanied by dramatic structural rearrangements within the viral polypeptide complexes (18). Though little is known of the coronavirus membrane fusion process (for a review, see (22)), the occurrence of conformational changes induced by various conditions has been described for MHV spikes (45). While MHV-A59 is quite stable at mildly acidic pH, it is rapidly and irreversibly inactivated at pH 8.0 and 37°C (60). Under these conditions the S1 subunit dissociates from the virions and the S2 subunit aggregates concomitantly resulting in the aggregation of the particles. Due to the structural rearrangements in the spike, virions can bind to liposomes and the S2 protein becomes sensitive to protease degradation (27). Similar conformational changes can apparently also be induced at pH 6.5 by the binding of spikes to the

(soluble) MHV receptor (21, 27) as this interaction enhances liposome binding and protease sensitivity as well (27). Virion binding to liposomes is presumably caused by the exposure of hydrophobic protein surfaces or of the fusion peptide as a result of the conformational change. It appears that the structural rearrangements in the spikes, whether elicited by elevated pH or soluble receptor interaction, reflect the process that naturally gives rise to the fusion of viral and cellular membranes. Accordingly, cell-cell fusion induced by MHV-A59 was maximal at slightly basic pH (60).

A number of studies on the MHV spike protein have shown the importance of the HR regions in membrane fusion. Three codon mutations (Q1067H, Q1094H and L1114R) in or close to the HR1 region of the spike protein were found to be responsible for the low pH requirement for fusion of some MHV-JHM variants isolated from persistently infected cells (23). Analysis of soluble receptor-resistant variants of this virus also pointed to an important role in fusion activity of the HR1 region and suggested that it interacts somehow with the N-terminal domain (S1N330-III; a.a. 278-288) of the spike protein (44). In yet another MHV-JHM variant, a great reduction in cell-cell fusion was attributed to the occurrence of two mutations in the spike protein, one of which was again located in the HR1 region (A1046V), the other (V870A) was located in a small nonconserved HR region (N helix) close to the S cleavage site (33). Acidification resulted in a clear enhancement of fusion by this double mutant. It was speculated that the three predicted helical regions (N helix, HR1 and HR2) all collapse into a low-energy coiled coil during the process of membrane fusion (33). Herein we provide evidence that the HR1 and HR2 regions indeed can form such a low-energy coiled coil. Studies with the MHV-A59 S protein showed that mutations introduced at "a" and "d" positions in an N-terminal part of the HR1 region, a fusion peptide candidate, severely affected cell-cell fusion ability (40). This effect was not due to defects in spike maturation or cell surface expression. Finally, also codon mutations in the HR2 region were found to significantly reduce cell-cell fusion (39). Though these mutant spike proteins were apparently impaired in oligomerization, their surface expression was hardly affected.

In conclusion, our structural and functional studies show that the coronavirus spike protein can be classified as a class I viral fusion protein. The protein has, however, several unusual features that set it apart. An important characteristic of all class I virus fusion proteins

known so far, is the cleavage of the precursor by host cell proteases into a membrane-distal and a membrane-anchored subunit, an event essential for membrane fusion. Consequently, the hydrophobic fusion peptide is then located at or close to the newly generated N-terminus of the membrane anchored subunit, just preceding the HR1 region. In contrast, the MHV-A59 spike does not have a hydrophobic stretch of residues at the distal end of S2, but carries a fusion peptide internally at a location that has yet to be determined (7, 40). Unlike other class I fusion proteins, cleavage of the S protein into S1 and S2 has been shown to enhance fusogenicity (25, 61) but not to be absolutely required (2, 26, 59, 61). Rather, spikes belonging to group 1 coronaviruses are not cleaved at all.

The invention is further explained by the use of the following illustrative examples.

Example 1:

MATERIALS AND METHODS:

Plasmid constructions: For the production of peptides corresponding to amino acid residues 953-1048 (HR1), 969-1048 (HR1a), 1003-1048 (HR1b), 969-1010 (HR1c) and 1216-1254 (HR2) of the MHV-A59 spike protein, PCR fragments were prepared using as a template the plasmid pTUMS which contains the MHV-A59 spike gene (64). Primers were designed (see Table 1) to introduce into the amplified fragment an upstream *Bam*HI site, a downstream *Eco*RI site as well as a stop codon preceding the *Eco*RI site. The fragments corresponding to a.a. 953-1048 and 1216-1254 were additionally provided with sequences specifying a factor Xa cleavage site immediately downstream from the *Bam*HI site. Fragments were cloned into the *Bam*HI/*Eco*RI site of the pGEX-2T bacterial expression vector (Amersham Bioscience) in frame with the GST gene just downstream of the thrombin cleavage site.

To establish a cell-cell fusion inhibition assay, the firefly luciferase gene was cloned under a T7 promoter and an EMCV IRES. The luciferase gene containing fragment was excised from the pSP-*luc*+ vector (Promega) by digestion with *Nco*I and *Eco*RV, treated with Klenow, and ligated into the *Bam*HI-linearized, Klenow-blunted pTN3 vector (65) yielding the pTN3-*luc*+ reporter plasmid.

Bacterial protein expression and purification: Freshly transformed BL21 cells (Novagen) were grown in 2 x YT (yeast-tryptone) medium to log phase (OD600~1.0) and subsequently induced by adding IPTG (GibcoBRL) to a final concentration of 0.4 mM. Two hours later, cells were pelleted, resuspended in 1/25 volume of 10 mM Tris (pH 8.0), 10 mM EDTA, 1 mM PMSF and sonicated on ice (5 times for 2 minutes). Cell homogenates were centrifuged at 20,000 x *g* for 60 minutes at 4°C. To each 50 ml of supernatant 2 ml glutathione-sepharose 4B (Amersham Bioscience; 50% v/v in PBS) was added and incubated overnight (O/N) at 4°C under rotation. Beads were washed three times with 50 ml PBS and resuspended in a final volume of 1ml PBS. Peptides were cleaved from the GST moiety on the beads using 20 U of thrombin (Amersham Bioscience) by incubation for 4 hours at room temperature (RT). Peptides in the supernatant were purified by high pressure reversed phase chromatography (RP-HPLC) using a Phenyl-5PW RP column (Tosoh) with a linear gradient of acetonitrile containing 0.1% trifluoroacetic acid. Peptide containing fractions were vacuum-dried O/N and dissolved in water. Peptide concentration was determined by measuring the absorbance at 280 nm (24) and by BCA protein analysis (Micro BCA™ Assay Kit, Pierce).

Temperature stability of HR1-HR2 complex: An equimolar mix of peptides HR1 and HR2 (80 μM each) in H_2O was incubated at room temperature for 1 hour. After addition of an equal volume of 2 x tricine sample buffer (0.125 M Tris pH 6.8, 4% SDS, 5% β-mercaptoethanol, 10% glycerol, 0.004 g bromophenol blue) (55), the mixtures were either left at room temperature or heated for 5 minutes at different temperatures and subsequently analyzed by SDS-polyacrylamide gel electrophoresis (PAGE) in 15% tricine gel (55).

CD spectroscopy: CD spectra of peptides (25 μM in H_2O) were recorded at room temperature on a Jasco J-810 spectropolarimeter, using a 0.1 mm path length, 1 nm bandwidth, 1 nm resolution, 0.5 second response time and a scan speed of 50 nm/min. The alpha-helix content was calculated using the program CDNN (http://bioinformatik.biochemtech.uni-halle.de/cd_spec/).

Electron Microscopy: A preincubated equimolar mix of the peptides HR1 and HR2 was subjected to size-exclusion chromatography (Superdex™ 75 HR 10/30, Amersham Pharmacia Biotech). A sample from the HR1-HR2 peptide complex containing fraction was

adsorbed onto a discharged carbon film, negatively stained with a 2% uranyl acetate solution and examined with a Philips CM200 microscope at 100 kV.

Proteinase K treatment: Stock solutions (1 mM) of the peptides HR1, HR1a, HR1b, HR1c and HR2 in water were diluted to 80 μM in PBS. Peptides on their own (80 μM) or after preincubation for 1 hour at 37°C with HR2 (80 μM each) were subsequently subjected to proteinase K digestion (1% wt/wt, proteinase K/peptide) for 2 hours at 4°C. Samples were immediately subjected to tricine SDS-PAGE analysis. Protease resistant fragments were also separated and purified by RP HPLC and characterized by mass spectrometry.

Virus-cell fusion assay: The potency of HR peptides in inhibiting viral infection was determined using a recombinant MHV-A59, MHV-EFLM that expresses the firefly luciferase gene (C.A.M. de Haan and P.J.M. Rottier, manuscript in preparation). LR7 cells (34) were maintained as monolayer cultures in Dulbecco's modified Eagle's medium (DMEM) supplemented with 10% fetal calf serum (FCS; GIBCO BRL). LR7 cells grown in 96-well plates were inoculated with MHV-EFLM in DMEM at a multiplicity of infection (MOI) of 5 in the presence of varying concentrations of peptide ranging from 0.4 - 50 μM. After 1 hour, cells were washed with DMEM and medium was replaced with DMEM containing 10% FCS. At 5 hours post infection (p.i.) cells were harvested in 50 μl 1x Passive Lysis buffer (Luciferase Assay System, Promega) according to the manufacturer's protocol. Upon mixing of 10 μl cell lysate with 40 μl substrate, luciferase activity was measured using a Wallac Betalumino meter.

Cell-cell fusion assay: $2x10^6$ LR7 cells, used as target cells, were washed with DMEM and overlaid with transfection medium consisting of 0.2 ml DMEM containing 10 μl of lipofectin (Life Technologies) and 4 μg of the plasmid pTN3-*luc*+. After 10 minutes at room temperature, 0.8 ml DMEM was added and incubation was continued at 37°C. BSR T7/5 cells - BHK cells constitutively expressing T7 RNA polymerase (3); a gift from Dr. K.K. Conzelmann - were grown in BHK-21 medium supplemented with 10% FCS, 100 IU of penicillin/ml and 1 mg/ml geneticin (GIBCO BRL). $1x10^4$ BSR T7/5 cells, designated as effector cells, were infected in 96-well plates with wild-type vaccinia virus at an MOI of 1 in DMEM at 37°C. After 1 hour, the cells were washed with DMEM and incubated for 3 hours at 37°C with transfection medium consisting

of 50 µl DMEM containing 1 µl lipofectin and 0.2 µg of the plasmid pTUMS (65), which carries the MHV-A59 spike gene under the control of a T7 promoter. Then, $3x10^4$ of target cells in 100µl DMEM were added and the cells were incubated for another 4 hours in the presence or absence of HR peptide. Cells were lysed and luciferase activity was measured as mentioned above.

RESULTS:

HR1 and HR2 regions in coronavirus spike proteins:

The S2 subunit ectodomain of coronaviruses contains two heptad repeat domains HR1 and HR2, which are conserved in sequence and position (15) (diagrammed in FIG. 1A). HR2 is located adjacent to the transmembrane domain while HR1 occurs at about 170 a.a. upstream of HR2. FIG. 1B shows a protein sequence alignment of the HR1 and HR2 regions for 6 coronaviruses from the three antigenic clusters. The sequence alignment reveals a remarkable insertion of exactly two heptad repeats (14 a.a.) in both the HR1 and the HR2 domain of the spike protein of the group 1 coronaviruses HCV-229E (human coronavirus strain 229E) and FIPV (feline infectious peritonitis virus strain) 79-1146. Another characteristic feature is that the length of the linker region between the HR2 region and the transmembrane region is strictly conserved in all coronavirus spike proteins.

HR1 and HR2 can form an hetero-oligomeric complex:

To study the heptad repeat regions in the S2 subunit of MHV-A59, peptides corresponding to the heptad repeat residues 953-1048 (HR1), 969-1048 (HR1a), 969-1048 (HR1b), 969-1003 (HR1c) and 1216-1254 (HR2) (FIG. 1B) were produced in bacteria as GST fusion proteins. Peptides were affinity purified using glutathione-sepharose beads, proteolytically cleaved from the resin and purified to homogeneity by reversed-phase HPLC. Masses of the peptides, as determined by mass spectrometry, matched their predicted Mw (HR1, 10,873 Da; HR1a, 8,653 Da; HR1b, 5,631 Da; HR1c, 4,447 Da; and HR2, 5,254 Da). To study an interaction between the two HR regions, the purified peptides HR1 and HR2 were incubated alone (80 µM) or in an equimolar (80 µM each) mixture for 1 hour at 37°C and the samples were subjected to SDS-PAGE either directly or after heating for 5 minutes at 95°C

(FIG. 2A). While the peptides migrated according to their molecular weight after separate incubation, most of the protein of the preincubated mixture of HR1 and HR2 migrated as a higher molecular weight complex with a slightly lower mobility than the 29 kDa marker. Upon heating, the complex dissociated giving rise to the individual subunits HR1 and HR2. We also tested the other HR1 peptides for interaction with HR2. While we did not observe complexes upon mixing of HR2 with HR1b or HR1c (data not shown), a higher molecular weight species co migrating with the 29 kDa marker was found when HR1a was incubated with HR2 (FIG. 2B), though the extent of complex formation appeared to be lower than with peptide HR1. Higher molecular weight species were not seen. The results indicated that the HR1 region contains the information to associate with the HR2 region into a hetero-oligomeric complex and that this complex was stable in the presence of 2% SDS.

HR1-HR2 complex is highly temperature resistant:

Next, we determined the stability of the HR1-HR2 complex at increasing temperatures. An equimolar (80 μM each) mix of the two peptides was again incubated for 1 hour at 37°C and subsequently heated for 5 minutes at different temperatures in 1x tricine sample buffer or left at room temperature. The complexes were analyzed by SDS-PAGE in 15% gel. As FIG. 3 demonstrates, the high molecular weight complexes remained intact up to 70°C, dissociated partly at 80°C and fully at 90°C. The stability of the complex at high temperatures indicates that the peptides are held together by strong interaction forces in an energetically favorable conformation.

HR1, HR2 and the HR1-HR2 complex are highly α-helical:

The secondary structure of the HR peptides was examined by circular dichroism. The CD spectra of HR1, HR2 and of an equimolar mixture of HR1 and HR2 were recorded (FIG. 4). The spectra showed clear minima at 208 nm and 222 nm, which is characteristic of alpha-helical structure. Calculations revealed that the alpha-helical contents of the individual HR1 and HR2 peptides and of the mixture of the two peptides were 89.2%, 89.3% and 81.9%, respectively.

The HR1-HR2 complex has a rod-like structure:

The overall shape of the HR1-HR2 complex was examined by electron microscopy. Complexes were purified and viewed after negative staining. Electron micrographs revealed rod-like structures (FIG. 5). Based on measurements of 40 particles, an average length of 14.5 nm (± 2 nm) was calculated. This length is consistent with an alpha-helix of approximately 90 a.a. in length, which corresponds approximately to the predicted length of the HR1 coiled coil region. Similar rod-shaped complexes have been reported for the influenza virus HA protein (12, 53), for portions of the HIV-1 gp41 protein (70) and for the Ebola virus GP2 protein (67).

HR1 and HR2 helices associate in an anti-parallel manner:

The relative orientation and position of HR2 with respect to HR1 in the complex was examined by limited proteolysis using proteinase K in combination with mass spectrometry. Complexes were generated by incubation of the HR2 peptide with each of peptides HR1, HR1a, HR1b and HR1c. The reaction mixtures as well as the individual peptides were then treated with proteinase K. Samples from each reaction were analyzed by tricine SDS-PAGE (data not shown). Using RP HPLC, the protease resistant fragments were purified and their molecular weight (MW) was determined by mass spectrometry, which allowed us to identify the protease resistant cores of the peptides. For each protease resistant core a unique amino acid composition could be deduced that allowed the unequivocal identification of the peptides in the different samples. FIG. 6 gives a schematic overview of the proteinase K resistant fragments. Digestion of HR1 alone left a protease-resistant fragment with an MW of 6,801 Da corresponding to residues 976-1040. Although CD spectra had indicated a folded structure, HR2 was completely degraded by proteinase K. However, in the presence of HR1, HR2 was fully protected from proteolytic degradation. HR2 was able to rescue 18 additional residues at the N-terminus of HR1, leaving a fragment of 8,675 Da corresponding to residues 958-1040.

Proteolysis of the HR1a peptide alone generated the same fragment (residues 976-1040) as obtained with HR1. In the HR1a-HR2 mixture, the HR2 peptide was completely protected against degradation by HR1a, while HR2 fully shielded the N-terminus

of HR1a for proteolysis, including the glycine and serine residues originating from the thrombin cleavage site.

Although a higher molecular weight species could not be detected by tricine SDS-PAGE (data not shown), the protease treatment of the HR1c-HR2 complex left a protease resistant core. HR1c was fully sensitive for proteinase K, but was completely protected in the presence of HR2. HR2 itself was partly protected against proteolysis by HR1c, yielding a fragment of 3,583 Da that represents residues 1225-1254. Importantly, this HR2 fragment has an intact C-terminus but is degraded at its N-terminus. HR1c has the same N-terminus as HR1a but is truncated at its C-terminus. Thus, its inability to protect the HR2 N-terminus combined with the full protection provided by HR1a implies an anti-parallel association of the HR1 and HR2 helices in the hetero-oligomeric complex. The peptide HR1b was fully sensitive to proteinase K both by itself and when mixed with HR2. HR1b could not prevent proteolysis of HR2 either. Altogether, the proteolysis results suggest the anti-parallel association of HR2 and HR1 to occur in the middle part of HR1.

HR2 strongly inhibits viral entry and syncytium formation:

The formation of stable HR complexes is supposedly an essential step in the process of membrane fusion during viral cell entry. Thus, we evaluated the potency of our HR peptides in inhibiting MHV entry, making use of a recombinant MHV-A59, MHV-EFLM that expresses the firefly luciferase reporter gene. Cells were inoculated with MHV-EFLM in the presence of different concentrations of the peptides HR1, HR1a, HR1b, HR1c and HR2. After 1 hour, the cells were washed and culture medium without peptide was added. At 4 hours post infection, i.e., before syncytium formation takes place, cells were lysed and tested for luciferase activity (FIG. 7A). HR1, HR1a and HR1b were not able to inhibit virus entry up to concentrations of 50 μM. In contrast, HR2 blocked viral entry in a concentration-dependent manner inhibition being almost complete at a concentration of 50 μM.

We also studied the ability of the HR peptides in blocking cell-cell fusion. To this end we established a sensitive fusion assay based on the co-culturing of BHK cells expressing the bacteriophage T7 polymerase as well as the MHV-A59 spike protein, with murine L cells transfected with a plasmid carrying a luciferase gene cloned behind a T7 promoter. Fusion of

the cells was determined by measuring luciferase activity. The effects of adding the HR peptides during the co-culturing of the cells are compiled in FIG. 7B. The HR2 peptide again appeared to be a potent inhibitor able to efficiently block cell-cell fusion. A 1000x reduction in luciferase activity was measured at a concentration of 10 μM, whereas essentially no activity was observed at a concentration of 50 μM. Of the HR1 peptides only the HR1b peptide had a minor effect at the highest concentration of 50 μM.

Example 2:

Inhibition of cell-cell fusion after FIPV infection:

FCWF cells were infected with FIPV strain 79-1146 with an moi of 1. 1 hour after infection the cells were washed and medium was replaced by medium containing the GST-FIPV fusion proteins at different concentrations. 8 hours after infection, cells were fixed and scored for syncytia formation (see, Table 2). The amino acid sequence of HR1 and HR2 of FIP is shown in FIG. 9.

Example 3:

Inhibition of SARS-CoV infection of Vero cells by peptides derived from the HR1 and/or HR2 region of SARS-CoV:

Material and methods:

Plasmid constructions: For the production of peptides corresponding to the HR1 and HR2 regions of the SARS-CoV spike protein, PCR fragments were prepared using as a template a SARS-CoV (strain 5688, Kuiken) cDNA covering the S gene. Primers were designed (see Table 3) to introduce into the amplified fragment an upstream *Bam*HI site, a downstream *Eco*RI site as well as a stop codon preceding the *Eco*RI site. Fragments were cloned into the *Bam*HI/*Eco*RI site of the pGEX-2T bacterial expression vector (Amersham Bioscience) in frame with the GST gene just downstream of the thrombin cleavage site. For the production of HR peptides with an N-terminal hydrophilic FLAG-tag (DYKDDDDK) a primer dimer (Table 3) containing the FLAG-tag encoding sequence was cloned into the *Bam*HI site of the pGEX-2T vector, thereby knocking out the 5' *Bam*HI site. The resulting

vector was used to clone the HR1 and HR2 PCR products of SARS-CoV spike gene into the *Bam*HI/*Eco*RI site.

Bacterial protein expression and purification: Freshly transformed BL21 cells (Novagen) were grown in 2 x YT (yeast-tryptone) medium to log phase (OD600 ~1.0) and subsequently induced by adding IPTG (GibcoBRL) to a final concentration of 0.4 mM. Two hours later, cells were pelleted, resuspended in 1/25 volume of 10 mM Tris (pH 8.0), 10 mM EDTA, 1 mM PMSF, and sonicated on ice (5 times for 2 minutes). Cell homogenates were centrifuged at 20,000 x *g* for 60 minutes at 4°C. To each 50 ml of supernatant, 2 ml glutathione-sepharose 4B (Amersham Bioscience; 50% v/v in PBS) was added and the suspensions were incubated overnight (O/N) at 4°C under rotation. Beads were washed three times with 50 ml PBS and resuspended in a final volume of 1 ml PBS. Peptides were cleaved from the GST moiety on the beads using 20 U of thrombin (Amersham Bioscience) by incubation for 4 hours at room temperature. Peptides in the supernatant were purified by reversed phase high pressure liquid chromatography (RP HPLC) using a Phenyl-5PW RP column (Tosoh) with a linear gradient of acetonitrile containing 0.1% trifluoroacetic acid. Peptide containing fractions were vacuum-dried O/N and dissolved in water. Peptide concentrations were determined by measuring the absorbance at 280 nm (Gill and von Hippel 1989) and by BCA protein analysis (Micro BCA™ Assay Kit, Pierce).

Inhibition of SARS-CoV infection:

Vero 118 cells were maintained in Iscove's modified Dulbecco's medium (IMDM; Biowhittaker, Belgium) supplemented with 5% fetal bovine serum (FBS; Greiner), penicillin (100 U/ml), streptomycin (100 µg/ml), and 2 mM L-glutamine. The initial experiments were performed on Vero 118 cells grown on cover slips in 24 well plates ($2x10^5$ cells/well) at 37°C. Cells were inoculated (MOI = 0.5) in the presence of HR peptide at different concentration (25, 5 and 0 µM). After 1 hour, the inoculum was removed, the cells were washed twice with IMDM and the cells were overlaid with IMDM containing 5% FBS and the peptide at similar concentration as used in the inoculum. After O/N incubation, plates were washed twice with PBS and fixed by 4% formaldehyde for 15 minutes and 70% ethanol

plus 0.5% H_2O_2 for 15 minutes at room temperature. After washing the plates twice with PBS + 0.5% Tween-20 and twice with PBS, the cover slips were incubated with a human polyclonal reconvalescent serum (1:50) for 1 hour at 37°C. FITC labeled antihuman serum was used as a conjugate in a 1:300 dilution. Pictures of FITC fluorescent cells were taken using a Olympus camera mounted on a Leitz microscope.

The second set of inhibition experiments was performed on Vero 118 cells in 96 well plates (10^4 cells/well). Cells were infected in triplicate with 100 $TCID_{50}$ of SARS-CoV (strain 5688, fourth passage) in the presence of various peptide concentrations, ranging from 0.4 μM to 50 μM, for 1 hour at 37°C in a CO_2-incubator. Cells were then washed twice with IMDM and the medium was replaced with IMDM containing 5% FBS. After incubation for 9 hours, plates were washed twice with PBS and fixed by 4% formaldehyde for 15 minutes and 70% ethanol plus 0.5% H_2O_2 for 15 minutes at room temperature. After washing the plates twice with PBS + 0.5% Tween-20 and twice with PBS, the fixed and permeabilized cells were incubated with a ferret polyclonal antiserum (1:40) for 1 hour at 37°C. Horse radish peroxidase (HRP) labeled goat-anti-ferret antibodies (DAKO, USA) were used as a conjugate in a 1:50 dilution. Reaction was developed with 3-amino-9-ethylcarbazole (AEC; Sigma, Zwijndrecht) according to the manufacturer's instructions. SARS-CoV positive cells were counted using the light microscope and the effective peptide concentration at which 50% of the infection was inhibited (EC_{50}) was determined. Inhibition of MHV by HR peptides was tested as described above but using LR7 cells (Kuo, Godeke et al. 2000) rather then VERO 118 cells. IPOX detection of MHV positive cells was carried out by using a rabbit polyclonal antibody against MHV (1:300) (Rottier, Armstrong et al. 1985) in combination with a HRP swine-anti rabbit antibody (1:300) (DAKO, USA). Experiments were performed in triplicate, and carried out in duplicate.

Temperature stability of SARS-CoV and MHV HR1-HR2 complex: Equimolar mixes of HR1 and HR2 peptides (100 μM each) of SARS-CoV and MHV were incubated in parallel at room temperature for 3 hours, to allow HR1-HR2 complex formation. 25 μl of each mix was pooled and an equal volume of 2 x Tricine sample buffer (0.125 M Tris pH 6.8,

4% SDS, 5% β-mercaptoethanol, 10% glycerol, 0.004 g bromophenol blue) (55) was added. The mixtures were either left at room temperature or heated for 5 minutes at different temperatures and subsequently analyzed by SDS-polyacrylamide gel electrophoresis (PAGE) in 15% Tricine gel (55).

CD spectroscopy: CD spectra of the HR1 and HR2 peptides (20 μM in H_2O) or a preincubated equimolar mix of HR1 and HR2 (20 μM each in H_2O) were recorded at room temperature on a Jasco J-810 spectropolarimeter, using a 0.1 mm path length, 1 nm bandwidth, 1 nm resolution, 0.5 second response time and a scan speed of 50 nm/min. The alpha-helical content of the peptides was calculated using the program k2d (http://www.embl-heidelberg.de/~andrade/k2d/).

Proteinase K treatment: Stock solutions (250 μM) of the peptides HR1a, HR1c and HR2 in water were diluted to 100 μM in 50 mM Tris pH 7.0. Peptides on their own (100 μM) or HR1-HR2 mixtures (100 μM each) preincubated for 3 hours at 37°C were subjected to proteinase K digestion (1% wt/wt, proteinase K/peptide) for 2 hours at 4°C. Protease resistant fragments were separated and purified by RP HPLC and characterized by mass spectrometry.

Results:

HR regions in the SARS-CoV spike protein:

As shown by the alignment in FIG. 1, two heptad repeat (HR) regions are present in the C-terminal S2 domain of the SARS-CoV spike protein as they were detected before in other coronavirus spike proteins (15). One region (HR2) is located adjacent to the transmembrane domain, the other (HR1) is located some 170 residues upstream. In all coronaviruses, HR1 is consistently larger than HR2. However, the group 1 coronaviruses show a remarkable insertion of two heptad repeats (14 aa) in both HR regions. This insertion is lacking in the SARS-CoV HR regions. The HR2 region of SARS-CoV contains three conserved N-glycosylation sites (N-X-S/T; FIG. 1B).

HR peptides and their infection inhibitory activities:

Peptides corresponding to the HR regions were expressed using the bacterial GST expression and purification system. They were purified to homogeneity using RP HPLC and their molecular masses were verified by mass spectrometry. Peptides were subsequently tested for their inhibitory potency in an infection inhibition assay. VERO cells were inoculated with SARS-CoV (MOI 0.5) in the absence or presence of different concentrations of a particular peptide and the extent of infection was evaluated using an indirect immunofluorescence assay. As shown in FIG. 11A, for one of the initial peptides tested, HR2-1, a clear concentration dependent inhibition of SARS-CoV infection could be observed. This effect was sequence specific as no inhibition was seen with a corresponding peptide derived from the HR2 region of MHV (mHR2), known to block MHV infection.

To study the sequence dependence and to optimize the efficacy of the inhibition, we prepared two sets of peptides, the sequences of which are compiled in FIG. 10B. One set consisted of HR2-1 based peptides: a series of peptides with increasing 4-residue N-terminal truncations (HR2-2 - HR2-7), one peptide with a 4-residue C-terminal extension (HR2-8) and two peptides with 4- and 8-residue C-terminal truncations (HR2-9 and HR2-10, respectively). The other set consisted of peptides corresponding to the HR1 region, with peptide HR1 comprising almost the entire heptad repeat region and peptides HR1a-c representing N-terminal and C-terminal truncations thereof. These peptides were tested similarly, but the infection levels were now determined in a technically different format using immune peroxidase staining followed by an automated read-out of the percentage of infected cells. FIG. 10B shows the EC_{50} values obtained, i.e., the concentrations calculated to cause a 50% reduction of infection. It is clear that only slight truncations at either side of the HR2-1 peptide are tolerated without loss of inhibitory activity. Actually, shortening HR2-1 just by 4 residues at the N-terminal (HR2-2) or the C-terminal side (HR2-9) resulted in significantly enhanced inhibition. The most effective peptide of the panel was HR2-8, which carried the C-terminal 4-residue extension. It had an EC_{50} value of 17 μM. The inhibition efficiency of this peptide was clearly lower than that of an HR2 peptide of MHV, mHR2, which had an EC_{50} value of 0.9 μM when tested in the MHV infection system. Of the panel of HR1

derived peptides none showed any measurable inhibitory effect on SARS-CoV infection under the conditions used in this experiment.

HR1-HR2 complex formation:

We have previously shown by Tricine SDS-PAGE analysis that the HR1 and HR2 peptides of the MHV S protein, when mixed together, assemble into an oligomeric complex that is resistant to 2% SDS, the SDS concentration used in this analysis. By the same approach we observed that the HR1 and HR2 peptides of the SARS-CoV spike protein behave likewise. As shown in FIG. 12A for equimolar mixtures of similar HR peptides from both viruses, SDS-stable oligomeric complexes are formed that dissociate upon heating.

These observations do not necessarily imply that the complexes are composed of both HR peptides: in the mixture one peptide might simply catalyze the homomultimerization of the other. To confirm the presence of both HR1 and HR2 in the complex, FLAG-tagged HR peptides were prepared in which the polar FLAG octapeptide (DYKDDDDK (SEQ ID NO: 51)) was appended to the N-termini of HR1 (FLAG-HR1) and HR2 (FLAG-HR2). Preincubated mixtures of HR1+HR2, FLAG-HR1+HR2, HR1+FLAG-HR2 and FLAG-HR1+FLAG-HR2 were analyzed in 15% Tricine SDS-PAGE together with the individual peptides (FIG. 12B). The individual FLAG-tagged HR peptides migrated slower in the gel than their nontagged homologues. All combinations of HR1 and HR2 peptide produced the higher molecular weight band, indicating that the addition of the FLAG tag did not prevent complex formation. The combination of FLAG-HR1+HR2 and HR1+FLAG-HR2 each produced a complex that had lower gel mobility than the nontagged HR1+HR2 complex. Combining the two tagged peptides resulted in an additional mobility decrease. These observations imply that both the HR1 and the HR2 peptide are present in the complex.

Stoichiometry of peptides in the HR1-HR2 complex:

The availability of the FLAG-tagged HR peptides provided us with the means to determine the stoichiometry of the peptides in the HR complex. As the FLAG-tag did not interfere with complex formation its distinctive effect on the electrophoretic mobility of the tagged peptides was exploited to determine the number of HR1 and HR2 peptides in the

complex. FLAG-tagged and nontagged HR2 peptides were mixed in different ratios and subsequently incubated for 3 hours at room temperature (RT) with equimolar amounts of HR1 peptide to allow complex formation. Subsequent SDS-PAGE analysis revealed four bands when the HR1 peptide had been incubated with a 1:1 mixture of FLAG-tagged and nontagged HR2 peptides (FIG. 13-I). The fastest migrating band comigrated with the complex obtained with nontagged HR2 peptide only, while the band with the lowest mobility corresponded to the complex obtained with the FLAG-tagged HR2 peptide. Consequently, the two intermediate bands represent complexes containing one and two FLAG-tagged HR2 peptides, respectively. Note that the relative intensities of the four bands correspond well with the predicted ratio of formation of the different complexes (1/8, 3/8, 3/8, 1/8 respectively), calculated under the assumption that the tag is fully inert.

The reciprocal approach was used to determine the number of HR1 peptides in the complex. In this case FLAG-tagged and nontagged HR1 peptides were combined with nontagged HR2 peptide. However, when a 1:1 mixture of the two HR1 forms was incubated with HR2, only two bands were observed in the gel (FIG. 13-II), the faster one comigrating with the HR1-HR2 complex, the slower one corresponding with the FLAG-HR1-HR2 complex. One interpretation of this result is that the complex contains just one HR1 peptide molecule. Alternatively, HR1 peptides in solution assemble into homo-oligomers already in the absence of HR2. These oligomers are sufficiently stable to prevent the exchange of peptides when tagged and nontagged HR1 complexes are mixed and, as a result, such a mixture will yield only two forms of hetero-oligomeric complexes upon addition of HR2. In view of this latter possibility we repeated the experiment after we had first denatured the putative HR1 oligomers. Thus, acetonitrile - an anorganic solvent - was added to solutions of HR1 and FLAG-tagged HR1 to a concentration of 50% (v/v). The solutions were mixed, briefly incubated after which the acetonitrile was removed by evaporation. Equimolar mixtures were again prepared of the different HR1 forms and HR2, which were incubated and finally analyzed by Tricine SDS-PAGE. As FIG. 13-III reveals, we now observed four bands in the sample containing both tagged and nontagged HR1, indicating the presence of three HR1 peptides in the complex. The combined results are consistent with HR1 and HR2 forming a hexameric complex composed of three molecules HR1 and HR2 each.

Temperature stability of HR1-HR2 complex:

The stability of the SARS-CoV HR1-HR2 complex to temperature dissociation was assessed in comparison to that of the corresponding MHV complex. Equal amounts of both complexes were combined and the solution was adjusted to 1x Tricine sample buffer. Equal samples were taken, incubated in parallel for 5 minutes at different temperatures and subsequently analyzed by 10% Tricine SDS-PAGE (FIG. 14). Due to their distinct electrophoretic mobilities, the SARS-CoV and MHV complexes could clearly be distinguished allowing the direct comparison of their temperature sensitivity. Surprisingly, the SARS-CoV HR complex appeared to be significantly less stable (dissociated at 70°C) than the MHV complex (dissociated at 90°C).

Secondary structure of HR1 and HR2 peptides and of HR1-HR2 complex:

Circular dichroism (CD) was used to determine the secondary structure of the individual peptides HR1 and HR2 and of the HR1-HR2 complex. The CD spectra show that the peptides have a high alpha-helicity both on their own and in the complex (FIG. 15). The calculated values of the helical content were 85% (HR1), 81% (HR2) and 88% (HR1-HR2).

Limited proteolysis on HR1-HR2 complex:

Strongly folded protein structures are often resistant to proteolytic degradation. To obtain structural information about the HR1-HR2 complex we carried out limited digestions with proteinase K, purified the resistant fragments by RP HPLC (FIG. 16, upper part) and analyzed the fragments by mass spectrometry (FIG. 16, lower part). For the individual peptides the results showed that HR2 was completely degraded by the enzyme while of the HR1a peptide only the C-terminal 6 residues were sensitive to proteinase K, indicating a strong folding of this latter peptide. When a mixture of the two peptides was analyzed, the HR2 peptide was entirely protected from proteolytic breakdown. A similar analysis carried out with a C-terminally truncated version of HR1a, HR1c, revealed that now the N-terminus of HR2 was no longer protected. These results indicate that in the HR1-HR2 complex, the HR1 and HR2 helices are oriented in an anti-parallel fashion.

Our functional and biochemical analyses of the SARS-CoV spike HR regions shows that the virus makes use of a membrane fusion mechanism that has similarities with the fusion mechanism of class I fusion proteins, in which the HR regions play a prominent role. We show that peptides corresponding to the HR2 domain, but not those derived of the HR1 domain of the SARS-CoV spike protein can inhibit virus infection. We show here that HR2 peptides are able to bind stably to HR1 peptides, as has been observed previously for coronavirus, retrovirus and paramyxovirus fusion proteins. Analogous to the HIV-1 gp41, SV5 F and HRSV F proteins (69, 8, 1, 80, the HR1-HR2 complex was found to consist of a six-helix bundle that is composed of three HR1 and three HR2 alpha-helical peptides. The high resistance of the HR1 peptide to proteinase-K, the inability of separately preincubated FLAG-tagged and nontagged HR1 peptides to form mixed hexamers unless first dissociated by acetonitrile, and the highly alpha-helical character of the peptide are all observations suggesting that SARS-CoV HR1, in the absence of HR2, already forms a (trimeric) coiled coil. The proteolysis data point to an anti-parallel packing of HR2 with respect to HR1, presumably through interaction of the hydrophobic interface of the HR2 helix with the hydrophobic groove in the HR1 coiled coil created by the - mostly hydrophobic - e and g residues of HR1. Formation of such an anti-parallel six-helix bundle has been shown to be essential in the membrane fusion process, by pulling the viral and cellular membrane together. In the full-length spike protein such a structure brings the fusion peptide - N-terminal of HR1 - in close proximity to the transmembrane domain - C-terminal of HR2 - thereby enabling membrane fusion. The infection inhibiting effect of peptides corresponding to HR2 can be explained by their competitive binding to the HR1 region of the SARS-CoV spike protein, which prevents formation of the six-helix bundle and, consequently, prevents membrane fusion.

The HR2-8 peptide can be used as a lead for the development of more effective SARS-CoV peptide inhibitors. Alternatively, the HR peptides might be used as a vaccine, since antibodies directed against the HR2 peptides of HIV-1 inhibit virus infection. Hence, the HR peptides provide a basis for therapeutic and/or prophylactic agents against SARS-CoV as well as against other coronaviruses.

Example 4:

The coronavirus fusion peptide:

Transmembrane prediction using the TMAP program:

The TMAP program, www.mbb.ki.se/tmap/index.html, was used to predict transmembrane segments in coronavirus spike proteins using multiple sequence alignments. A Clustal W alignment was used of spike protein sequences from nine coronaviruses including FIPV (feline infectious peritonitis virus, strain 79-1146; VGIH79), TGEV (porcine transmissible gastroenteritis virus, strain Purdue; P07946), PEDV (porcine epidemic diarrhea virus; NP_598310), HCoV-229E (human coronavirus, strain 229E; VGIHHC), BCoV (bovine coronavirus, strain F15; P25190), MHV (mouse hepatitis virus, strain A59; P11224), HCoV-OC43 (human coronavirus, strain OC43; CAA83661), SARS-CoV (strain TOR2; P59594), and IBV (infectious bronchitis virus, strain Beaudette; P11223).

The TMAP program, designed to identify transmembrane domains in proteins, was used in the search for the coronavirus fusion peptide. Nine coronaviral spike protein sequences (FIG. 17, lower part) were used for the Clustal W alignment on which the prediction by the TMAP program is based. Three hydrophobic regions were identified (FIG. 17, middle part). Two of these, i.e., the regions in the N- and C-terminal part of the protein, represent the well-known signal sequence and transmembrane anchor, respectively. The third domain is found immediately upstream of HR1. This location combined with its hydrophobicity and the presence of a conserved proline in it are characteristics indicating that this domain functions as the coronavirus fusion peptide.

The identity of the fusion peptide in the coronavirus spike protein has not yet been established. Generally, class I fusion proteins require cleavage for fusion activation. As a result, the fusion peptide ends up at or close to the N-terminus of the membrane-anchored subunit. Unlike other class I fusion proteins, coronavirus spike proteins lack the cleavage requirement for virus infectivity. Cleavage inhibition of the MHV spike protein by a furin blocker does not affect virus infectivity, rather, group 1 coronaviruses are not cleaved at all. We could not observe any significant cleavage of the expressed spike protein. Additionally, the cleavable coronavirus spike proteins lack a hydrophobic region adjacent to the cleavage site. This suggests that coronavirus spike proteins use an internal fusion peptide like the VSV

G protein and class II fusion proteins, such as the TBEV E and SFV E1 fusion proteins. In order to predict the location of the fusion peptide, we have used a transmembrane prediction program TMAP], which predicts transmembrane domains (TM) in protein sequences using multiple alignments. In the Clustal W alignment of all known coronavirus spike sequences, the TMAP program predicted three TM domains (FIG. 17). One represented the signal sequence (SARS-CoV-S residues 1 - 15), the other represented the transmembrane anchor (residues 1195 - 1223), and the third hydrophobic region was predicted immediately N-terminal of the HR1 region (residues 858 - 886). Careful inspection of this region reveals that it has fusion peptide characteristics like a high alanine and glycine content and a conserved proline residue (residue 879), which is characteristic of internal fusion peptides. This region was previously recognized by Chambers and coworkers (7) as a potential fusion peptide for coronaviruses. The formation of the anti-parallel six-helix bundle during the fusion reaction brings this fusion peptide in close proximity to the transmembrane anchor of the full-length protein, which results in the merging of viral and cellular membranes.

REFERENCES

1. **Baker, K. A., R. E. Dutch, R. A. Lamb, and T. S. Jardetzky.** 1999. Structural basis for paramyxovirus-mediated membrane fusion. Mol Cell **3**:309-19.
2. **Bos, E. C., L. Heijnen, W. Luytjes, and W. J. Spaan.** 1995. Mutational analysis of the murine coronavirus spike protein: effect on cell-to-cell fusion. Virology **214**:453-63.
3. **Buchholz, U. J., S. Finke, and K. K. Conzelmann.** 1999. Generation of bovine respiratory syncytial virus (BRSV) from cDNA: BRSV NS2 is not essential for virus replication in tissue culture, and the human RSV leader region acts as a functional BRSV genome promoter. J Virol **73**:251-9.
4. **Bullough, P. A., F. M. Hughson, J. J. Skehel, and D. C. Wiley.** 1994. Structure of influenza haemagglutinin at the pH of membrane fusion. Nature **371**:37-43.
5. **Caffrey, M., M. Cai, J. Kaufman, S. J. Stahl, P. T. Wingfield, D. G. Covell, A. M. Gronenborn, and G. M. Clore.** 1998. Three-dimensional solution structure of the 44 kDa ectodomain of SIV gp41. Embo J **17**:4572-84.
6. **Cavanagh, D.** 1995. The Coronavirus Surface Glycoprotein, p. 73-113. *In* S. G. Siddell (ed.), The Coronaviridae. Plenum Press, New York.
7. **Chambers, P., C. R. Pringle, and A. J. Easton.** 1990. Heptad repeat sequences are located adjacent to hydrophobic regions in several types of virus fusion glycoproteins. J Gen Virol **71**:3075-80.
8. **Chan, D. C., D. Fass, J. M. Berger, and P. S. Kim.** 1997. Core structure of gp41 from the HIV envelope glycoprotein. Cell **89**:263-73.
9. **Chen, C. H., T. J. Matthews, C. B. McDanal, D. P. Bolognesi, and M. L. Greenberg.** 1995. A molecular clasp in the human immunodeficiency virus (HIV) type 1 TM protein determines the anti-HIV activity of gp41 derivatives: implication for viral fusion. J Virol **69**:3771-7.
10. **Chen, J., K. H. Lee, D. A. Steinhauer, D. J. Stevens, J. J. Skehel, and D. C. Wiley.** 1998. Structure of the hemagglutinin precursor cleavage site, a determinant of influenza pathogenicity and the origin of the labile conformation. Cell **95**:409-17.

11. **Chen, J., J. J. Skehel, and D. C. Wiley.** 1999. N- and C-terminal residues combine in the fusion-pH influenza hemagglutinin HA(2) subunit to form an N cap that terminates the triple-stranded coiled coil. Proc Natl Acad Sci U S A **96:**8967-72.

12. **Chen, J., S. A. Wharton, W. Weissenhorn, L. J. Calder, F. M. Hughson, J. J. Skehel, and D. C. Wiley.** 1995. A soluble domain of the membrane-anchoring chain of influenza virus hemagglutinin (HA2) folds in Escherichia coli into the low-pH-induced conformation. Proc Natl Acad Sci U S A **92:**12205-9.

13. **Chen, L., J. J. Gorman, J. McKimm-Breschkin, L. J. Lawrence, P. A. Tulloch, B. J. Smith, P. M. Colman, and M. C. Lawrence.** 2001. The structure of the fusion glycoprotein of Newcastle disease virus suggests a novel paradigm for the molecular mechanism of membrane fusion. Structure (Camb) **9:**255-66.

14. **Davies, H. A., and M. R. Macnaughton.** 1979. Comparison of the morphology of three coronaviruses. Arch Virol **59:**25-33.

15. **de Groot, R. J., W. Luytjes, M. C. Horzinek, B. A. van der Zeijst, W. J. Spaan, and J. A. Lenstra.** 1987. Evidence for a coiled-coil structure in the spike proteins of coronaviruses. J Mol Biol **196:**963-6.

16. **Delmas, B., and H. Laude.** 1990. Assembly of coronavirus spike protein into trimers and its role in epitope expression. J Virol **64:**5367-75.

17. **Eckert, D. M., and P. S. Kim.** 2001. Design of potent inhibitors of HIV-1 entry from the gp41 N-peptide region. Proc Natl Acad Sci U S A **98:**11187-92.

18. **Eckert, D. M., and P. S. Kim.** 2001. Mechanisms of viral membrane fusion and its inhibition. Annu Rev Biochem **70:**777-810.

19. **Fass, D., S. C. Harrison, and P. S. Kim.** 1996. Retrovirus envelope domain at 1.7 angstrom resolution. Nat Struct Biol **3:**465-9.

20. **Furuta, R. A., C. T. Wild, Y. Weng, and C. D. Weiss.** 1998. Capture of an early fusion-active conformation of HIV-1 gp41. Nat Struct Biol **5:**276-9.

21. **Gallagher, T. M.** 1997. A role for naturally occurring variation of the murine coronavirus spike protein in stabilizing association with the cellular receptor. J Virol **71:**3129-37.

22. **Gallagher, T. M., and M. J. Buchmeier.** 2001. Coronavirus spike proteins in viral entry and pathogenesis. Virology **279:**371-4.

23. **Gallagher, T. M., C. Escarmis, and M. J. Buchmeier.** 1991. Alteration of the pH dependence of coronavirus-induced cell fusion: effect of mutations in the spike glycoprotein. J Virol **65:**1916-28.

24. **Gill, S. C., and P. H. von Hippel.** 1989. Calculation of protein extinction coefficients from amino acid sequence data. Anal Biochem **182:**319-26.

25. **Gombold, J. L., S. T. Hingley, and S. R. Weiss.** 1993. Fusion-defective mutants of mouse hepatitis virus A59 contain a mutation in the spike protein cleavage signal. J Virol **67:**4504-12.

26. **Hingley, S. T., I. Leparc-Goffart, and S. R. Weiss.** 1998. The spike protein of murine coronavirus mouse hepatitis virus strain A59 is not cleaved in primary glial cells and primary hepatocytes. J Virol **72:**1606-9.

27. **Holmes, K. V., B.D. Zelus, J.H. Schickli and S.R. Weiss.** 2001. Receptor specificity and receptor-induced conformational changes in mouse hepatitis virus spike glycoprotein. Adv Exp Med Biol **494:**173-181.

28. **Jiang, S., K. Lin, N. Strick, and A. R. Neurath.** 1993. HIV-1 inhibition by a peptide. Nature **365:**113.

29. **Joshi, S. B., R. E. Dutch, and R. A. Lamb.** 1998. A core trimer of the paramyxovirus fusion protein: parallels to influenza virus hemagglutinin and HIV-1 gp41. Virology **248:**20-34.

30. **Judice, J. K., J. Y. Tom, W. Huang, T. Wrin, J. Vennari, C. J. Petropoulos, and R. S. McDowell.** 1997. Inhibition of HIV type 1 infectivity by constrained alpha-helical peptides: implications for the viral fusion mechanism. Proc Natl Acad Sci U S A **94:**13426-30.

31. **Kliger, Y., and Y. Shai.** 2000. Inhibition of HIV-1 entry before gp41 folds into its fusion-active conformation. J Mol Biol **295:**163-8.

32. **Kobe, B., R. J. Center, B. E. Kemp, and P. Poumbourios.** 1999. Crystal structure of human T cell leukemia virus type 1 gp21 ectodomain crystallized as a maltose-binding

protein chimera reveals structural evolution of retroviral transmembrane proteins. Proc Natl Acad Sci U S A **96:**4319-24.

33. **Krueger, D. K., S. M. Kelly, D. N. Lewicki, R. Ruffolo, and T. M. Gallagher.** 2001. Variations in disparate regions of the murine coronavirus spike protein impact the initiation of membrane fusion. J Virol **75:**2792-802.

34. **Kuo, L., G. J. Godeke, M. J. Raamsman, P. S. Masters, and P. J. Rottier.** 2000. Retargeting of coronavirus by substitution of the spike glycoprotein ectodomain: crossing the host cell species barrier. J Virol **74:**1393-406.

35. **Lambert, D. M., S. Barney, A. L. Lambert, K. Guthrie, R. Medinas, D. E. Davis, T. Bucy, J. Erickson, G. Merutka, and S. R. Petteway, Jr.** 1996. Peptides from conserved regions of paramyxovirus fusion (F) proteins are potent inhibitors of viral fusion. Proc Natl Acad Sci U S A **93:**2186-91.

36. **Lescar, J., A. Roussel, M. W. Wien, J. Navaza, S. D. Fuller, G. Wengler, and F. A. Rey.** 2001. The Fusion glycoprotein shell of Semliki Forest virus: an icosahedral assembly primed for fusogenic activation at endosomal pH. Cell **105:**137-48.

37. **Lewicki, D. N., and T. M. Gallagher.** 2002. Quaternary structure of coronavirus spikes in complex with carcinoembryonic antigen-related cell adhesion molecule cellular receptors. J Biol Chem **277:**19727-34.

38. **Lu, M., S. C. Blacklow, and P. S. Kim.** 1995. A trimeric structural domain of the HIV-1 transmembrane glycoprotein. Nat Struct Biol **2:**1075-82.

39. **Luo, Z., A. M. Matthews, and S. R. Weiss.** 1999. Amino acid substitutions within the leucine zipper domain of the murine coronavirus spike protein cause defects in oligomerization and the ability to induce cell-to-cell fusion. J Virol **73:**8152-9.

40. **Luo, Z., and S. R. Weiss.** 1998. Roles in cell-to-cell fusion of two conserved hydrophobic regions in the murine coronavirus spike protein. Virology **244:**483-94.

41. **Malashkevich, V. N., D. C. Chan, C. T. Chutkowski, and P. S. Kim.** 1998. Crystal structure of the simian immunodeficiency virus (SIV) gp41 core: conserved helical interactions underlie the broad inhibitory activity of gp41 peptides. Proc Natl Acad Sci U S A **95:**9134-9.

42. **Malashkevich, V. N., B. J. Schneider, M. L. McNally, M. A. Milhollen, J. X. Pang, and P. S. Kim.** 1999. Core structure of the envelope glycoprotein GP2 from Ebola virus at 1.9- A resolution. Proc Natl Acad Sci U S A **96:**2662-7.

43. **Malashkevich, V. N., M. Singh, and P. S. Kim.** 2001. The trimer-of-hairpins motif in membrane fusion: Visna virus. Proc Natl Acad Sci U S A **98:**8502-6.

44. **Matsuyama, S., and F. Taguchi.** 2002. Communication between S1N330 and a region in S2 of murine coronavirus spike protein is important for virus entry into cells expressing CEACAM1b receptor. Virology **295:**160-71.

45. **Matsuyama, S., and F. Taguchi.** 2002. Receptor-induced conformational changes of murine coronavirus spike protein. J Virol **76:**11819-26.

46. **Melikyan, G. B., R. M. Markosyan, H. Hemmati, M. K. Delmedico, D. M. Lambert, and F. S. Cohen.** 2000. Evidence that the transition of HIV-1 gp41 into a six-helix bundle, not the bundle configuration, induces membrane fusion. J Cell Biol **151:**413-23.

47. **Munoz-Barroso, I., S. Durell, K. Sakaguchi, E. Appella, and R. Blumenthal.** 1998. Dilation of the human immunodeficiency virus-1 envelope glycoprotein fusion pore revealed by the inhibitory action of a synthetic peptide from gp41. J Cell Biol **140:**315-23.

48. **Nash, T. C., and M. J. Buchmeier.** 1997. Entry of mouse hepatitis virus into cells by endosomal and nonendosomal pathways. Virology **233:**1-8.

49. **Nehete, P. N., R. B. Arlinghaus, and K. J. Sastry.** 1993. Inhibition of human immunodeficiency virus type 1 infection and syncytium formation in human cells by V3 loop synthetic peptides from gp120. J Virol **67:**6841-6.

50. **Parry, D. A.** 1978. Fibrinogen: A preliminary analysis of the amino acid sequences of the portions of the alpha, beta, and gamma-chains postulated to form the interdomainal link between globular regions of the molecule. J. Mol. Biol. **248:**180-189.

51. **Rapaport, D., M. Ovadia, and Y. Shai.** 1995. A synthetic peptide corresponding to a conserved heptad repeat domain is a potent inhibitor of Sendai virus-cell fusion: an emerging similarity with functional domains of other viruses. Embo J **14:**5524-31.

52. **Rimsky, L. T., D. C. Shugars, and T. J. Matthews.** 1998. Determinants of human immunodeficiency virus type 1 resistance to gp41-derived inhibitory peptides. J Virol **72:**986-93.

53. **Ruigrok, R. W., A. Aitken, L. J. Calder, S. R. Martin, J. J. Skehel, S. A. Wharton, W. Weis, and D. C. Wiley.** 1988. Studies on the structure of the influenza virus haemagglutinin at the pH of membrane fusion. J Gen Virol **69:**2785-95.

54. **Russell, C. J., T. S. Jardetzky, and R. A. Lamb.** 2001. Membrane fusion machines of paramyxoviruses: capture of intermediates of fusion. Embo J **20:**4024-34.

55. **Schagger, H., and G. von Jagow.** 1987. Tricine-sodium dodecyl sulfate-polyacrylamide gel electrophoresis for the separation of proteins in the range from 1 to 100 kDa. Anal Biochem **166:**368-79.

56. **Siddell, S. G.** 1995. The Coronaviridae; an introduction. Plenum Press, New York.

57. **Skehel, J. J., and D. C. Wiley.** 1998. Coiled coils in both intracellular vesicle and viral membrane fusion. Cell **95:**871-4.

58. **Slepushkin, V. A., G. V. Kornilaeva, S. M. Andreev, M. V. Sidorova, A. O. Petrukhina, G. R. Matsevich, S. V. Raduk, V. B. Grigoriev, T. V. Makarova, V. V. Lukashov, and Karamov, E. V.** 1993. Inhibition of human immunodeficiency virus type 1 (HIV-1) penetration into target cells by synthetic peptides mimicking the N-terminus of the HIV-1 transmembrane glycoprotein. Virology **194:**294-301.

59. **Stauber, R., M. Pfleiderera, and S. Siddell.** 1993. Proteolytic cleavage of the murine coronavirus surface glycoprotein is not required for fusion activity. J Gen Virol **74:**183-91.

60. **Sturman, L. S., C. S. Ricard, and K. V. Holmes.** 1990. Conformational change of the coronavirus peplomer glycoprotein at pH 8.0 and 37 degrees C correlates with virus aggregation and virus- induced cell fusion. J Virol **64:**3042-50.

61. **Taguchi, F.** 1993. Fusion formation by the uncleaved spike protein of murine coronavirus JHMV variant cl-2. J Virol **67:**1195-202.

62. **Taguchi, F.** 1995. The S2 subunit of the murine coronavirus spike protein is not involved in receptor binding. J Virol **69:**7260-3.

63. **Tan, K., J. Liu, J. Wang, S. Shen, and M. Lu.** 1997. Atomic structure of a thermostable subdomain of HIV-1 gp41. Proc Natl Acad Sci U S A **94:**12303-8.

64. **Vennema, H., G. J. Godeke, J. W. Rossen, W. F. Voorhout, M. C. Horzinek, D. J. Opstelten, and P. J. Rottier.** 1996. Nucleocapsid-independent assembly of coronavirus-like particles by co- expression of viral envelope protein genes. Embo J **15:**2020-8.

65. **Vennema, H., R. Rijnbrand, L. Heijnen, M. C. Horzinek, and W. J. Spaan.** 1991. Enhancement of the vaccinia virus/phage T7 RNA polymerase expression system using encephalomyocarditis virus 5'-untranslated region sequences. Gene **108:**201-9.

66. **Vennema, H., P. J. Rottier, L. Heijnen, G. J. Godeke, M. C. Horzinek, and W. J. Spaan.** 1990. Biosynthesis and function of the coronavirus spike protein. Adv Exp Med Biol **276:**9-19.

67. **Weissenhorn, W., L. J. Calder, S. A. Wharton, J. J. Skehel, and D. C. Wiley.** 1998. The central structural feature of the membrane fusion protein subunit from the Ebola virus glycoprotein is a long triple-stranded coiled coil. Proc Natl Acad Sci U S A **95:**6032-6.

68. **Weissenhorn, W., A. Carfi, K. H. Lee, J. J. Skehel, and D. C. Wiley.** 1998. Crystal structure of the Ebola virus membrane fusion subunit, GP2, from the envelope glycoprotein ectodomain. Mol Cell **2:**605-16.

69. **Weissenhorn, W., A. Dessen, S. C. Harrison, J. J. Skehel, and D. C. Wiley.** 1997. Atomic structure of the ectodomain from HIV-1 gp41. Nature **387:**426-30.

70. **Weissenhorn, W., S. A. Wharton, L. J. Calder, P. L. Earl, B. Moss, E. Aliprandis, J. J. Skehel, and D. C. Wiley.** 1996. The ectodomain of HIV-1 env subunit gp41 forms a soluble, alpha-helical, rod-like oligomer in the absence of gp120 and the N-terminal fusion peptide. Embo J **15:**1507-14.

71. **Westenberg, M., H. Wang, W. F. IJkel, R. W. Goldbach, J. M. Vlak, and D. Zuidema.** 2002. Furin is involved in baculovirus envelope fusion protein activation. J Virol **76:**178-84.

72. **Wild, C., T. Oas, C. McDanal, D. Bolognesi, and T. Matthews.** 1992. A synthetic peptide inhibitor of human immunodeficiency virus replication: correlation between solution structure and viral inhibition. Proc Natl Acad Sci U S A **89:**10537-41.

73. **Wild, C. T., D. C. Shugars, T. K. Greenwell, C. B. McDanal, and T. J. Matthews.** 1994. Peptides corresponding to a predictive alpha-helical domain of human immunodeficiency virus type 1 gp41 are potent inhibitors of virus infection. Proc Natl Acad Sci U S A **91:**9770-4.

74. **Williams, R. K., G. S. Jiang, and K. V. Holmes.** 1991. Receptor for mouse hepatitis virus is a member of the carcinoembryonic antigen family of glycoproteins. Proc Natl Acad Sci U S A **88:**5533-6.

75. **Wilson, I. A., J. J. Skehel, and D. C. Wiley.** 1981. Structure of the haemagglutinin membrane glycoprotein of influenza virus at 3 A resolution. Nature **289:**366-73.

76. **Yang, Z. N., T. C. Mueser, J. Kaufman, S. J. Stahl, P. T. Wingfield, and C. C. Hyde.** 1999. The crystal structure of the SIV gp41 ectodomain at 1.47 A resolution. J Struct Biol **126:**131-44.

77. **Yao, Q., and R. W. Compans.** 1996. Peptides corresponding to the heptad repeat sequence of human parainfluenza virus fusion protein are potent inhibitors of virus infection. Virology **223:**103-12.

78. **Yoo, D. W., M. D. Parker, and L. A. Babiuk.** 1991. The S2 subunit of the spike glycoprotein of bovine coronavirus mediates membrane fusion in insect cells. Virology **180:**395-9.

79. **Young, J. K., R. P. Hicks, G. E. Wright, and T. G. Morrison.** 1997. Analysis of a peptide inhibitor of paramyxovirus (NDV) fusion using biological assays, NMR, and molecular modeling. Virology **238:**291-304.

80. **Zhao, X., M. Singh, V. N. Malashkevich, and P. S. Kim.** 2000. Structural characterization of the human respiratory syncytial virus fusion protein core. Proc Natl Acad Sci U S A **97:**14172-7.

Table 1. Primers used for PCR of HR regions

Primer	*Polarity*	*Sequence (5'- 3')*	*HR product*
973	+	GTGGATCCATCGAAGGTCGTCAATATAGA ATTAATGGTTTAG (SEQ ID NO: 41)	HR1
974	+	GTGGATCCATCGAAGGTCGTAATGCAAAT GCTGAAGC (SEQ ID NO: 47)	HR1b
975	-	GGAATTCAATTAATAAGACGATCTATCTG (SEQ ID NO: 43)	HR1, HR1a, HR1b
976	-	CGAATTCATTCCTTGAGGTTGATGTAG (SEQ ID NO: 44)	HR2
990	+	GCGGATCCATCGAAGGTCGTGATTTATCTC TCGATTTC (SEQ ID NO: 45)	HR2
1151	+	GTGGATCCAACCAAAAGATGATTGC (SEQ ID NO: 46)	HR1a, HR1c
1152	-	GGAATTCAATTGAGTGCTTCAGCATTTG (SEQ ID NO: 47)	HR1c

Table 2

Inhibition of cell-to-cell fusion

FCFW cells/FIPV infected		
	GST-HR1	**GST-HR2**
10 ng	+++	-
1 ng	+++	+
0.1ng	+++	++
0 ng	+++	+++

Syncytia formation +++

Table 3. Primers used for PCR of HR regions

Primer	*Polarity*	*Sequence (5'- 3')*	*product*
2006	+	GCGGATCCGCATATAGGTTCAATGG (SEQ ID NO: 48)	HR1
2007	-	CGAATTCATGTAATTAACCTGTCAA (SEQ ID NO: 49)	HR1, HR1a, HR1b
2008	+	GCGGATCCAACCAAAAACAAATCGC (SEQ ID NO: 50)	HR1a, HR1c
2009	+	GCGGATCCAACCAGAATGCTCAAGC (SEQ ID NO: 51)	HR1b
2010	-	CGAATTCATTGTTTAACAAGTGTGT (SEQ ID NO: 52)	HR1c
1998	+	CGAATTCACTCATATTTTCCCAATT (SEQ ID NO: 53)	HR2
1999	+	GCGGATCCGAGCTTGACTCATTCAA (SEQ ID NO: 54)	HR2-1, HR2-8, HR2-9, HR2-10
2064	+	GCGGATCCTTCAAAGAAGAGCTGGA (SEQ ID NO: 55)	HR2-2
2065	+	GCGGATCCCTGGACAAGTACTTCAA (SEQ ID NO: 56)	HR2-3
2066	+	GCGGATCCTTCAAAAATCATACATC (SEQ ID NO: 57)	HR2-4
2067	+	GCGGATCCACATCACCAGATGTTGA (SEQ ID NO: 58)	HR2-5
2068	+	GCGGATCCGTTGATCTTGGCGACAT (SEQ ID NO: 59)	HR2-6
2069	+	GCGGATCCGACATTTCAGGCATTAA (SEQ ID NO: 60)	HR2-7
1998	-	CGAATTCACTCATATTTTCCCAATT (SEQ ID NO: 53)	HR2-1 – HR2-7
2034	-	CGAATTCATTTAATATATTGCTCAT (SEQ ID NO: 61)	HR2-8
2070	-	CGAATTCACAATTCTTGAAGGTCAA (SEQ ID NO: 62)	HR2-9
2071	-	CGAATTCAGTCAATGAGTGATTCAT (SEQ ID NO: 63)	HR2-10
2072	+	GATCAGACTACAAGGATGACGATGACA AAG (SEQ ID NO: 64)	FLAG-tag
2073	-	GATCCTTTGTCATCGTCATCCTTGTAGT CT (SEQ ID NO: 65)	FLAG-tag

CLAIMS

What is claimed is:

1. A method for at least in part inhibiting anti-parallel coiled coil formation of a coronavirus spike protein of a coronavirus, said method comprising:

decreasing contact between heptad repeat regions of said coronavirus spike protein.

2. The method according to claim 1 wherein a peptide and/or a functional fragment and/or an equivalent thereof decreases contact between heptad repeat regions of said coronavirus spike protein.

3. The method according to claim 2 wherein the peptide and/or a functional fragment and/or an equivalent thereof comprises a heptad repeat region of a coronavirus spike protein.

4. The method according to claim 1, claim 2, or claim 3, wherein said heptad repeat region comprises an amino acid sequence of SARS HR2 and/or HR1 according to FIG. 1 (SEQ ID NOS: 23 & 118, respectively), and/or a functional fragment and/or a derivative thereof.

5. The method according to claim 1, wherein an antibody and/or a functional fragment and/or an equivalent thereof decreases contact between heptad repeat regions of said coronavirus spike protein.

6. The method according to claim 1, claim 2, claim 3, claim 4, or claim 5, wherein the coronavirus comprises a group 1 coronavirus.

7. The method according to claim 6, wherein the coronavirus comprises a feline corona virus.

8. The method according to claim 7, wherein the coronavirus comprises a feline infectious peritonitis (FIP) virus.

9. The method according to claim 6, wherein the coronavirus comprises a human corona virus.

10. The method according to claim 1, claim 2, claim 3, claim 4, or claim 5, wherein the coronavirus comprises a group 2 coronavirus.

11. The method according to claim 10, wherein said coronavirus comprises a mouse hepatitis virus (MHV).

12. A method according to claim 1, claim 2, claim 3, claim 4, or claim 5, wherein the coronavirus causes Severe Acute Respiratory Syndrome (SARS).

13. A method for inhibiting of coronavirus spike protein mediated cell to cell fusion, said method comprising:

decreasing contact between heptad repeat regions of said coronavirus spike protein.

14. A method of selecting a compound that binds to a heptad repeat region of a coronavirus spike protein, said method comprising:

contacting *in vitro* at least one heptad region of a coronavirus spike protein with a collection of compounds, and

measuring the formation of an anti-parallel coiled coil in said coronavirus spike protein.

15. A compound selected by the method of claim 14.

16. An antibody, functional fragment, and/or derivative thereof, said antibody, functional fragment, and/or derivative thereof capable of decreasing the contact between heptad repeat regions of a coronavirus spike protein.

17. A composition comprising:

the compound of claim 15, and/or

an antibody and/or a functional fragment and/or a derivative thereof, capable of decreasing the contact between heptad repeat regions of a coronavirus spike protein, and

a suitable diluent and/ or carrier.

18. A method of treating coronavirus infections in a subject, said method comprising:

providing to the subject the composition of claim 17.

19. A diagnostic kit for detecting coronavirus infection in a sample of a subject, said diagnostic kit comprising:

the compound of claim 15 or an antibody, functional fragment, and/or derivative thereof, said antibody, functional fragment, and/or derivative thereof capable of decreasing the contact between heptad repeat regions of a coronavirus spike protein, together with

means of detecting binding of said compound or antibody functional fragment, and/or derivative thereof to the coronavirus.

20. A diagnostic kit for detecting antibodies directed against coronavirus in a sample from a subject, said diagnostic kit comprising:

the compound according to claim 15, and

means for detecting binding of said compound to said antibodies.

21. A method of attenuating a coronavirus, said method comprising:

decreasing the contact between heptad repeat regions of the spike protein of said coronavirus.

22. An attenuated coronavirus having decreased contact between heptad repeat regions of the spike protein of said attenuated coronavirus.

23. The method according to claim 3 wherein said peptide comprises an amino acid sequence according to peptide sHR2-1, and/or sHR2-2, and/or sHR2-8, and/or sHR2-9 as depicted in FIG. 11B, and/or a functional fragment and/or an equivalent thereof.

24. A method for at least in part inhibiting a fusion of a coronavirus with a cell membrane, said method comprising decreasing binding of a fusion peptide with said cell membrane.

25. The method according to claim 24, wherein said fusion peptide comprises the amino acid sequence of SARS-CoV as depicted in FIG. 17.

26. The method according to claim 24, wherein a specific binding molecule for said fusion peptide decreases binding of a fusion peptide with said cell membrane.

27. The method according to claim 26, wherein said specific binding molecule is an antibody, functional fragment thereof, and/or derivative thereof.

ABSTRACT

The invention relates to the field of coronaviruses and diagnosis, therapeutic use, and vaccines therefor. Methods are shown for at least in part inhibiting anti-parallel coiled coil formation of a coronavirus spike protein which methods include decreasing the contact between heptad repeat regions of the coronavirus spike protein. The invention provides a peptide comprising a heptad repeat region of a coronaviral spike protein and/or a functional fragment and/or a derivative thereof. The invention also provides antibodies and compounds inhibiting coronaviral infection of cells, and/or cell-to-cell fusion. The invention also includes heptad repeat regions and a fusion peptide of SARS-CoV.

APPENDIX B

(VERSION OF SUBSTITUTE SPECIFICATION EXCLUDING CLAIMS WITH MARKINGS TO SHOW CHANGES MADE)

(Serial No. 10/750,411)

PATENT
Attorney Docket 2183-6265US

NOTICE OF EXPRESS MAILING

Express Mail Mailing Label Number: _____

Date of Deposit with USPS: _____

Person making Deposit: _____

APPLICATION FOR LETTERS PATENT

for

~~CORONA~~ CORONAVIRUS-LIKE PARTICLES COMPRISING FUNCTIONALLY DELETED GENOMES

Inventors:
Petrus J. M. Rottier
Cornelis A. M. de Haan
Bert J. Haijema
Berend J. Bosch

Attorney:
Allen C. Turner
Registration No. 33,041
TraskBritt, P.C.
P.O. Box 2550
Salt Lake City, Utah 84110
(801) 532-1922

TITLE OF THE INVENTION

~~CORONA~~ CORONAVIRUS-LIKE PARTICLES COMPRISING FUNCTIONALLY DELETED GENOMES

CROSS-REFERENCE TO RELATED APPLICATIONS

This application is a continuation-in-part of co-pending application, serial no. 10/714,534, filed November 14, 2003, and a continuation-in-part of co-pending application serial no. 10/414,256, filed April 14, 2003, which are both continuations of PCT International Patent Application No. PCT/NL/02/00318, filed ~~May 17 2002,~~ May 17, 2002, designating the United States of America, and published, in English, as PCT International Publication No. WO 02/092827 A2 on November 21, 2002, the contents of the entirety of all of which are incorporated herein by this reference.

TECHNICAL FIELD

The invention relates generally to biotechnology, and more specifically to the field of coronaviruses and diagnosis, therapeutic use and associated vaccines.

BACKGROUND

Coronavirions have a rather simple structure. They consist of a nucleocapsid surrounded by a lipid membrane. The helical nucleocapsid is composed of the RNA genome packaged by one type of protein, the nucleocapsid protein N. The viral envelope generally contains 3 membrane proteins: the spike protein (S), the membrane protein (M) and the envelope protein (E). Some coronaviruses have a fourth protein in their membrane, the hemaglutinin-esterase protein (HE). Like all ~~viruses~~ viruses, coronaviruses encode a wide variety of different gene products and proteins. Most important among these are obviously the proteins responsible for functions related to viral replication and virion structure. But besides these elementary ~~functions~~ functions, viruses generally specify a diverse collection of ~~proteins~~ proteins, the function of which is often still unknown but which are known or assumed to be in some way beneficial to the virus. These proteins may either be essential - operationally defined as being required for virus replication in cell culture - or dispensable. Coronaviruses constitute a family of large, positive-sense RNA viruses that usually cause respiratory and

intestinal infections in many different species. Based on antigenic, genetic and structural protein criteria they have been divided into three distinct groups: group I, II and III. Actually, in view of the great differences between the ~~groups~~ groups, their classification into three different genera is presently being discussed by the responsible ICTV Study Group. The features that all these viruses have in common are a characteristic set of essential genes encoding replication and structural functions. Interspersed between and flanking these ~~genes~~ genes, sequences occur that differ profoundly among the groups and that are, more or less, specific for each group.

To successfully initiate an infection, viruses need to overcome the cell membrane barrier. Enveloped viruses achieve this by membrane fusion, a process mediated by specialized viral fusion proteins. Most viral fusion proteins are expressed as precursor proteins, which are endoproteolytically cleaved by cellular proteases giving rise to a metastable complex of a receptor binding and a membrane fusion subunit.

SUMMARY OF THE INVENTION

The present invention provides methods and means to interfere with fusion of ~~corona~~ coronaviruses. According to the ~~invention~~ invention, after receptor binding at the cell membrane, the fusion proteins undergo a dramatic conformational transition. A hydrophobic fusion peptide becomes exposed and inserts into the target membrane. The free energy released upon subsequent refolding of the fusion protein to its most stable conformation is believed not only to facilitate the close apposition of viral and cellular membranes but also to effect the actual membrane merger (1, 46, 54).

~~SUMMARY OF THE INVENTION~~

The present invention further provides methods and means to use the biochemical and functional characteristics of the heptad repeat (HR) regions of the ~~corona~~ coronavirus spike proteins. ~~We show here~~The inventors show herein that peptides corresponding to the HR regions assemble into a thermostable, oligomeric, alpha-helical rod-like complex, with the HR1 and HR2 helices oriented in an anti-parallel manner.

Furthermore, we have found that HR2 of the ~~corona~~ coronavirus spike protein such as MHV-A59 spike protein is a strong inhibitor of both virus-cell and cell-cell fusion.

The invention also provides the amino acid sequences of the HR regions of a coronavirus belonging to another group such as Feline infectious peritonitis ~~(FIP)~~ virus (FIPV) spike protein, and of the inhibition of cell-to-cell fusion in FIPV infected cells by administration of HR2 of viruses such as FIPV. We demonstrate that the same mechanism is valid in different groups of coronaviruses.

The present invention also provides the amino acid sequences of the HR regions of the spike protein of a coronavirus, which causes a severe acute respiratory syndrome (SARS) in humans and which has been designated provisionally as SARS coronavirus (SARS-CoV). The inhibitory effect of SARS-CoV HR derived peptides on infection of cells by SARS-CoV is also disclosed, and peptides have been identified that can be used as a vaccine against SARS-CoV infections or for the preparation of a medicine against a SARS-CoV caused disease. In addition, this invention discloses the amino acid sequence of the fusion peptide of SARS-CoV. The fusion peptide can also be used as a vaccine against SARS-CoV infections or for the preparation of a medicament against a SARS-CoV caused disease.

The invention makes use of the discovery that in coronaviruses the energy necessary for the membrane fusion process is at least partly provided by the formation of an anti-parallel coiled coil structure by folding of the spike protein and interaction of the HR1 and HR2 repeat region. Decreasing the contact of the heptad repeat regions in the spike protein results in a less optimal fit of the coiled coil and thus in less energy for the fusion of membranes. Therefore, this invention teaches a method for at least in part inhibiting anti-parallel coiled coil formation of a coronavirus spike protein comprising decreasing the contact between heptad repeat regions of the protein. Of course, blocking the coiled coil formation by occupying the sequence of either HR1 or HR2 is a good way of decreasing, or even preventing coiled coil ~~formation,~~ formation.

The contact of the heptad repeat regions can be disturbed by a molecule or compound that binds to HR1 or HR2 and by binding to these regions, or in close proximity, the compound blocks the site for binding to another HR site. This will result in ~~decreasing~~ decreasing, or ~~inhibiting~~ inhibiting, the ability of the coronavirus to fuse with a membrane and

enter a cell. Of course, if binding of a compound occurs in the vicinity of these regions, contact of the heptad repeat regions may also be decreased and/or inhibited. Such a compound ~~may~~ may for ~~example~~ example, be a peptide and/or a functional fragment and/or an equivalent thereof with an amino acid sequence as shown in FIG. 1.

A functional fragment of a protein or peptide is defined as a part which has the same kind of biological properties in kind, not necessarily in amount. A "functional equivalent" of a peptide is defined as a ~~compound~~ compound, be it a peptide or proteinaceous or ~~non~~ nonproteinaceous molecule with essentially the same functional properties in kind, not necessarily in amount. A functional equivalent can be provided in many ways, for ~~instance~~ instance, through conservative amino acid substitution.

A person skilled in the art is well able to generate analogous equivalents of a protein. This ~~can~~ can, for ~~instance~~ instance, be done through screening of a peptide library. Such an equivalent has essentially the same biological properties of the protein or peptide in kind, not necessarily in amount.

Therefore, this invention teaches a method for at least in part inhibiting anti-parallel coiled coil formation of a coronavirus spike protein comprising decreasing the contact between heptad repeat regions of the protein, wherein the decreasing is provided by a peptide and/or a functional fragment and/or an equivalent thereof.

Decreasing the contact between heptad regions may also be provided by a peptide comprising a heptad repeat region of a coronaviral spike protein and/or a functional fragment and/or an equivalent thereof. Therefore, this invention provides a method to decrease and/or inhibit contact between heptad regions wherein the decreasing and/or inhibiting is provided by a peptide comprising a heptad repeat region of a coronaviral spike protein and/or a functional fragment and/or an equivalent thereof. The disclosure of the amino acid sequence of HR2 of SARS-CoV enables the production and/or selection of peptides comprising SARS-CoV HR2 of spike protein and/or a functional fragment and/or an equivalent thereof.

In another embodiment, such decreasing can be achieved by providing an antibody directed against a part of HR1 or HR2. The antibody will inhibit the binding of a heptad repeat region to another heptad repeat region, thus ~~preventing~~ preventing, at least in ~~part~~ part, the formation of an anti-parallel coiled coil. Of course, binding of an antibody to a region in

close proximity to the heptad region may also disturb the correct fit of the heptad repeat regions in a coiled coil. Therefore, the present invention teaches a method for at least in part inhibiting anti-parallel coiled coil formation of a coronavirus spike protein comprising decreasing the contact between heptad repeat regions of the protein, wherein the decreasing is provided by an antibody and/or a functional fragment and/or an equivalent thereof.

The present invention shows comparative data on the amino acid sequences of the HR1and HR2 region of a number of coronaviruses and of SARS coronavirus (FIG. 1). The human coronavirus HCV-229E and the feline infectious peritonitis virus (FIPV), which both belong to the group 1 ~~coronaviruses~~ coronaviruses, show an insertion of 14 amino acids in the HR1 and in the HR2 region, which the other ~~coronaviruses~~ coronaviruses, like mouse hepatitis virus and another human coronavirus (HCV-OC43) (group 2), and infectious bronchitis virus of poultry (group 3) and ~~SARS-CoV~~ SARS-CoV, do not have. This insertion of 14 amino acids in each heptad region may generate more electrostatic power for the fusion of a membrane, once the ~~coiled~~ coiled coil is formed, because the total length of each heptad alpha helix is elongated by 2 coils. The fact that FIPV and HCV-229E have these extra 2 coils per heptad repeat region may indicate that these viruses need extra energy to fuse their membrane with that of their host cell. Decreasing this energy by ~~inhibiting~~ inhibiting, at least in ~~part~~ part, the formation of a coiled coil will effectively decrease the penetrating power of the viruses. Therefore, the invention teaches a method ~~for~~ for, at least in ~~part~~ part, inhibiting anti-parallel coiled coil formation of a coronavirus spike protein comprising decreasing the contact between heptad repeat regions of the protein, wherein the coronavirus comprises a feline coronavirus and/or a human coronavirus, and/or a mouse hepatitis virus MHV and/or a SARS virus.

After infection of a cell by a coronavirus, the infected cell exhibits coronaviral spike protein on its surface. Coronaviral spike protein present on the cell membrane surface mediates the fusion of cell membranes of other cells, thus allowing cell-to-cell fusion and allowing the virus to passage from the infected cell to a neighboring cell without the need to leave the cell. An important step in decreasing viral infection of cells ~~is by~~ is preventing the cell-to-cell fusion. By providing a compound such as a peptide or an antibody that decreases and/or inhibits the contact of heptad regions, cell-to-cell fusion will be decreased and/or

inhibited. The present invention teaches a method for inhibiting coronavirus spike protein mediated cell-to-cell fusion, comprising decreasing and/or inhibiting the contact between heptad repeat regions of the spike protein.

The present invention also provides methods for selecting further inhibitors of coiled coil formation in ~~corona~~ coronaviruses. For example, the HR1 and HR2 peptides may be used *in vitro* to select binding compounds from libraries of molecules. Any compound that binds to at least part of an HR1 or HR2 peptide is selected and is used as an inhibitor of the formation of an anti-parallel coiled coil in a spike protein of coronavirus. Therefore, this invention teaches a method to select a compound binding to a heptad repeat region of a coronavirus spike protein, comprising contacting *in vitro* at least one heptad region of a coronavirus spike protein with a collection of compounds and measuring the formation of an anti-parallel coiled coil in the protein.

The present invention also teaches a compound selected by contacting *in vitro* at least one heptad region of a coronavirus spike protein with a collection of compounds and measuring the formation of an anti-parallel coiled coil in the protein. With this method, non-proteinaceous compounds, proteinaceous compounds and antibodies are selected for their capacity to bind to the heptad repeat regions. Of course, a functional fragment and/or derivative of an antibody may also bind to heptad repeat regions. Therefore, this invention also teaches an antibody or a functional fragment and/or derivative thereof, capable of decreasing and/or inhibiting the contact between heptad repeat regions of a coronavirus spike protein. The ~~above~~above-mentioned compounds and/or antibodies may be incorporated into a pharmaceutical composition with a suitable diluent and/or or carrier compound. Therefore, the invention teaches a pharmaceutical composition comprising the compound and/or the antibody or a functional fragment and/or derivative thereof, and a suitable diluent and/ or carrier. Administration of the pharmaceutical composition to a cell or a subject with a coronaviral infection will inhibit the infection of cells and at least in part decrease the coronaviral infection. Therefore, the invention teaches a method of treatment of coronavirus infections comprising providing to a subject the pharmaceutical composition.

In another embodiment, the compounds and/or antibodies may be used to detect the presence of coronavirus in a cell or in a subject by contacting a sample of the cells or of

the subject to the compound or the antibody and visualizing any binding of the coronavirus to the compound and/or the antibody. The visualizing may be performed by any method known in the art, for example by ELISA techniques or by fluorescence or histochemistry. Therefore, the present invention also teaches a diagnostic kit for detecting coronavirus infection in a sample of a subject comprising the compound or the antibody, further comprising a means of detecting binding of the compound or antibody to the coronavirus. In yet another embodiment, the compound may be used to measure antibody titers of a subject. This may be done to diagnose whether a subject is undergoing a coronaviral infection, or has undergone a coronaviral infection in the past. This may be useful, not only for diagnostic purposes, but also for assessing the possible risk of a subject for a coronaviral infection, and for evaluating vaccination efficiency and strategy. Therefore, the present invention also teaches a diagnostic kit for detecting coronavirus antibodies in a sample of a subject comprising the compound, further comprising a means of detecting binding of the compound to the antibodies.

In another embodiment, the amino acid sequence of the heptad repeat regions is manipulated by recombination, insertion, or deletion techniques that are known in the art. Such a manipulation of the coronaviral genome in or around the heptad repeat regions will result in decreased and/or inhibited contact of the heptad repeat regions; it will result in attenuation of the coronavirus. Therefore, the invention teaches a method to attenuate a coronavirus comprising decreasing and/or ~~inhibited~~ inhibiting the contact between heptad repeat regions of the spike protein of the coronavirus. The method enables the production of an attenuated coronavirus with a decreased contact between the heptad repeat regions. Therefore, the invention teaches an attenuated coronavirus characterized in that the contact between heptad repeat regions of the spike protein of the coronavirus is decreased and/or inhibited.

The invention also discloses a number of peptides derived from SARS-C0V HR2 region that inhibited infection of cells by ~~SARS-CoV, therefore,~~ SARS-CoV. Therefore, the present invention discloses a method for at least in part inhibiting anti-parallel coiled coil formation of a coronavirus spike protein comprising decreasing the contact between heptad repeat regions of the protein, wherein the peptide comprises an amino acid sequence according to peptide ~~sHR2-1,and/or~~ sHR2-1, (SEQ ID NO: 1) and/or sHR2-2, (SEQ ID NO: 2)

and/or sHR2-8 (SEQ ID NO: 3), and/or sHR2-9 (SEQ ID NO: 4) as described in ~~FIG. 11 B,~~ FIG. 11B, and/or a functional fragment and/or an equivalent thereof.

In another embodiment, the invention discloses amino acid sequences of the fusion peptide of SARS-CoV. Therefore, the present invention discloses a method for at least in part inhibiting anti-parallel coiled coil formation of a coronavirus spike protein comprising decreasing the contact between heptad repeat regions of the protein, for at least in part inhibiting a fusion of a coronavirus with a cell membrane comprising decreasing binding of a fusion peptide with the cell membrane. Furthermore, the present invention discloses ~~above~~ the above-described method, wherein the fusion peptide comprises the amino acid sequence of SARS-CoV as described in FIG. 17 (SEQ ID NO: 5).

Because the fusion peptide of SARS-CoV is disclosed, inhibition of fusion may be used to find and select molecules that specifically bind to the fusion protein. Therefore, the present invention discloses the ~~above~~ above-described method, wherein the decreased binding is provided by a specific binding molecule for the fusion peptide. The disclosed fusion peptide is used to select antibodies and/or a functional fragment and/or a derivative thereof that specifically bind ~~the~~ to the fusion peptide, according to well known techniques in the art, such ~~as~~ as, for ~~example~~ example, phage display. Therefore, the present invention also discloses a method for at least in part inhibiting anti-parallel coiled coil formation of a coronavirus spike protein comprising decreasing the contact between heptad repeat regions of the protein, for at least in part inhibiting a fusion of a coronavirus with a cell membrane comprising decreasing binding of a fusion peptide with the cell membrane, wherein the specific binding molecule is an antibody and/or a functional fragment and/or a derivative thereof.

BRIEF DESCRIPTION OF THE FIGURES

FIG. 1. (A) Schematic representation of the coronavirus spike protein structure. The glycoprotein has an N-terminal signal sequence (SS) and a transmembrane domain (TM) close to the C-terminus. Group 2 and 3 coronavirus spike proteins are proteolytically cleaved (arrow) ~~in~~ into an S1 and an S2 subunit, which are non-covalently linked. S2 contains two heptad repeat regions (shaded bars), HR1 and HR2, as indicated. (B) Sequence alignment

of HR1 and HR2 domains of the newly identified SARS-CoV (strain TOR2) (SEQ ID NOS: 6 and 7, respectively) with those of the group 1 coronaviruses FIPV (feline infectious peritonitis virus strain 79-1146) (SEQ ID NOS: 8 and 9, respectively) and HCoV-229E (human coronavirus strain 229E) (SEQ ID NOS: 10 and 11, respectively), the group 2 coronaviruses MHV-A59 (mouse hepatitis virus strain A59) (SEQ ID NOS: 12 and 13, respectively) and HCoV-OC43 (human coronavirus strain OC43) (SEQ ID NOS: 14 and 15, respectively), and the group 3 coronavirus IBV (infectious bronchitis virus strain Beaudette) (SEQ ID NOS: 16 and 17, respectively) (GenBank accession nos. P59594, VGIH79, VGIHHC, P11224, CAA83661 and P11223, respectively). Dark shading marks sequence identity while lighter shading represents sequence similarity. The alignment shows a remarkable insertion of exactly two heptad repeats (14 a.a.) in both HR1 ~~(SEQ ID NO:)~~ and HR2 ~~(SEQ ID NO:)~~ of HCoV-229E ~~(SEQ ID NO:)~~ (SEQ ID NOS: 10 and 11, respectively), and FIPV ~~(SEQ ID NO:)~~ (SEQ ID NOS. 8 and 9, respectively), a characteristic of all group 1 viruses. The predicted hydrophobic heptad repeat ~~'a' and 'd'~~ "a" and "d" residues are indicated above the sequence. Asterisks denote conserved residues, dots represent similar residues. The amino acid sequences of the HR1 derived peptides HR1 (SEQ ID NO: 18), HR1a (SEQ ID NO: 9), HR1b (SEQ ID NO: 20), HR1c (SEQ ID NO: 21), and a FLAG-tagged HR1 (Fl.HR1) (SEQ NO: 22) and of the HR2 derived peptides HR2 (SEQ ID NO: 23), HR2-1 (SEQ ID NO: 24), and a FLAG-tagged HR2 (Fl-HR2) (SEQ ID NO: 25) of SARS-CoV ~~(SEQ ID NO:)~~ used in this study are presented in italics below the alignments. N-terminal glycine and serine residues derived from the thrombin proteolytic cleavage site of the GST fusion protein are in parentheses.

FIG. 2. Hetero-oligomeric complex formation of HR1 and HR1a with HR2. (A) HR1 and HR2 on their own or as a preincubated equimolar (80 μM) mix were subjected to 15% tricine SDS-PAGE. Before gel loading, samples were either heated at 100°C or left at ~~RT.~~ room temperature. Positions of HR1, HR2 and HR1-HR2 complex are indicated on the left, while the positions of molecular mass markers are indicated at the right. (B) Same as (A) but with peptide HR1a instead of HR1.

FIG. 3. Temperature stability of HR1-HR2 complex. An equimolar mix of HR1 and HR2 (80 μM) was incubated at ~~RT~~ room temperature for 1 ~~h.~~ hour. Samples were

subsequently heated for 5 ~~min~~ minutes at the indicated temperatures in 1x tricine sample buffer and analyzed by SDS-PAGE in a 15% tricine gel, together with HR1 and HR2 alone. Positions of HR1, HR2 and HR1-HR2 complex are indicated on the left, while the molecular mass markers are indicated at the right.

FIG. 4. Circular dichroism spectra (mean residue ~~eliplicity)~~ ellipticity of the HR1 (25 μM; open square) peptide, the HR2 (25 μM; filled triangle) peptide, and of the HR1-HR2 complex (25 μM; filled square) in water at ~~RT.~~ room temperature. Note that the HR1 and HR2 spectra virtually coincide.

FIG. 5. Electron micrographs of HR1-HR2 complex.

FIG. 6. Proteinase K treatment of HR peptides. The peptides HR2, HR1, HR1a, HR1b and HR1c were subjected to Proteinase K either individually in solution or after mixing of the different HR1 peptides with HR2 at equimolar concentration followed by 1 ~~h~~ hour of incubation at 37°C. Proteolytic fragments were separated and purified by HPLC and characterized by mass spectrometry. Peptides are schematically indicated by bars. Hatched bars indicate the protease sensitive part(s) of the peptide. ~~N~~ N- and C-terminal position of the peptide and the amino acid numbering are indicated.

FIG. 7. Inhibition of virus-cell and cell-cell fusion by HR peptides. (A) Virus-cell inhibition by HR peptides using a luciferase gene expressing MHV. LR7 cells were inoculated with virus at an MOI of 5 in the presence of varying concentrations of peptide ranging from 0.4 - 50 μM. At 5 ~~h p.i.~~ hours post infection cells were lysed and luciferase activity was measured. (B) Inhibition of spike mediated cell-cell fusion by HR peptides. BSR T7/5 effector cells - BHK cells constitutively expressing T7 RNA polymerase (3), were infected with vaccinia virus for 1 ~~h~~ hour and subsequently transfected with a plasmid containing the S gene under a T7 promoter. Three hours post transfection, LR7 target cells transfected with a plasmid carrying the luciferase gene behind a T7 promoter, were added to the effector cells. Cells were incubated for another 4 ~~h~~ hours in the presence or absence of HR peptide. Cells were lysed and luciferase activity was measured.

FIG. 8. Schematic representation (approximately to scale) of the viral fusion proteins of six different virus families; MHV-A59 S (*Coronaviridae*), Influenza HA (*Orthomyxoviridae*), HIV-1 gp160 (*Retroviridae*), SV5 F, (*Paramyxoviridae*), Ebola Gp2

(*Filoviridae*) and Se*M*NPV F (*Baculoviridae*). Cleavage sites are indicated by triangles; the black bars represent the (putative) fusion peptides, the vertically hatched bars represent the HR1 domains and the horizontally hatched bars represent the HR2 domains. Transmembrane domains are indicated by the vertical, dashed lines. For each ~~polypeptide~~ polypeptide, the total length is given at the right.

FIG. 9. GST-FIPV fusion protein sequences of GST-HR1 (SEQ ID NO:—26) and GST-HR2 (SEQ ID NO:—27).

FIG. ~~10~~ 10. SARS nucleotide and deduced protein sequence as derived from the RT-PCR fragment (SEQ ID NO:—28).

FIG. 11. Inhibition of SARS-CoV infection by HR peptides. (A) VERO cells were mock infected or infected with SARS-CoV (MOI = 0.5) in the presence of the HR2-1 peptide (sHR2-1) at concentrations of 0, 5, or 25 μM and incubated in medium containing the same concentration of peptide. An infection in the presence of peptide (25 μM) corresponding to the HR2 domain of MHV (mHR2) was taken along as a negative control. At 16 ~~h p.i.~~ hours post infection, cells were fixed and SARS-CoV positive cells were visualized by immunofluorescence staining. The Table (panel B) shows amino acid sequences of HR2 (B1) (sHR2-1 through sHR2-10 and mHR2 (SEQ ID NOs:——1, 2, 29-33, 3, 4, 34, and 35, respectively) and HR1 (B2) (sHR1, sHR1a, sHR1b, and sHR1c (SEQ ID NOs:——36 through 39, respectively) derived peptides of SARS-CoV (SCV) and MHV and their EC_{50} values as determined in a 96 wells format infection inhibition assay. (EC_{50}: 50% inhibitory concentration; SD: standard deviation).

FIG. 12. Complex formation of SARS-CoV HR1 and HR2 peptides. (A).. Comparison of SARS-CoV and MHV. HR1 and HR2 peptides on their own or as a preincubated equimolar (100 μM) mixture were subjected to 15% Tricine SDS-PAGE. Just before loading onto the gel, some samples were heated at 100°C. (B) HR1-HR2 complex formation using FLAG-tagged and ~~non~~ nontagged SARS-CoV HR peptides. Samples of the individual peptides HR1 (1), HR2 (2), FLAG-tagged HR1 (F1) and FLAG-tagged HR2 (F2), and of preincubated mixtures of these peptides (1+2, F1+2, 1+F2 and F1+F2) were subjected to 15% Tricine SDS-PAGE. The positions of molecular mass markers are indicated at the left.

FIG. 13. Stoichiometry of peptides in HR1-HR2 complexes. (A) FLAG-tagged HR2 and ~~non-~~nontagged HR2 were mixed in different ~~ratio's~~ ratios and incubated with an equimolar amount of HR1 to allow complex formation for 3 ~~h~~ hours followed by analysis in a 10% Tricine SDS-PAGE. (B) FLAG-tagged HR1, ~~non-~~nontagged HR1 and a 1:1 mixture of the two peptides were incubated with an equimolar amount of HR2 for 3 ~~h~~ hours and subsequently analyzed in a 10% Tricine SDS-PAGE. (C) Acetonitrile was added to a concentration of 50% (v/v) to solutions of FLAG-tagged HR1 (100 μM), ~~non-~~nontagged HR1 (100 μM) or to a 1:1 mixture of these two solutions. After mixing and incubation for 5 ~~min,~~ minutes, the acetonitrile was evaporated and an equimolar amount of HR2 was added to allow complex formation. After 3 ~~h~~ hours samples were analyzed in a 10% Tricine SDS-PAGE. Only the part of the gel containing the complexes is shown. The positions of molecular mass markers are indicated at the left.

FIG. 14. Comparative temperature stabilities of HR1-HR2 complexes of SARS-CoV and MHV. Equal amounts of SARS-CoV and MHV HR1-HR2 complexes were pooled, subsequently incubated for 5 ~~min~~ minutes at the indicated temperatures in 1x Tricine sample buffer and analyzed directly by SDS-PAGE in a 15% Tricine gel. Positions of the HR1-HR2 complex of SARS-CoV and MHV are indicated on the right, while the molecular mass markers are indicated at the left.

FIG. 15. Circular dichroism spectra (mean residue ~~eliplicity~~ ellipticity Φ) of the HR1 (20 μM; filled square) peptide, the HR2 (20 μM; open square) peptide, and of the HR1-HR2 complex (20 μM; filled triangle) in water at ~~RT.~~ room temperature. Note that the three spectra virtually coincide.

FIG. 16. Proteolytic analysis of the HR1-HR2 complex. The peptides HR2 (SEQ ID NO:—40), HR1a (SEQ ID NO:—41) or preincubated equimolar mixtures of HR2 (SEQ ID NO:—40) with HR1a (SEQ ID NO:—41) or HR1c (SEQ ID NO:—42) were subjected to Proteinase K (pK) digestion and analyzed by RP HPLC (upper part). The peaks representing the protected fragments were purified by RP HPLC. The molecular masses of the protected fragments were determined by mass spectrometry (lower part), allowing the identification of the protease-resistant cores of the peptides. The molecular masses of the protected fragments

determined by mass spectrometry (Ms Mw) matched their predicted masses (Pred. Mw) within 1 Da.

FIG. 17. Hydrophobic domains in coronavirus spike proteins. The TMAP program was applied on a Clustal W alignment of nine coronavirus spike sequences (see Methods section). In the hydrophobicity plot obtained, the three predicted transmembrane domains are indicated by black bars (middle part). Arrows point to the corresponding hydrophobic regions in the schematic drawing of the spike protein (upper part), which represent the N-terminal signal sequence (SS), the C-terminal transmembrane anchor (TM) downstream of the HR2 domain, and the putative fusion peptide (FP) immediately upstream of the HR1 domain. In the bottom part of the figure the Clustal W multiple sequence alignment of this latter domain is shown for the nine coronavirus spike proteins (SEQ ID NOs:——43-49, 5, and 50, respectively).

DETAILED DESCRIPTION OF THE INVENTION

With a positive stranded RNA genome of 28-32 kb, the *Coronaviridae* are the largest enveloped RNA viruses. Coronaviruses exhibit a broad host range, infecting mammalian and avian species. They are responsible for a variety of acute and chronic diseases of the respiratory, hepatic, gastrointestinal and neurological systems (56).

Recently, coronavirus induced pneumonia (Severe Acute Respiratory Syndrome, SARS) has spread rapidly from China via Hong Kong to the rest of the world. The spike (S) protein is the sole viral membrane protein responsible for cell entry. It binds to the receptor on the target cell and mediates subsequent virus-cell fusion (6). Spikes can be seen under the electron microscope as clear, 20 nm large, bulbous surface projections on the virion membrane (14). The spike protein of mouse hepatitis virus (MHV-A59) is a 180 kDa heavily N-glycosylated type I membrane protein which occurs in a homodimeric (37, 66) or homotrimeric (16) complex. In most murine hepatitis strains, the S protein is cleaved intracellularly into an N-terminal subunit (S1) and a membrane anchored subunit (S2) of similar size, which are ~~non-~~noncovalently linked and have distinct functions. Binding to the MHV receptor (MHVR) (74) has been mapped to the N-terminal 330 amino acids (a.a.) of the S1 subunit (62), whereas the membrane fusion function resides in the S2 subunit (78). It

has been suggested that the S1 subunit forms the globular head while the S2 subunit constitutes the stalk-like region of the spike (15). Binding of S1 to soluble MHVR, or exposure to 37°C and an elevated pH (pH 8.0) induces a conformational change which is accompanied by the separation of S1 and S2 and which might be involved in triggering membrane fusion (21, 27, 60). Cleavage of the S protein into S1 and S2 has been shown to enhance fusogenicity (25, 61) but cleavage is not absolutely required for fusion (2, 26, 59, 61).

The ectodomain of the S2 subunit contains two regions with a 4,3 hydrophobic (heptad) repeat (15), a sequence motif characteristic of coiled coils. These two heptad repeat (HR) regions, designated here as HR1 and HR2, are conserved in position and sequence among the members of the three coronavirus antigenic clusters (FIG. 1). A number of studies have shown that the HR1 and HR2 regions are involved in viral fusion. First, a putative internal fusion peptide has been proposed to occur close to (7) or within (40) the HR1 region. Second, viruses with mutations in the membrane-proximal HR2 region exhibited defects in spike oligomerization and in fusion ability (39). Third, it has been suggested that the MHV-4 (JHM) strain can utilize both endosomal and nonendosomal pathways for cell entry but does not require acidification of endosomes for fusion activation (48). However, mutations found in murine hepatitis viruses which do require a low pH for fusion, appeared to map to the HR1 region (23).

HR regions appear to be a common motif in many viral fusion proteins (57). There are usually two of them; one N-terminal HR region (HR1) adjacent to the fusion peptide and a C-terminal HR region (HR2) close to the transmembrane anchor. Structural studies on viral fusion proteins reveal that the HR regions form a six-helix bundle structure implicated in viral entry (reviewed in ~~(18).~~ (18)). The structure consists of a homotrimeric coiled coil of HR1 domains in the exposed hydrophobic grooves of which the HR2 regions are packed in an anti-parallel manner. This conformation brings the N-terminal fusion peptide in close proximity to the transmembrane anchor. Because the fusion peptide inserts into the cell membrane during the fusion event, such a conformation facilitates a close apposition of the cellular and viral membrane (reviewed in (18)). Recent evidence suggests that the actual six-helix bundle formation is directly coupled to the merging of the membranes (46, 54). The similarities in the structures of the six-helix bundle complexes elucidated for influenza virus

HA (4, 11), human and simian immunodeficiency virus (HIV-1, SIV) gp41 (5, 8, 41, 63, 69, 76), Moloney murine leukemia virus typel (MoMLV) gp21 (19), Ebola virus GP2 (42, 68), human T-cell leukemia virus type I (HTLV-1) gp21 (32), Visna virus TM, (43), simian parainfluenza virus (SV5) F1 (1), and human respiratory syncytial virus (HRSV) F1 (80), all point to a common fusion mechanism for these viruses.

Based on structural similarities, two classes of viral fusion proteins have been distinguished (36). Proteins containing HR regions and an N-terminal or N-proximal fusion peptide are classified as class I viral fusion proteins. Class II viral fusion proteins (e.g., the alphavirus E1 and the flavivirus E fusion protein) lack HR regions and have an internal fusion peptide. Their fusion protein is folded in tight association with a second protein as a heterodimer. Here, fusion activation takes place upon cleavage of the second protein.

The coronavirus fusion protein (S) shares several features with class I virus fusion proteins. It is a type I membrane protein, synthesized in the ER, and is transported to the plasma membrane. It contains two heptad repeat sequences, one located downstream of the fusion peptide and one in close proximity to the transmembrane region.

However, despite its similarity to class I fusion proteins, there are several characteristics that make the coronavirus S protein exceptional. One is the absence of an N-terminal or even N-proximal fusion peptide in the membrane-anchored subunit. Another peculiarity is the relatively large sizes of the HR regions (~100 and ~40 a.a.). Third, cleavage of the S protein is not required for membrane fusion; rather, it does not occur at all in the group 1 coronaviruses. For these reasons, it is not likely to assume that coronavirus fusion protein is a class 1 fusion protein.

Heptad repeat regions play an important role in viral membrane fusion. Fusion proteins from widely disparate virus families have been shown to contain two such regions, one located close to the fusion peptide, the other generally in the vicinity of the viral membrane ((7); summarized in FIG. 8). Distances between the HR regions vary greatly, from some 50 a.a. as in HIV-1 to about 300 residues in *Spodoptera exigua* multicapsid nucleopolyhedrosis virus (71). The crystal structures resolved for influenza HA (4, 10, 75) HIV-1 and SIV gp41 (5, 8, 41, 63, 69, 76), MuMLV gp21 (19), Ebola virus GP2 (42, 68), HTLV-1 gp21 (32), Visna virus TM, (43), SV5 F1 (1), HRSV F1 (80) and NDV F (13) all

show a central trimeric coiled coil constituted by three HR1 regions. In some of these structures (e.g., HIV-1 and SIV gp41, SV5 F1, Ebola virus gp2, Visna virus TM and HRSV F1) a second layer of helices or elongated peptide chains was observed contributed by HR2 domains which were packed in an anti-parallel manner into the hydrophobic grooves of the HR1 coiled coil, forming a six-helix bundle. In the full-length protein, such a conformation brings the fusion peptide present at the N-terminus of HR1 close to the transmembrane region that occurs at the C-terminal of HR2. With the fusion peptide inserted in the cellular membrane and the transmembrane region anchored in the viral membrane, such a hairpin-like structure facilitates the close apposition of cellular and viral membrane and enables subsequent membrane fusion (reviewed in (18)). Combined with the findings that peptides derived from these HR domains can act as potent inhibitors of fusion (reviewed in (18)), the biological relevance of the heptad repeat regions in the viral life cycle is obvious. Our studies of the heptad repeat motifs in coronavirus spike protein presented here show that coronaviruses use coiled coil formation for membrane fusion and cell entry mechanisms comparable to some other viruses, probably allowing coronavirus spike proteins to be classified as class I viral fusion proteins (36).

The coronavirus (MHV-A59) derived HR peptides exhibited a number of typical class I characteristics. First of all, the purified HR1 and HR2 peptides assembled spontaneously into unique, homogeneous multimeric complexes. These complexes were highly stable surviving, for instance, high concentrations (2%) of SDS and high temperatures (70-80°C). The peptides apparently associate with great specificity into an energetically very favorable structure. Another typical feature was the observed secondary structure in the peptides. The CD spectra of both the individual and the complexed HR1 and HR2 peptides showed patterns characteristic of alpha-helical structure. Alpha-helix contents were calculated to be about 89% for the separate peptides and about 82% for their equimolar mixture. Consistent with these observations, the HR complex revealed a rod-like structure when examined by electron microscopy. The length of this structure (~14.5 nm) correlates well with the length predicted for an alpha-helix the size of HR1 (96 a.a.). Similar rod-like structures have been observed for other class I virus fusion proteins such as the influenza virus HA protein (12, 53), portions of the HIV-1 gp41 protein (70), and the Ebola

virus GP2 protein (67) but the length of the MHV-A59 derived structures is substantially larger. This is presumably even more so for type I coronaviruses which have an insertion of two heptad repeats (14 a.a.; see FIG. 1) in both HR regions. These insertions into otherwise conserved areas suggest these additional sequences to associate with each other in the HR1-HR2 complex thereby extending the alpha-helical complex by exactly four turns. The significance of the exceptional lengths of coronavirus HR complexes may be that the higher energy gain of their formation corresponds with higher energy requirements for membrane fusion by these viruses.

Another important characteristic of class I viral fusion proteins is the formation of a heterotrimeric six-helix bundle during the membrane fusion process, resulting in a close allocation of the fusion peptide and the transmembrane domain. Consistently, protein dissection studies using proteinase K demonstrated an anti-parallel organization of the HR1 and HR2 alpha-helical peptides in the MHV-A59 HR complex. So far, no fusion peptides have been identified in any coronavirus spike protein but predictions for MHV S have located such fusion sequences at (7) or in (40) the N-terminus of HR1. In both ~~cases~~ cases, an anti-parallel orientation of the HR1 and HR2 alpha helices ensures that the fusion peptide is brought into close proximity to the transmembrane region. Sequence analysis reveals that the ~~'e' and 'g'~~ "e" and "g" positions in the HR1 regions of all coronaviruses are primarily occupied by hydrophobic residues, unlike the ~~'e' and 'g'~~ "e" and "g" positions in the HR2 regions, which are mostly polar (see FIG. 1). The HR2 region also contains a strictly conserved N-linked glycosylation sequence, indicating its surface accessibility. Preliminary X-ray data on the HR1-HR2 complex show a six-helix bundle structure in the electron dense region (Bosch, B.J., Rottier, P.J.M, and Rey F.A., unpublished results). The combined observations suggest a packing analogous to the fusion proteins of other class I viruses (e.g., HIV, SV5), where the HR1 and HR2 peptides can form a six-helix bundle with the long HR1 peptide centered in the middle as a three-stranded ~~coiled~~ coiled coil with the hydrophobic ~~'a' and 'd'~~ "a" and "d" residues in its inner core. The shorter HR2 peptide packs with its apolar interface in the hydrophobic grooves of the HR1 coiled coil, which expose the mostly hydrophobic residues on 'e' and 'g' positions.

Peptides derived from the heptad repeat regions of retrovirus (28, 30, 38, 47, 49, 58, 72, 73) and paramyxovirus (29, 35, 51, 77, 79) fusion proteins have been shown to strongly interfere with the fusion activity of these proteins. We observed the same effect when we tested the HR2 peptide of the MHV-A59 spike protein. Using a recombinant luciferase-expressing MHV-A59, the peptide acted as an effective inhibitor of virus entry at micromolar concentrations. Cell-cell fusion inhibition was even more efficiently blocked by the peptide as tested in a cell fusion luciferase assay system. However, peptides derived from the HR1 region had no or only a minor effect on virus entry and syncytia formation. HIV-1 gp41 derived HR peptides that inhibit membrane fusion have been shown not to bind to the native protein or to the six-helix bundle. They can only bind to an intermediate stage of gp41 occurring during the fusion process (9, 20, 31). Repeated passage of HIV in the presence of the inhibitory peptide DP178, which is derived from the C-terminal gp41 HR region, resulted in resistant viruses containing mutations in the N-terminal HR region (52). Inhibition of membrane fusion by the MHV HR2 peptide most likely takes place during an intermediate stage of the fusion process by binding of the peptide to the HR1 region in the spike protein. This binding, which may occur before, during or after the association of the HR1 regions into the inner trimeric coiled coil, presumably inhibits the subsequent interaction with native HR2 and, consequently, membrane fusion. For the HIV-1 gp41 and SV5 F protein also peptides corresponding to the HR1 region show membrane fusion inhibition, supposedly by binding to the native HR2 region (29, 72). It has been reported previously for HIV-1 that the HR1 peptide aggregates in solution (38) and that its inhibitory activity could be enhanced by fusing it to a designed soluble trimeric coiled coil, making the HR1 peptide more soluble (17). The MHV-A59 HR1 peptide is soluble in water but appeared to precipitate in salt solutions (data not shown). This solubility feature may have obscured the inhibitory potency of our HR1 derived peptides and accounts for the negative results with these peptides in our fusion assays. The HR2 peptide (as well ~~as,~~ as soluble forms of HR1) provides powerful antivirals for the therapy of coronavirus induced diseases both in animals and man.

Membrane fusion mediated by class I fusion proteins is accompanied by dramatic structural rearrangements within the viral polypeptide complexes (18). Though little is known of the coronavirus membrane fusion process (for a review, see (22)), the occurrence of

conformational changes induced by various conditions has been described for MHV spikes (45). While MHV-A59 is quite stable at mildly acidic ~~pH~~ pH, it is rapidly and irreversibly inactivated at pH 8.0 and 37°C (60). Under these conditions the S1 subunit dissociates from the virions and the S2 subunit aggregates concomitantly resulting in the aggregation of the particles. Due to the structural rearrangements in the spike, virions can bind to liposomes and the S2 protein becomes sensitive to protease degradation (27). Similar conformational changes can apparently also be induced at pH 6.5 by the binding of spikes to the (soluble) MHV receptor (21, 27) as this interaction enhances liposome binding and protease sensitivity as well (27). Virion binding to liposomes is presumably caused by the exposure of hydrophobic protein surfaces or of the fusion peptide as a result of the conformational change. It appears that the structural rearrangements in the spikes, whether elicited by elevated pH or soluble receptor interaction, reflect the process that naturally gives rise to the fusion of viral and cellular membranes. Accordingly, cell-cell fusion induced by MHV-A59 was maximal at slightly basic pH (60).

A number of studies on the MHV spike protein have shown the importance of the HR regions in membrane fusion. Three codon mutations (Q1067H, Q1094H and L1114R) in or close to the HR1 region of the spike protein were found to be responsible for the low pH requirement for fusion of some MHV-JHM variants isolated from persistently infected cells (23). Analysis of soluble receptor-resistant variants of this virus also pointed to an important role in fusion activity of the HR1 region and suggested that it interacts somehow with the N-terminal domain (S1N330-III; a.a. 278-288) of the spike protein (44). In yet another MHV-JHM ~~variant~~ variant, a great reduction in cell-cell fusion was attributed to the occurrence of two mutations in the spike ~~protein~~ protein, one of which ~~again~~ was again located in the HR1 region (A1046V), the other (V870A) was located in a small ~~non~~ nonconserved HR region (N helix) close to the S cleavage site (33). Acidification resulted in a clear enhancement of fusion by this double mutant. It was speculated that the three predicted helical regions (N helix, HR1 and HR2) all collapse into a low-energy ~~coiled~~ coiled coil during the process of membrane fusion (33). Herein we provide evidence that the HR1 and HR2 regions indeed can form such a low-energy coiled coil. Studies with the MHV-A59 S protein showed that mutations introduced at ~~'a' and 'd'~~ "a" and "d" positions in an

N-terminal part of the HR1 region, a fusion peptide candidate, severely affected cell-cell fusion ability (40). This effect was not due to defects in spike maturation or cell surface expression. Finally, also codon mutations in the HR2 region were found to significantly reduce cell-cell fusion (39). Though these mutant spike ~~protein~~ proteins were apparently impaired in ~~oligomerization~~ oligomerization, their surface expression was hardly affected.

In conclusion, our structural and functional studies show that the coronavirus spike protein can be classified as a class I viral fusion protein. The protein has, however, several unusual features that set it apart. An important characteristic of all class I virus fusion proteins known so far, is the cleavage of the precursor by host cell proteases into a membrane-distal and a membrane-anchored subunit, an event essential for membrane fusion. Consequently, the hydrophobic fusion peptide is then located at or close to the newly generated N-terminus of the membrane anchored subunit, just preceding the HR1 region. In contrast, the MHV-A59 spike does not have a hydrophobic stretch of residues at the distal end of S2, but carries a fusion peptide internally at a location that has yet to be determined (7, 40). Unlike other class I fusion ~~proteins~~ proteins, cleavage of the S protein into S1 and S2 has been shown to enhance fusogenicity (25, 61) but not to be absolutely required (2, 26, 59, 61). Rather, spikes belonging to group 1 coronaviruses are not cleaved at all.

The invention is further explained by the use of the following illustrative examples.

Example ~~1~~ 1:

MATERIALS AND ~~METHODS~~ METHODS:

Plasmid ~~constructions.~~ constructions: For the production of peptides corresponding to amino acid residues 953-1048 (HR1), 969-1048 (HR1a), 1003-1048 (HR1b), 969-1010 (HR1c) and 1216-1254 (HR2) of the MHV-A59 spike protein, PCR fragments were prepared using as a template the plasmid pTUMS which contains the MHV-A59 spike gene (64). Primers were designed (see Table 1) to introduce into the amplified fragment an upstream *Bam*HI site, a downstream *Eco*RI site as well as a stop codon preceding the *Eco*RI site. The fragments corresponding to a.a. 953-1048 and 1216-1254 were additionally provided with sequences specifying a factor Xa cleavage site immediately downstream from the *Bam*HI site. Fragments were cloned into the *Bam*HI/*Eco*RI site of the pGEX-2T bacterial expression

vector (Amersham Bioscience) in frame with the GST gene just downstream of the thrombin cleavage site.

To establish a cell-cell fusion inhibition assay, the firefly luciferase gene was cloned under a T7 promoter and an EMCV IRES. The luciferase gene containing fragment was excised from the pSP-*luc*+ vector (Promega) by digestion with *Nco*I and *Eco*RV, treated with Klenow, and ligated into the *Bam*HI-linearized, Klenow-blunted pTN3 vector (65) yielding the pTN3-*luc*+ reporter plasmid.

Bacterial protein expression and ~~purification.~~ purification: Freshly transformed BL21 cells (Novagen) were grown in 2 x YT (yeast-tryptone) medium to log phase (OD600~1.0) and subsequently induced by adding IPTG (GibcoBRL) to a final concentration of 0.4 mM. Two hours ~~later~~ later, cells were pelleted, resuspended in 1/25 volume of 10 mM Tris (pH 8.0), 10 mM EDTA, 1 mM PMSF and sonicated on ice (5 times for 2 ~~min~~ minutes). Cell homogenates were centrifuged at 20,000 x *g* for 60 ~~min~~ minutes at 4°C. To each 50 ml of supernatant 2 ml glutathione-sepharose 4B (Amersham Bioscience; 50% v/v in PBS) was added and incubated overnight (O/N) at 4°C under rotation. Beads were washed three times with 50 ml PBS and resuspended in a final volume of 1ml PBS. Peptides were cleaved from the GST moiety on the beads using 20 U of thrombin (Amersham Bioscience) by incubation for 4 ~~h~~ hours at room temperature (RT). Peptides in the supernatant were purified by high pressure reversed phase chromatography (RP-HPLC) using a Phenyl-5PW RP column (Tosoh) with a linear gradient of acetonitrile containing 0.1% trifluoroacetic acid. Peptide containing fractions were vacuum-dried O/N and dissolved in water. Peptide concentration was determined by measuring the absorbance at 280 nm (24) and by BCA protein analysis (Micro BCA™ Assay Kit, Pierce).

Temperature stability of HR1-HR2 ~~complex.~~ complex: An equimolar mix of peptides HR1 and HR2 (80 µM each) in H_2O was incubated at ~~RT~~ room temperature for 1 ~~h.~~ hour. After addition of an equal volume of 2 x tricine sample buffer (0.125 M Tris pH 6.8, 4% SDS, 5% β-mercaptoethanol, 10% glycerol, 0.004 g bromophenol blue) (55), the mixtures were either left at ~~RT~~ room temperature or heated for 5 ~~min~~ minutes at different temperatures and subsequently analyzed by SDS-polyacrylamide gel electrophoresis (PAGE) in 15% tricine gel (55).

CD ~~spectroscopy.~~ spectroscopy: CD spectra of peptides (25 μM in H_2O) were recorded at ~~RT~~ room temperature on a Jasco J-810 spectropolarimeter, using a 0.1 mm path length, 1 nm bandwidth, 1 nm resolution, 0.5 ~~s~~ second response time and a scan speed of 50 nm/min. The alpha-helix content was calculated using the program CDNN (http://bioinformatik.biochemtech.uni-halle.de/cd_spec/).

Electron ~~Microscopy.~~ Microscopy: A preincubated equimolar mix of the peptides HR1 and HR2 was subjected to size-exclusion chromatography (Superdex™ 75 HR 10/30, Amersham Pharmacia Biotech). A sample from the HR1-HR2 peptide complex containing fraction was adsorbed onto a discharged carbon film, negatively stained with a 2% uranyl acetate solution and examined with a Philips CM200 microscope at 100 kV.

Proteinase K ~~treatment.~~ treatment: Stock solutions (1 mM) of the peptides HR1, HR1a, HR1b, HR1c and HR2 in water were diluted to 80 μM in PBS. Peptides on their own (80 μM) or after preincubation for 1 ~~h~~ hour at 37°C with HR2 (80 μM each) were subsequently subjected to proteinase K digestion (1% wt/wt, proteinase K/peptide) for 2 ~~h~~ hours at 4°C. Samples were immediately subjected to tricine SDS-PAGE analysis. Protease resistant fragments were also separated and purified by RP HPLC and characterized by mass spectrometry.

Virus-cell fusion ~~assay.~~ assay: The potency of HR peptides in inhibiting viral infection was determined using a recombinant MHV-A59, MHV-EFLM that expresses the firefly luciferase gene (C.A.M. de Haan and P.J.M. Rottier, manuscript in preparation). LR7 cells (34) were maintained as monolayer cultures in Dulbecco's modified Eagle's medium (DMEM) supplemented with 10% fetal calf serum (FCS; GIBCO BRL). LR7 cells grown in ~~96-wells~~ 96-well plates were inoculated with MHV-EFLM in DMEM at a multiplicity of infection (MOI) of 5 in the presence of varying concentrations of peptide ranging from 0.4 - 50 μM. After 1 ~~h,~~ hour, cells were washed with DMEM and medium was replaced with DMEM containing 10% FCS. At 5 ~~h~~ hours post infection (p.i.) cells were harvested in 50 μl 1x Passive Lysis buffer (Luciferase Assay System, Promega) according to the manufacturer's protocol. Upon mixing of 10 μl cell lysate with 40 μl substrate, luciferase activity was measured using a Wallac Betalumino meter.

Cell-cell fusion ~~assay.~~ assay: $2x10^6$ LR7 cells, used as target cells, were washed with DMEM and overlaid with transfection medium consisting of 0.2 ml DMEM containing 10 µl of lipofectin (Life Technologies) and 4 µg of the plasmid pTN3-*luc*+. After 10 ~~min~~ minutes at ~~RT,~~ room temperature, 0.8 ml DMEM was added and incubation was continued at 37°C. BSR T7/5 cells - BHK cells constitutively expressing T7 RNA polymerase (3); a gift from Dr. K.K. Conzelmann - were grown in BHK-21 medium supplemented with 10% FCS, 100 IU of penicillin/ml and 1 mg/ml geneticin (GIBCO BRL). $1x10^4$ BSR T7/5 cells, designated as effector cells, were infected in ~~96-wells~~ 96-well plates with wild-type vaccinia virus at an MOI of 1 in DMEM at 37°C. After 1 ~~h,~~ hour, the cells were washed with DMEM and incubated for 3 ~~h~~ hours at 37°C with transfection medium consisting of 50 µl DMEM containing 1 µl lipofectin and 0.2 µg of the plasmid pTUMS (65), which carries the MHV-A59 spike gene under the control of a T7 promoter. Then, $3x10^4$ of target cells in 100µl DMEM were added and the cells were incubated for another 4 ~~h~~ hours in the presence or absence of HR peptide. Cells were lysed and luciferase activity was measured as mentioned above.

~~RESULTS~~RESULTS:

HR1 and HR2 regions in coronavirus spike ~~proteins.~~ proteins:

The S2 subunit ectodomain of coronaviruses contains two heptad repeat domains HR1 and HR2, which are conserved in sequence and position (15) (diagrammed in FIG. 1A). HR2 is located adjacent to the transmembrane domain while HR1 occurs at about 170 a.a. upstream of HR2. FIG. 1B shows a protein sequence alignment of the HR1 and HR2 regions for 6 coronaviruses from the three antigenic clusters. The sequence alignment reveals a remarkable insertion of exactly two heptad repeats (14 a.a.) in both the HR1 and the HR2 domain of the spike protein of the group 1 coronaviruses HCV-229E (human coronavirus strain 229E) and FIPV (feline infectious peritonitis virus strain) ~~79-1146).~~ 79-1146. Another characteristic feature is that the length of the linker region between the HR2 region and the transmembrane region is strictly conserved in all coronavirus spike proteins.

HR1 and HR2 can form an hetero-oligomeric ~~complex.~~ complex:

To study the heptad repeat regions in the S2 subunit of MHV-A59, peptides corresponding to the heptad repeat residues 953-1048 (HR1), 969-1048 (HR1a), 969-1048 (HR1b), 969-1003 (HR1c) and 1216-1254 (HR2) (FIG. 1B) were produced in bacteria as GST fusion proteins. Peptides were affinity purified using glutathione-sepharose beads, proteolytically cleaved from the resin and purified to homogeneity by reversed-phase HPLC. Masses of the peptides, as determined by mass spectrometry, matched their predicted Mw (HR1, 10,873 Da; HR1a, 8,653 Da; HR1b, 5,631 Da; HR1c, 4,447 Da; and HR2, 5,254 Da). To study an interaction between the two HR regions, the purified peptides HR1 and HR2 were incubated alone (80 μM) or in an equimolar (80 μM each) mixture for 1 ~~h~~ hour at 37°C and the samples were subjected to SDS-PAGE either directly or after heating for 5 ~~min~~ minutes at 95°C (FIG. 2A). While the peptides migrated according to their molecular weight after separate incubation, most of the protein of the preincubated mixture of HR1 and HR2 migrated as a higher molecular weight complex with a slightly lower mobility than the 29 kDa marker. Upon heating, the complex dissociated giving rise to the individual subunits HR1 and HR2. We also tested the other HR1 peptides for interaction with HR2. While we did not observe complexes upon mixing of HR2 with HR1b or HR1c (data not shown), a higher molecular weight species co migrating with the 29 kDa marker was found when HR1a was incubated with HR2 (FIG. 2B), though the extent of complex formation appeared to be lower than with peptide HR1. Higher molecular weight species were not seen. The results indicated that the HR1 region contains the information to associate with the HR2 region into a hetero-oligomeric complex and that this complex was stable in the presence of 2% SDS.

HR1-HR2 complex is highly temperature ~~resistant.~~ resistant:

Next, we determined the stability of the HR1-HR2 complex at increasing temperatures. An equimolar (80 μM each) mix of the two peptides was again incubated for 1 ~~h~~ hour at 37°C and subsequently heated for 5 minutes at different temperatures in 1x tricine sample buffer or left at ~~RT.~~ room temperature. The complexes were analyzed by SDS-PAGE in 15% gel. As FIG. 3 demonstrates, the high molecular weight complexes remained intact up to 70°C, dissociated partly at 80°C and fully at 90°C. The stability of the complex at high temperatures

indicates that the peptides are held together by strong interaction forces in an energetically favorable conformation.

HR1, HR2 and the HR1-HR2 complex are highly ~~α-helical.~~ α-helical:

The secondary structure of the HR peptides was examined by circular dichroism. The CD spectra of HR1, HR2 and of an equimolar mixture of HR1 and HR2 were recorded (FIG. 4). The spectra showed clear minima at 208 nm and 222 nm, which is characteristic of alpha-helical structure. Calculations revealed that the alpha-helical contents of the individual HR1 and HR2 peptides and of the mixture of the two peptides were 89.2%, 89.3% and 81.9%, respectively.

The HR1-HR2 complex has a rod-like ~~structure.~~ structure:

The overall shape of the HR1-HR2 complex was examined by electron microscopy. Complexes were purified and viewed after negative staining. Electron micrographs revealed rod-like structures (FIG. 5). Based on measurements of 40 ~~particles~~ particles, an average length of 14.5 nm (± 2 nm) was calculated. This length is consistent with an alpha-helix of approximately 90 a.a. in length, which corresponds approximately to the predicted length of the HR1 coiled coil region. Similar rod-shaped complexes have been reported for the influenza virus HA protein (12, 53), for portions of the HIV-1 gp41 protein (70) and for the Ebola virus GP2 protein (67).

HR1 and HR2 helices associate in an anti-parallel ~~manner.~~ manner:

The relative orientation and position of HR2 with respect to HR1 in the complex was examined by limited proteolysis using proteinase K in combination with mass spectrometry. Complexes were generated by incubation of the HR2 peptide with each of peptides HR1, HR1a, HR1b and HR1c. The reaction mixtures as well as the individual peptides were then treated with proteinase K. Samples from each reaction were analyzed by tricine SDS-PAGE (data not shown). Using ~~RP HPLC~~ RP HPLC, the protease resistant fragments were purified and their molecular weight (MW) was determined by mass spectrometry, which allowed us to identify the protease resistant cores of the peptides. For

each protease resistant core a unique amino acid composition could be deduced that allowed the unequivocal identification of the peptides in the different samples. FIG. 6 gives a schematic overview of the proteinase K resistant fragments. Digestion of HR1 alone left a protease-resistant fragment with ~~a~~ an MW of 6,801 Da corresponding to residues 976-1040. Although CD spectra had indicated a folded structure, HR2 was completely degraded by proteinase K. However, in the presence of ~~HR1~~ HR1, HR2 was fully protected from proteolytic degradation. HR2 was able to rescue 18 additional residues at the ~~N~~ N-terminus of HR1, leaving a fragment of 8,675 Da corresponding to residues 958-1040.

Proteolysis of the HR1a peptide alone generated the same fragment (residues 976-1040) as obtained with HR1. In the HR1a-HR2 mixture, the HR2 peptide was completely protected against degradation by HR1a, while HR2 fully shielded the N-terminus of HR1a for proteolysis, including the glycine and serine residues originating from the thrombin cleavage site.

Although a higher molecular weight species could not be detected by tricine SDS-PAGE (data not shown), the protease treatment of the HR1c-HR2 complex left a protease resistant core. HR1c was fully sensitive for proteinase K, but was completely protected in the presence of HR2. HR2 itself was partly protected against proteolysis by HR1c, yielding a fragment of 3,583 Da that represents residues 1225-1254. Importantly, this HR2 fragment has an intact C-terminus but is degraded at its N-terminus. HR1c has the same N-terminus as HR1a but is truncated at its C-terminus. Thus, its inability to protect the HR2 N-terminus combined with the full protection provided by HR1a implies an anti-parallel association of the HR1 and HR2 helices in the hetero-oligomeric complex. The peptide HR1b was fully sensitive to proteinase K both by itself and when mixed with HR2. HR1b could not prevent proteolysis of HR2 either. Altogether, the proteolysis results suggest the anti-parallel association of HR2 and HR1 to occur in the middle part of HR1.

HR2 strongly inhibits viral entry and syncytium ~~formation.~~ formation:

The formation of stable HR complexes is supposedly an essential step in the process of membrane fusion during viral cell entry. Thus, we evaluated the potency of our HR peptides in inhibiting MHV ~~entry~~ entry, making use of a recombinant MHV-A59, MHV-EFLM that

expresses the firefly luciferase reporter gene. Cells were inoculated with MHV-EFLM in the presence of different concentrations of the peptides HR1, HR1a, HR1b, HR1c and HR2. After 1 ~~h,~~ hour, the cells were washed and culture medium without peptide was added. At 4 ~~h~~ hours ~~p.i.~~ post infection, ~~i.e.~~ i.e., before syncytium formation takes place, cells were lysed and tested for luciferase activity (FIG. 7A). HR1, HR1a and HR1b were not able to inhibit virus entry up to concentrations of 50 μM. In contrast, HR2 blocked viral entry in a concentration-dependent manner inhibition being almost complete at a concentration of 50 μM.

We also studied the ability of the HR peptides in blocking cell-cell fusion. To this end we established a sensitive fusion assay based on the co-culturing of BHK cells expressing the bacteriophage T7 polymerase as well as the MHV-A59 spike protein, with murine L cells transfected with a plasmid carrying a luciferase gene cloned behind a T7 promoter. Fusion of the cells was determined by measuring luciferase activity. The effects of adding the HR peptides during the co-culturing of the cells are compiled in FIG. 7B. The HR2 peptide again appeared to be a potent inhibitor able to efficiently block cell-cell fusion. A 1000x reduction in luciferase activity was measured at a concentration of 10 μM, whereas essentially no activity was observed at a concentration of 50 μM. Of the HR1 peptides only the HR1b peptide had a minor effect at the highest concentration of 50 μM.

Example ~~2~~ 2:

Inhibition of cell-cell fusion after FIPV ~~infection~~ infection:

FCWF cells were infected with FIPV strain 79-1146 with an moi of 1. 1 hour after infection the cells were washed and medium was replaced by medium containing the GST-FIPV fusion proteins at different concentrations. 8 hours after infection, cells were fixed and scored for syncytia formation (see, Table 2). The amino acid sequence of HR1 and HR2 of FIP is shown in ~~FIG.9~~ FIG. 9.

Example ~~3~~ 3:

Inhibition of SARS-CoV infection of Vero cells by peptides derived from the HR1 and/or HR2 region of ~~SARS-CoV.~~ SARS-CoV:

Material and ~~methods~~ methods:

Plasmid ~~constructions.~~ constructions: For the production of peptides corresponding to the HR1 and HR2 regions of the SARS-CoV spike protein, PCR fragments were prepared using as a template a SARS-CoV (strain 5688, Kuiken) cDNA covering the S gene. Primers were designed (see Table 3) to introduce into the amplified fragment an upstream *Bam*HI site, a downstream *Eco*RI site as well as a stop codon preceding the *Eco*RI site. Fragments were cloned into the *Bam*HI/*Eco*RI site of the pGEX-2T bacterial expression vector (Amersham Bioscience) in frame with the GST gene just downstream of the thrombin cleavage site. For the production of HR peptides with an N-terminal hydrophilic FLAG-tag (DYKDDDDK) a primer dimer (Table 3) containing the FLAG-tag encoding sequence was cloned into the *Bam*HI site of the pGEX-2T vector, thereby knocking out the 5' *Bam*HI site. The resulting vector was used to clone the HR1 and HR2 PCR products of SARS-CoV spike gene into the *Bam*HI/*Eco*RI site.

Bacterial protein expression and ~~purification.~~ purification: Freshly transformed BL21 cells (Novagen) were grown in 2 x YT (yeast-tryptone) medium to log phase (OD600 ~1.0) and subsequently induced by adding IPTG (GibcoBRL) to a final concentration of 0.4 mM. Two hours ~~later~~ later, cells were pelleted, resuspended in 1/25 volume of 10 mM Tris (pH 8.0), 10 mM EDTA, 1 mM PMSF, and sonicated on ice (5 times for 2 ~~min~~ minutes). Cell homogenates were centrifuged at 20,000 x *g* for 60 ~~min~~ minutes at 4°C. To each 50 ml of ~~supernatant~~ supernatant, 2 ml glutathione-sepharose 4B (Amersham Bioscience; 50% v/v in PBS) was added and the suspensions were incubated overnight (O/N) at 4°C under rotation. Beads were washed three times with 50 ml PBS and resuspended in a final volume of ~~1ml~~ 1 ml PBS. Peptides were cleaved from the GST moiety on the beads using 20 U of thrombin (Amersham Bioscience) by incubation for 4 ~~h~~ hours at ~~RT.~~ room temperature. Peptides in the supernatant were purified by reversed phase high pressure liquid chromatography (RP HPLC) using a Phenyl-5PW RP column (Tosoh) with a linear gradient of

acetonitrile containing 0.1% trifluoroacetic acid. Peptide containing fractions were vacuum-dried O/N and dissolved in water. Peptide concentrations were determined by measuring the absorbance at 280 nm (Gill and von Hippel 1989) and by BCA protein analysis (Micro BCA™ Assay Kit, Pierce).

Inhibition of SARS-CoV ~~infection.~~ infection:

Vero 118 cells were maintained in Iscove's modified Dulbecco's medium (IMDM; Biowhittaker, Belgium) supplemented with 5% fetal bovine serum (FBS; Greiner), penicillin (100 U/ml), streptomycin (100 µg/ml), and 2 mM L-glutamine. The initial experiments were performed on Vero 118 cells grown on cover slips in 24 well plates ($2x10^5$ ~~cells/ well)~~ cells/well) at 37°C. Cells were inoculated (MOI = 0.5) in the presence of HR peptide at different concentration (25, 5 and 0 µM). After 1 ~~h,~~ hour, the inoculum was removed, the cells were washed twice with IMDM and the cells were overlaid with IMDM containing 5% FBS and the peptide at similar concentration as used in the inoculum. After O/N incubation, plates were washed twice with PBS and fixed by 4% formaldehyde for 15 ~~min~~ minutes and 70% ethanol plus ~~0,5%~~ 0.5% H_2O_2 for 15 ~~min~~ minutes at ~~RT~~ room temperature. After washing the plates twice with PBS + 0.5% Tween-20 and twice with PBS, the cover slips were incubated with a human polyclonal reconvalescent ~~serum(1: 50)~~ serum (1:50) for 1 ~~hr~~ hour at 37°C. FITC labeled ~~anti~~ antihuman serum was used as a conjugate in a 1:300 dilution. Pictures of FITC fluorescent cells were taken using a Olympus camera mounted on a Leitz microscope.

The second set of inhibition experiments was performed on Vero 118 cells in 96 well plates (10^4 ~~cells/ well).~~ cells/well). Cells were infected in triplicate with 100 $TCID_{50}$ of SARS-CoV (strain 5688, fourth passage) in the presence of various peptide concentrations, ranging from 0.4 µM to 50 µM, for 1 ~~h~~ hour at 37°C in a CO_2 incubator. Cells were then washed twice with IMDM and the medium was replaced with IMDM containing 5% FBS. After incubation for 9 ~~h,~~ hours, plates were washed twice with PBS and fixed by 4% formaldehyde for 15 ~~min~~ minutes and 70% ethanol plus 0.5% H_2O_2 for 15 ~~min~~ minutes at ~~RT.~~ room temperature. After washing the plates twice with PBS + 0.5% Tween-20 and twice with PBS, the fixed and permeabilized cells were incubated with a ferret polyclonal

antiserum (1:40) for 1 ~~hr~~ hour at 37°C. Horse radish peroxidase (HRP) labeled goat-anti-ferret antibodies (DAKO, USA) were used as a conjugate in a 1:50 dilution. Reaction was developed with 3-amino-9-ethylcarbazole (AEC; Sigma, Zwijndrecht) according to the manufacturer's instructions. SARS-CoV positive cells were counted using the light microscope and the effective peptide concentration at which 50% of the infection was inhibited (EC_{50}) was determined. Inhibition of MHV by HR peptides was tested as described above but using LR7 cells (Kuo, Godeke et al. 2000) rather then VERO 118 cells. IPOX detection of MHV positive cells was carried out by using a rabbit polyclonal antibody against MHV (1:300) (Rottier, Armstrong et al. 1985) in combination with a HRP swine-anti rabbit antibody (1:300) (DAKO, USA). Experiments were performed in triplicate, and carried out in duplicate.

Temperature stability of SARS-CoV and MHV HR1-HR2 ~~complex.~~ complex: Equimolar mixes of HR1 and HR2 peptides (100 μM each) of SARS-CoV and MHV were incubated in parallel at ~~RT~~ room temperature for 3 ~~h,~~ hours, to allow HR1-HR2 complex formation. 25 μl of each mix was pooled and an equal volume of 2 x Tricine sample buffer (0.125 M Tris pH 6.8, 4% SDS, 5% β-mercaptoethanol, 10% glycerol, 0.004 g bromophenol blue) ~~(55)~~ (55) was added. The mixtures were either left at ~~RT~~ room temperature or heated for 5 ~~min~~ minutes at different temperatures and subsequently analyzed by SDS-polyacrylamide gel electrophoresis (PAGE) in 15% Tricine gel ~~(55)~~ (55).

CD ~~spectroscopy.~~ spectroscopy: CD spectra of the HR1 and HR2 peptides (20 μM in H_2O) or a preincubated equimolar mix of HR1 and HR2 (20 μM each in H_2O) were recorded at ~~RT~~ room temperature on a Jasco J-810 spectropolarimeter, using a 0.1 mm path length, 1 nm bandwidth, 1 nm resolution, 0.5 ~~s~~ second response time and a scan speed of 50 nm/min. The alpha-helical content of the peptides was calculated using the program k2d (http://www.embl-heidelberg.de/~andrade/k2d/).

Proteinase K~~—treatment.~~ treatment: Stock solutions (250 μM) of the peptides HR1a, HR1c and HR2 in water were diluted to 100 μM in 50 mM Tris pH 7.0. Peptides on their own (100 μM) or HR1-HR2 mixtures (100 μM each) preincubated for 3 ~~h~~ hours at 37°C were subjected to proteinase K digestion (1% wt/wt, proteinase K/peptide) for 2 ~~h~~ hours at 4°C. Protease resistant fragments were separated and purified by RP HPLC and characterized by mass spectrometry.

~~Results~~**Results:**

HR regions in the SARS-CoV spike ~~protein~~ protein:

As shown by the alignment in FIG. 1, two heptad repeat (HR) regions are present in the C-terminal S2 domain of the SARS-CoV spike protein as they were detected before in other coronavirus spike proteins (15). One region (HR2) is located adjacent to the transmembrane domain, the other (HR1) is located some 170 residues upstream. In all coronaviruses, HR1 is consistently larger than HR2. However, the group 1 coronaviruses show a remarkable insertion of two heptad repeats (14 aa) in both HR regions. This insertion is lacking in the SARS-CoV HR regions. The HR2 region of SARS-CoV contains three conserved N-glycosylation sites (N-X-S/T; FIG. 1B).

HR peptides and their infection inhibitory ~~activities~~ activities:

Peptides corresponding to the HR regions were expressed using the bacterial GST expression and purification system. They were purified to homogeneity using RP HPLC and their molecular masses were verified by mass spectrometry. Peptides were subsequently tested for their inhibitory potency in an infection inhibition assay. VERO cells were inoculated with SARS-CoV (MOI 0.5) in the absence or presence of different concentrations of a particular peptide and the extent of infection was evaluated using an indirect immunofluorescence assay. As shown in FIG. 11A, for one of the initial peptides tested, HR2-1, a clear concentration dependent inhibition of SARS-CoV infection could be observed. This effect was sequence specific as no inhibition was seen with a corresponding peptide derived from the HR2 region of MHV (mHR2), known to block MHV infection.

To study the sequence dependence and to optimize the efficacy of the ~~inhibition~~ inhibition, we prepared two sets of ~~peptides~~ peptides, the sequences of which are compiled in FIG. 10B. One set consisted of HR2-1 based peptides: a series of peptides with increasing 4-residue N-terminal truncations (HR2-2 - HR2-7), one peptide with a 4-residue C-terminal extension (HR2-8) and two peptides with 4- and 8-residue C-terminal truncations (HR2-9 and HR2-10, respectively). The other set consisted of peptides corresponding to the HR1 region, with peptide HR1 comprising almost the entire heptad repeat region and peptides HR1a-c representing N-terminal and C-terminal truncations thereof. These peptides were tested similarly, but the infection levels were now determined in a technically different format using immune peroxidase staining followed by an automated read-out of the percentage of infected cells. FIG. 10B shows the EC_{50} values obtained, ~~i.e.~~ i.e., the concentrations calculated to cause a 50% reduction of infection. It is clear that only slight truncations at either side of the HR2-1 peptide are tolerated without loss of inhibitory activity. Actually, shortening HR2-1 just by 4 residues at the N-terminal (HR2-2) or the C-terminal side (HR2-9) resulted in significantly enhanced inhibition. The most effective peptide of the panel was HR2-8, which carried the C-terminal 4-residue extension. It had an EC_{50} value of 17 μM. The inhibition efficiency of this peptide was clearly lower than that of an HR2 peptide of MHV, mHR2, which had an EC_{50} value of 0.9 μM when tested in the MHV infection system. Of the panel of HR1 derived peptides none showed any measurable inhibitory effect on SARS-CoV infection under the conditions used in this ~~experiment.~~ experiment.

HR1-HR2 complex ~~formation~~ formation:

We have previously shown by Tricine SDS-PAGE analysis that the HR1 and HR2 peptides of the MHV S protein, when mixed together, assemble into an oligomeric complex that is resistant to 2% SDS, the SDS concentration used in this analysis. By the same approach we observed that the HR1 and HR2 peptides of the SARS-CoV spike protein behave likewise. As shown in FIG. 12A for equimolar mixtures of similar HR peptides from both viruses, SDS-stable oligomeric complexes are formed that dissociate upon heating.

These observations do not necessarily imply that the complexes are composed of both HR peptides: in the mixture one peptide might simply catalyze the homomultimerization

of the other. To confirm the presence of both HR1 and HR2 in the complex, FLAG-tagged HR peptides were prepared in which the polar FLAG octapeptide (DYKDDDDK (SEQ ID NO:~~—~~ 51)) was appended to the N-termini of HR1 (FLAG-HR1) and HR2 (FLAG-HR2). Preincubated mixtures of HR1+HR2, FLAG-HR1+HR2, HR1+FLAG-HR2 and FLAG-HR1+FLAG-HR2 were analyzed in 15% Tricine ~~SDS-PAG~~ SDS-PAGE together with the individual peptides (FIG. 12B). The individual FLAG-tagged HR peptides migrated slower in the gel than their ~~non-~~nontagged homologues. All combinations of HR1 and HR2 peptide produced the higher molecular weight band, indicating that the addition of the FLAG tag did not prevent complex formation. The combination of FLAG-HR1+HR2 ~~and of~~ and HR1+FLAG-HR2 each produced a complex that had lower gel mobility than the ~~non-~~nontagged HR1+HR2 complex. Combining the two tagged peptides resulted in an additional mobility decrease. These observations imply that both the HR1 and the HR2 peptide are present in the complex.

Stoichiometry of peptides in the HR1-HR2 ~~complex~~ complex:

The availability of the FLAG-tagged HR peptides provided us with the means to determine the stoichiometry of the peptides in the HR complex. As the FLAG-tag did not interfere with complex formation its distinctive effect on the electrophoretic mobility of the tagged peptides was exploited to determine the number of HR1 and HR2 peptides in the complex. FLAG-tagged and ~~non-~~nontagged HR2 peptides were mixed in different ratios and subsequently incubated for 3 ~~h~~ hours at room temperature (RT) with equimolar amounts of HR1 peptide to allow complex formation. Subsequent SDS-PAGE analysis revealed four bands when the HR1 peptide had been incubated with a 1:1 mixture of FLAG-tagged and ~~non-~~nontagged HR2 peptides (FIG. 13-I). The fastest migrating band ~~co-~~comigrated with the complex obtained with ~~non-~~nontagged HR2 peptide only, while the band with the lowest mobility corresponded to the complex obtained with the FLAG-tagged HR2 peptide. Consequently, the two intermediate bands represent complexes containing one and two FLAG-tagged HR2 peptides, respectively. Note that the relative intensities of the four bands correspond well with the predicted ratio of formation of the different complexes (1/8, 3/8, 3/8, 1/8 respectively), calculated under the assumption that the tag is fully inert.

The reciprocal approach was used to determine the number of HR1 peptides in the complex. In this case FLAG-tagged and ~~non-~~nontagged HR1 peptides were combined with ~~non-~~nontagged HR2 peptide. However, when a 1:1 mixture of the two HR1 forms was incubated with HR2, only two bands were observed in the gel (FIG. 13-II), the faster one comigrating with the HR1-HR2 complex, the slower one corresponding with the FLAG-HR1-HR2 complex. One interpretation of this result is that the complex contains just one HR1 peptide molecule. Alternatively, HR1 peptides in solution assemble into homo-oligomers already in the absence of HR2. These oligomers are sufficiently stable to prevent the exchange of peptides when tagged and ~~non-~~nontagged HR1 complexes are mixed and, as a result, such a mixture will yield only two forms of hetero-oligomeric complexes upon addition of HR2. In view of this latter possibility we repeated the experiment after we had first denatured the putative HR1 oligomers. Thus, acetonitrile - an anorganic solvent - was added to solutions of HR1 and FLAG-tagged HR1 to a concentration of 50% (v/v). The solutions were mixed, briefly incubated after which the acetonitrile was removed by evaporation. Equimolar mixtures were again prepared of the different HR1 forms and HR2, which were incubated and finally analyzed by Tricine SDS-PAGE. As FIG. 13-III reveals, we now observed four bands in the sample containing both tagged and ~~non-~~nontagged HR1, indicating the presence of three HR1 peptides in the complex. The combined results are consistent with HR1 and HR2 forming a hexameric complex composed of three molecules HR1 and HR2 each.

Temperature stability of HR1-HR2 ~~complex~~ complex:

The stability of the SARS-CoV HR1-HR2 complex to temperature dissociation was assessed in comparison to that of the corresponding MHV complex. Equal amounts of both complexes were combined and the solution was adjusted to 1x Tricine sample buffer. Equal samples were taken, incubated in parallel for 5 ~~min~~ minutes at different temperatures and subsequently analyzed by 10% Tricine SDS-PAGE (FIG. 14). Due to their distinct electrophoretic mobilities, the SARS-CoV and MHV complexes could clearly be distinguished allowing the direct comparison of their temperature sensitivity. Surprisingly, the SARS-CoV

HR complex appeared to be significantly less stable (dissociated at 70°C) than the MHV complex (dissociated at 90°C).

Secondary structure of HR1 and HR2 peptides and of HR1-HR2 ~~complex~~ complex:

Circular dichroism (CD) was used to determine the secondary structure of the individual peptides HR1 and HR2 and of the HR1-HR2 complex. The CD spectra show that the peptides have a high alpha-helicity both on their own and in the complex (FIG. 15). The calculated values of the helical content were 85% (HR1), 81% (HR2) and 88% (HR1-HR2).

Limited proteolysis on HR1-HR2 ~~complex~~ complex:

Strongly folded protein structures are often resistant to proteolytic degradation. To obtain structural information about the HR1-HR2 complex we carried out limited digestions with proteinase K, purified the resistant fragments by RP HPLC (FIG. 16, upper part) and analyzed the fragments by mass spectrometry (FIG. 16, lower part). For the individual peptides the results showed that HR2 was completely degraded by the enzyme while of the HR1a peptide only the C-terminal 6 residues were sensitive to proteinase K, indicating a strong folding of this latter peptide. When a mixture of the two peptides was ~~analyzed~~ analyzed, the HR2 peptide was entirely protected from proteolytic breakdown. A similar analysis carried out with a C-terminally truncated version of HR1a, HR1c, revealed that now the N-terminus of HR2 was no longer protected. These results indicate that in the HR1-HR2 complex, the HR1 and HR2 helices are oriented in an anti-parallel fashion.

Our functional and biochemical analyses of the SARS-CoV spike HR regions shows that the virus makes use of a membrane fusion mechanism that has similarities with the fusion mechanism of class I fusion proteins, in which the HR regions play a prominent role. We show that peptides corresponding to the HR2 domain, but not those derived of the HR1 domain of the SARS-CoV spike protein can inhibit virus infection. We show here that HR2 peptides are able to bind stably to HR1 peptides, as has been observed previously for coronavirus, retrovirus and paramyxovirus fusion proteins. Analogous to the HIV-1 gp41, SV5 F and HRSV F proteins (69, 8, 1, 80, the HR1-HR2 complex was found to consist of a six-helix bundle that is composed of three HR1 and three HR2 alpha-helical peptides. The

high resistance of the HR1 peptide to proteinase K, the inability of separately preincubated FLAG-tagged and ~~non-~~nontagged HR1 peptides to form mixed hexamers unless first dissociated by acetonitrile, and the highly alpha-helical character of the peptide are all observations suggesting that SARS-CoV HR1, in the absence of HR2, already forms a (trimeric) coiled coil. The proteolysis data point to an anti-parallel packing of HR2 with respect to HR1, presumably through interaction of the hydrophobic interface of the HR2 helix with the hydrophobic groove in the HR1 coiled coil created by the - mostly hydrophobic - e and g residues of HR1. Formation of such an anti-parallel six-helix bundle has been shown to be essential in the membrane fusion process, by pulling the viral and cellular membrane together. In the full-length spike protein such a structure brings the fusion peptide - N-terminal of HR1 - in close proximity to the transmembrane domain - C-terminal of HR2 - thereby enabling membrane fusion. The infection inhibiting effect of peptides corresponding to HR2 can be explained by their competitive binding to the HR1 region of the SARS-CoV spike protein, which prevents formation of the six-helix bundle and, consequently, prevents membrane~~-fusion~~ fusion.

The HR2-8 peptide can be used as a lead for the development of more effective SARS-CoV peptide inhibitors. Alternatively, the HR peptides might be used as a vaccine, since antibodies directed against the HR2 peptides of HIV-1 inhibit virus infection. Hence, the HR peptides provide a basis for therapeutic and/or prophylactic agents against SARS-CoV as well as against other coronaviruses.

Example ~~4~~ 4:

The coronavirus fusion ~~peptide~~ peptide:

Transmembrane prediction using the TMAP ~~program~~ program:

The TMAP ~~program~~ program, www.mbb.ki.se/tmap/index.html ~~was~~, was used to predict transmembrane segments in coronavirus spike proteins using multiple sequence alignments. A Clustal W alignment was used of spike protein sequences from nine coronaviruses including FIPV (feline infectious peritonitis virus, strain 79-1146; VGIH79), TGEV (porcine transmissible gastroenteritis virus, strain Purdue; P07946), PEDV (porcine epidemic diarrhea virus; NP_598310), HCoV-229E (human coronavirus, strain 229E;

VGIHHC), BCoV (bovine coronavirus, strain F15; P25190), MHV (mouse hepatitis virus, strain A59; P11224), HCoV-OC43 (human coronavirus, strain OC43; CAA83661), SARS-CoV (strain TOR2; P59594), and IBV (infectious bronchitis virus, strain Beaudette; P11223).

The TMAP program, designed to identify transmembrane domains in proteins, was used ~~in~~ in the search for the coronavirus fusion peptide. Nine coronaviral spike protein sequences (FIG. 17, lower part) were used for the Clustal W alignment on which the prediction by the TMAP program is based. Three hydrophobic regions were identified (FIG. 17, middle part). Two of these, ~~i.e.~~ i.e., the regions in the N- and C-terminal part of the protein, represent the well-known signal sequence and transmembrane anchor, respectively. The third domain is found immediately upstream of HR1. This location combined with its hydrophobicity and the presence of a conserved proline in it are characteristics indicating that this domain functions as the coronavirus fusion peptide.

The identity of the fusion peptide in the coronavirus spike protein has not yet been established. Generally, class I fusion proteins require cleavage for fusion activation. As a ~~result~~ result, the fusion peptide ends up at or close to the N-terminus of the membrane-anchored subunit. Unlike other class I fusion proteins, coronavirus spike proteins lack the cleavage requirement for virus infectivity. Cleavage inhibition of the MHV spike protein by a furin blocker does not affect virus infectivity, rather, group 1 coronaviruses are not cleaved at all. We could not observe any significant cleavage of the expressed spike protein. Additionally, the cleavable coronavirus spike proteins lack a hydrophobic region adjacent to the cleavage site. This suggests that coronavirus spike proteins use an internal fusion peptide like the VSV G protein and class II fusion proteins, such as the TBEV E and SFV E1 fusion proteins. In order to predict the location of the fusion peptide, we have used a transmembrane prediction program TMAP], which predicts transmembrane domains (TM) in protein sequences using multiple alignments. In the Clustal W alignment of all known coronavirus spike sequences, the TMAP program predicted three TM domains (FIG. 17). One represented the signal sequence (SARS-CoV-S residues 1 - 15), the other represented the transmembrane anchor (residues 1195 - 1223), and the third hydrophobic region was predicted immediately N-terminal of the HR1 region (residues 858 - 886). Careful

inspection of this region reveals that it has fusion peptide characteristics like a high alanine and glycine content and a conserved proline residue (residue 879), which is characteristic of internal fusion peptides. This region was previously recognized by Chambers and coworkers (7) as a potential fusion peptide for coronaviruses. The formation of the anti-parallel six-helix bundle during the fusion reaction brings this fusion peptide in close proximity to the transmembrane anchor of the full-length protein, which results in the merging of viral and cellular membranes.

REFERENCES

1. **Baker, K. A., R. E. Dutch, R. A. Lamb, and T. S. Jardetzky.** 1999. Structural basis for paramyxovirus-mediated membrane fusion. Mol Cell **3**:309-19.
2. **Bos, E. C., L. Heijnen, W. Luytjes, and W. J. Spaan.** 1995. Mutational analysis of the murine coronavirus spike protein: effect on cell-to-cell fusion. Virology **214**:453-63.
3. **Buchholz, U. J., S. Finke, and K. K. Conzelmann.** 1999. Generation of bovine respiratory syncytial virus (BRSV) from cDNA: BRSV NS2 is not essential for virus replication in tissue culture, and the human RSV leader region acts as a functional BRSV genome promoter. J Virol **73**:251-9.
4. **Bullough, P. A., F. M. Hughson, J. J. Skehel, and D. C. Wiley.** 1994. Structure of influenza haemagglutinin at the pH of membrane fusion. Nature **371**:37-43.
5. **Caffrey, M., M. Cai, J. Kaufman, S. J. Stahl, P. T. Wingfield, D. G. Covell, A. M. Gronenborn, and G. M. Clore.** 1998. Three-dimensional solution structure of the 44 kDa ectodomain of SIV gp41. Embo J **17**:4572-84.
6. **Cavanagh, D.** 1995. The Coronavirus Surface Glycoprotein, p. 73-113. *In* S. G. Siddell (ed.), The Coronaviridae. Plenum Press, New York.
7. **Chambers, P., C. R. Pringle, and A. J. Easton.** 1990. Heptad repeat sequences are located adjacent to hydrophobic regions in several types of virus fusion glycoproteins. J Gen Virol **71**:3075-80.
8. **Chan, D. C., D. Fass, J. M. Berger, and P. S. Kim.** 1997. Core structure of gp41 from the HIV envelope glycoprotein. Cell **89**:263-73.
9. **Chen, C. H., T. J. Matthews, C. B. McDanal, D. P. Bolognesi, and M. L. Greenberg.** 1995. A molecular clasp in the human immunodeficiency virus (HIV) type 1 TM protein determines the anti-HIV activity of gp41 derivatives: implication for viral fusion. J Virol **69**:3771-7.
10. **Chen, J., K. H. Lee, D. A. Steinhauer, D. J. Stevens, J. J. Skehel, and D. C. Wiley.** 1998. Structure of the hemagglutinin precursor cleavage site, a determinant of influenza pathogenicity and the origin of the labile conformation. Cell **95**:409-17.

11. **Chen, J., J. J. Skehel, and D. C. Wiley.** 1999. N- and C-terminal residues combine in the fusion-pH influenza hemagglutinin HA(2) subunit to form an N cap that terminates the triple-stranded coiled coil. Proc Natl Acad Sci U S A **96:**8967-72.

12. **Chen, J., S. A. Wharton, W. Weissenhorn, L. J. Calder, F. M. Hughson, J. J. Skehel, and D. C. Wiley.** 1995. A soluble domain of the membrane-anchoring chain of influenza virus hemagglutinin (HA2) folds in Escherichia coli into the low-pH-induced conformation. Proc Natl Acad Sci U S A **92:**12205-9.

13. **Chen, L., J. J. Gorman, J. McKimm-Breschkin, L. J. Lawrence, P. A. Tulloch, B. J. Smith, P. M. Colman, and M. C. Lawrence.** 2001. The structure of the fusion glycoprotein of Newcastle disease virus suggests a novel paradigm for the molecular mechanism of membrane fusion. Structure (Camb) **9:**255-66.

14. **Davies, H. A., and M. R. Macnaughton.** 1979. Comparison of the morphology of three coronaviruses. Arch Virol **59:**25-33.

15. **de Groot, R. J., W. Luytjes, M. C. Horzinek, B. A. van der Zeijst, W. J. Spaan, and J. A. Lenstra.** 1987. Evidence for a coiled-coil structure in the spike proteins of coronaviruses. J Mol Biol **196:**963-6.

16. **Delmas, B., and H. Laude.** 1990. Assembly of coronavirus spike protein into trimers and its role in epitope expression. J Virol **64:**5367-75.

17. **Eckert, D. M., and P. S. Kim.** 2001. Design of potent inhibitors of HIV-1 entry from the gp41 N-peptide region. Proc Natl Acad Sci U S A **98:**11187-92.

18. **Eckert, D. M., and P. S. Kim.** 2001. Mechanisms of viral membrane fusion and its inhibition. Annu Rev Biochem **70:**777-810.

19. **Fass, D., S. C. Harrison, and P. S. Kim.** 1996. Retrovirus envelope domain at 1.7 angstrom resolution. Nat Struct Biol **3:**465-9.

20. **Furuta, R. A., C. T. Wild, Y. Weng, and C. D. Weiss.** 1998. Capture of an early fusion-active conformation of HIV-1 gp41. Nat Struct Biol **5:**276-9.

21. **Gallagher, T. M.** 1997. A role for naturally occurring variation of the murine coronavirus spike protein in stabilizing association with the cellular receptor. J Virol **71:**3129-37.

22. **Gallagher, T. M., and M. J. Buchmeier.** 2001. Coronavirus spike proteins in viral entry and pathogenesis. Virology **279:**371-4.

23. **Gallagher, T. M., C. Escarmis, and M. J. Buchmeier.** 1991. Alteration of the pH dependence of coronavirus-induced cell fusion: effect of mutations in the spike glycoprotein. J Virol **65:**1916-28.

24. **Gill, S. C., and P. H. von Hippel.** 1989. Calculation of protein extinction coefficients from amino acid sequence data. Anal Biochem **182:**319-26.

25. **Gombold, J. L., S. T. Hingley, and S. R. Weiss.** 1993. Fusion-defective mutants of mouse hepatitis virus A59 contain a mutation in the spike protein cleavage signal. J Virol **67:**4504-12.

26. **Hingley, S. T., I. Leparc-Goffart, and S. R. Weiss.** 1998. The spike protein of murine coronavirus mouse hepatitis virus strain A59 is not cleaved in primary glial cells and primary hepatocytes. J Virol **72:**1606-9.

27. **Holmes, K. V., B.D. Zelus, J.H. Schickli and S.R. Weiss.** 2001. Receptor specificity and receptor-induced conformational changes in mouse hepatitis virus spike glycoprotein. Adv Exp Med Biol **494:**173-181.

28. **Jiang, S., K. Lin, N. Strick, and A. R. Neurath.** 1993. HIV-1 inhibition by a peptide. Nature **365:**113.

29. **Joshi, S. B., R. E. Dutch, and R. A. Lamb.** 1998. A core trimer of the paramyxovirus fusion protein: parallels to influenza virus hemagglutinin and HIV-1 gp41. Virology **248:**20-34.

30. **Judice, J. K., J. Y. Tom, W. Huang, T. Wrin, J. Vennari, C. J. Petropoulos, and R. S. McDowell.** 1997. Inhibition of HIV type 1 infectivity by constrained alpha-helical peptides: implications for the viral fusion mechanism. Proc Natl Acad Sci U S A **94:**13426-30.

31. **Kliger, Y., and Y. Shai.** 2000. Inhibition of HIV-1 entry before gp41 folds into its fusion-active conformation. J Mol Biol **295:**163-8.

32. **Kobe, B., R. J. Center, B. E. Kemp, and P. Poumbourios.** 1999. Crystal structure of human T cell leukemia virus type 1 gp21 ectodomain crystallized as a maltose-binding

protein chimera reveals structural evolution of retroviral transmembrane proteins. Proc Natl Acad Sci U S A **96:**4319-24.

33. **Krueger, D. K., S. M. Kelly, D. N. Lewicki, R. Ruffolo, and T. M. Gallagher.** 2001. Variations in disparate regions of the murine coronavirus spike protein impact the initiation of membrane fusion. J Virol **75:**2792-802.

34. **Kuo, L., G. J. Godeke, M. J. Raamsman, P. S. Masters, and P. J. Rottier.** 2000. Retargeting of coronavirus by substitution of the spike glycoprotein ectodomain: crossing the host cell species barrier. J Virol **74:**1393-406.

35. **Lambert, D. M., S. Barney, A. L. Lambert, K. Guthrie, R. Medinas, D. E. Davis, T. Bucy, J. Erickson, G. Merutka, and S. R. Petteway, Jr.** 1996. Peptides from conserved regions of paramyxovirus fusion (F) proteins are potent inhibitors of viral fusion. Proc Natl Acad Sci U S A **93:**2186-91.

36. **Lescar, J., A. Roussel, M. W. Wien, J. Navaza, S. D. Fuller, G. Wengler, and F. A. Rey.** 2001. The Fusion glycoprotein shell of Semliki Forest virus: an icosahedral assembly primed for fusogenic activation at endosomal pH. Cell **105:**137-48.

37. **Lewicki, D. N., and T. M. Gallagher.** 2002. Quaternary structure of coronavirus spikes in complex with carcinoembryonic antigen-related cell adhesion molecule cellular receptors. J Biol Chem **277:**19727-34.

38. **Lu, M., S. C. Blacklow, and P. S. Kim.** 1995. A trimeric structural domain of the HIV-1 transmembrane glycoprotein. Nat Struct Biol **2:**1075-82.

39. **Luo, Z., A. M. Matthews, and S. R. Weiss.** 1999. Amino acid substitutions within the leucine zipper domain of the murine coronavirus spike protein cause defects in oligomerization and the ability to induce cell-to-cell fusion. J Virol **73:**8152-9.

40. **Luo, Z., and S. R. Weiss.** 1998. Roles in cell-to-cell fusion of two conserved hydrophobic regions in the murine coronavirus spike protein. Virology **244:**483-94.

41. **Malashkevich, V. N., D. C. Chan, C. T. Chutkowski, and P. S. Kim.** 1998. Crystal structure of the simian immunodeficiency virus (SIV) gp41 core: conserved helical interactions underlie the broad inhibitory activity of gp41 peptides. Proc Natl Acad Sci U S A **95:**9134-9.

42. **Malashkevich, V. N., B. J. Schneider, M. L. McNally, M. A. Milhollen, J. X. Pang, and P. S. Kim.** 1999. Core structure of the envelope glycoprotein GP2 from Ebola virus at 1.9- A resolution. Proc Natl Acad Sci U S A **96:**2662-7.

43. **Malashkevich, V. N., M. Singh, and P. S. Kim.** 2001. The trimer-of-hairpins motif in membrane fusion: Visna virus. Proc Natl Acad Sci U S A **98:**8502-6.

44. **Matsuyama, S., and F. Taguchi.** 2002. Communication between S1N330 and a region in S2 of murine coronavirus spike protein is important for virus entry into cells expressing CEACAM1b receptor. Virology **295:**160-71.

45. **Matsuyama, S., and F. Taguchi.** 2002. Receptor-induced conformational changes of murine coronavirus spike protein. J Virol **76:**11819-26.

46. **Melikyan, G. B., R. M. Markosyan, H. Hemmati, M. K. Delmedico, D. M. Lambert, and F. S. Cohen.** 2000. Evidence that the transition of HIV-1 gp41 into a six-helix bundle, not the bundle configuration, induces membrane fusion. J Cell Biol **151:**413-23.

47. **Munoz-Barroso, I., S. Durell, K. Sakaguchi, E. Appella, and R. Blumenthal.** 1998. Dilation of the human immunodeficiency virus-1 envelope glycoprotein fusion pore revealed by the inhibitory action of a synthetic peptide from gp41. J Cell Biol **140:**315-23.

48. **Nash, T. C., and M. J. Buchmeier.** 1997. Entry of mouse hepatitis virus into cells by endosomal and nonendosomal pathways. Virology **233:**1-8.

49. **Nehete, P. N., R. B. Arlinghaus, and K. J. Sastry.** 1993. Inhibition of human immunodeficiency virus type 1 infection and syncytium formation in human cells by V3 loop synthetic peptides from gp120. J Virol **67:**6841-6.

50. **Parry, D. A.** 1978. Fibrinogen: A preliminary analysis of the amino acid sequences of the portions of the alpha, beta, and gamma-chains postulated to form the interdomainal link between globular regions of the molecule. J. Mol. Biol. **248:**180-189.

51. **Rapaport, D., M. Ovadia, and Y. Shai.** 1995. A synthetic peptide corresponding to a conserved heptad repeat domain is a potent inhibitor of Sendai virus-cell fusion: an emerging similarity with functional domains of other viruses. Embo J **14:**5524-31.

52. **Rimsky, L. T., D. C. Shugars, and T. J. Matthews.** 1998. Determinants of human immunodeficiency virus type 1 resistance to gp41-derived inhibitory peptides. J Virol **72:**986-93.

53. **Ruigrok, R. W., A. Aitken, L. J. Calder, S. R. Martin, J. J. Skehel, S. A. Wharton, W. Weis, and D. C. Wiley.** 1988. Studies on the structure of the influenza virus haemagglutinin at the pH of membrane fusion. J Gen Virol **69:**2785-95.

54. **Russell, C. J., T. S. Jardetzky, and R. A. Lamb.** 2001. Membrane fusion machines of paramyxoviruses: capture of intermediates of fusion. Embo J **20:**4024-34.

55. **Schagger, H., and G. von Jagow.** 1987. Tricine-sodium dodecyl sulfate-polyacrylamide gel electrophoresis for the separation of proteins in the range from 1 to 100 kDa. Anal Biochem **166:**368-79.

56. **Siddell, S. G.** 1995. The Coronaviridae; an introduction. Plenum Press, New York.

57. **Skehel, J. J., and D. C. Wiley.** 1998. Coiled coils in both intracellular vesicle and viral membrane fusion. Cell **95:**871-4.

58. **Slepushkin, V. A., G. V. Kornilaeva, S. M. Andreev, M. V. Sidorova, A. O. Petrukhina, G. R. Matsevich, S. V. Raduk, V. B. Grigoriev, T. V. Makarova, V. V. Lukashov, and Karamov, E. V.** 1993. Inhibition of human immunodeficiency virus type 1 (HIV-1) penetration into target cells by synthetic peptides mimicking the N-terminus of the HIV-1 transmembrane glycoprotein. Virology **194:**294-301.

59. **Stauber, R., M. Pfleiderera, and S. Siddell.** 1993. Proteolytic cleavage of the murine coronavirus surface glycoprotein is not required for fusion activity. J Gen Virol **74:**183-91.

60. **Sturman, L. S., C. S. Ricard, and K. V. Holmes.** 1990. Conformational change of the coronavirus peplomer glycoprotein at pH 8.0 and 37 degrees C correlates with virus aggregation and virus- induced cell fusion. J Virol **64:**3042-50.

61. **Taguchi, F.** 1993. Fusion formation by the uncleaved spike protein of murine coronavirus JHMV variant cl-2. J Virol **67:**1195-202.

62. **Taguchi, F.** 1995. The S2 subunit of the murine coronavirus spike protein is not involved in receptor binding. J Virol **69:**7260-3.

63. **Tan, K., J. Liu, J. Wang, S. Shen, and M. Lu.** 1997. Atomic structure of a thermostable subdomain of HIV-1 gp41. Proc Natl Acad Sci U S A **94:**12303-8.

64. **Vennema, H., G. J. Godeke, J. W. Rossen, W. F. Voorhout, M. C. Horzinek, D. J. Opstelten, and P. J. Rottier.** 1996. Nucleocapsid-independent assembly of coronavirus-like particles by co- expression of viral envelope protein genes. Embo J **15:**2020-8.

65. **Vennema, H., R. Rijnbrand, L. Heijnen, M. C. Horzinek, and W. J. Spaan.** 1991. Enhancement of the vaccinia virus/phage T7 RNA polymerase expression system using encephalomyocarditis virus 5'-untranslated region sequences. Gene **108:**201-9.

66. **Vennema, H., P. J. Rottier, L. Heijnen, G. J. Godeke, M. C. Horzinek, and W. J. Spaan.** 1990. Biosynthesis and function of the coronavirus spike protein. Adv Exp Med Biol **276:**9-19.

67. **Weissenhorn, W., L. J. Calder, S. A. Wharton, J. J. Skehel, and D. C. Wiley.** 1998. The central structural feature of the membrane fusion protein subunit from the Ebola virus glycoprotein is a long triple-stranded coiled coil. Proc Natl Acad Sci U S A **95:**6032-6.

68. **Weissenhorn, W., A. Carfi, K. H. Lee, J. J. Skehel, and D. C. Wiley.** 1998. Crystal structure of the Ebola virus membrane fusion subunit, GP2, from the envelope glycoprotein ectodomain. Mol Cell **2:**605-16.

69. **Weissenhorn, W., A. Dessen, S. C. Harrison, J. J. Skehel, and D. C. Wiley.** 1997. Atomic structure of the ectodomain from HIV-1 gp41. Nature **387:**426-30.

70. **Weissenhorn, W., S. A. Wharton, L. J. Calder, P. L. Earl, B. Moss, E. Aliprandis, J. J. Skehel, and D. C. Wiley.** 1996. The ectodomain of HIV-1 env subunit gp41 forms a soluble, alpha-helical, rod-like oligomer in the absence of gp120 and the N-terminal fusion peptide. Embo J **15:**1507-14.

71. **Westenberg, M., H. Wang, W. F. IJkel, R. W. Goldbach, J. M. Vlak, and D. Zuidema.** 2002. Furin is involved in baculovirus envelope fusion protein activation. J Virol **76:**178-84.

72. **Wild, C., T. Oas, C. McDanal, D. Bolognesi, and T. Matthews.** 1992. A synthetic peptide inhibitor of human immunodeficiency virus replication: correlation between solution structure and viral inhibition. Proc Natl Acad Sci U S A **89:**10537-41.

73. **Wild, C. T., D. C. Shugars, T. K. Greenwell, C. B. McDanal, and T. J. Matthews.** 1994. Peptides corresponding to a predictive alpha-helical domain of human immunodeficiency virus type 1 gp41 are potent inhibitors of virus infection. Proc Natl Acad Sci U S A **91:**9770-4.

74. **Williams, R. K., G. S. Jiang, and K. V. Holmes.** 1991. Receptor for mouse hepatitis virus is a member of the carcinoembryonic antigen family of glycoproteins. Proc Natl Acad Sci U S A **88:**5533-6.

75. **Wilson, I. A., J. J. Skehel, and D. C. Wiley.** 1981. Structure of the haemagglutinin membrane glycoprotein of influenza virus at 3 A resolution. Nature **289:**366-73.

76. **Yang, Z. N., T. C. Mueser, J. Kaufman, S. J. Stahl, P. T. Wingfield, and C. C. Hyde.** 1999. The crystal structure of the SIV gp41 ectodomain at 1.47 A resolution. J Struct Biol **126:**131-44.

77. **Yao, Q., and R. W. Compans.** 1996. Peptides corresponding to the heptad repeat sequence of human parainfluenza virus fusion protein are potent inhibitors of virus infection. Virology **223:**103-12.

78. **Yoo, D. W., M. D. Parker, and L. A. Babiuk.** 1991. The S2 subunit of the spike glycoprotein of bovine coronavirus mediates membrane fusion in insect cells. Virology **180:**395-9.

79. **Young, J. K., R. P. Hicks, G. E. Wright, and T. G. Morrison.** 1997. Analysis of a peptide inhibitor of paramyxovirus (NDV) fusion using biological assays, NMR, and molecular modeling. Virology **238:**291-304.

80. **Zhao, X., M. Singh, V. N. Malashkevich, and P. S. Kim.** 2000. Structural characterization of the human respiratory syncytial virus fusion protein core. Proc Natl Acad Sci U S A **97:**14172-7.

Table 1. Primers used for PCR of HR regions

Primer	*Polarity*	*Sequence (5'- 3')*	*HR product*
973	+	GTGGATCCATCGAAGGTCGTCAATATAGA ATTAATGGTTTAG (SEQ ID NO:—41)	HR1
974	+	GTGGATCCATCGAAGGTCGTAATGCAAAT GCTGAAGC (SEQ ID NO:—47)	HR1b
975	-	GGAATTCAATTAATAAGACGATCTATCTG (SEQ ID NO:—43)	HR1, HR1a, HR1b
976	-	CGAATTCATTCCTTGAGGTTGATGTAG (SEQ ID NO:—44)	HR2
990	+	GCGGATCCATCGAAGGTCGTGATTTATCTC TCGATTTC (SEQ ID NO:—45)	HR2
1151	+	GTGGATCCAACCAAAAGATGATTGC ~~(SEQ~~ (SEQ ID NO:—46)	HR1a, HR1c
1152	-	GGAATTCAATTGAGTGCTTCAGCATTTG (SEQ ID NO:—47)	HR1c

Table 2

Inhibition of cell-to-cell fusion

	FCFW cells/FIPV infected	
	GST-HR1	**GST-HR2**
10 ng	+++	-
1 ng	+++	+
0.1ng	+++	++
0 ng	+++	+++

Syncytia formation +++

Table 3. Primers used for PCR of HR regions

Primer	*Polarity*	*Sequence (5'- 3')*	*product*
2006	+	GCGGATCCGCATATAGGTTCAATGG (SEQ ID NO:—48)	HR1
2007	-	CGAATTCATGTAATTAACCTGTCAA (SEQ ID NO:—49)	HR1, HR1a, HR1b
2008	+	GCGGATCCAACCAAAAACAAATCGC (SEQ ID NO:—50)	HR1a, HR1c
2009	+	GCGGATCCAACCAGAATGCTCAAGC (SEQ ID NO:—51)	HR1b
2010	-	CGAATTCATTGTTTAACAAGTGTGT (SEQ ID NO:—52)	HR1c
1998	+	CGAATTCACTCATATTTTCCCAATT (SEQ ID NO:—53)	HR2
1999	+	GCGGATCCGAGCTTGACTCATTCAA (SEQ ID NO:—54)	HR2-1, HR2-8, HR2-9, HR2-10
2064	+	GCGGATCCTTCAAAGAAGAGCTGGA (SEQ ID NO:—55)	HR2-2
2065	+	GCGGATCCCTGGACAAGTACTTCAA (SEQ ID NO:—56)	HR2-3
2066	+	GCGGATCCTTCAAAAATCATACATC (SEQ ID NO:—57)	HR2-4
2067	+	GCGGATCCACATCACCAGATGTTGA (SEQ ID NO:—58)	HR2-5
2068	+	GCGGATCCGTTGATCTTGGCGACAT (SEQ ID NO:—59)	HR2-6
2069	+	GCGGATCCGACATTTCAGGCATTAA (SEQ ID NO:—60)	HR2-7
1998	-	CGAATTCACTCATATTTTCCCAATT (SEQ ID NO:—53)	HR2-1 – HR2-7
2034	-	CGAATTCATTTAATATATTGCTCAT (SEQ ID NO:—61)	HR2-8
2070	-	CGAATTCACAATTCTTGAAGGTCAA (SEQ ID NO:—62)	HR2-9
2071	-	CGAATTCAGTCAATGAGTGATTCAT (SEQ ID NO:—63)	HR2-10
2072	+	GATCAGACTACAAGGATGACGATGACA AAG (SEQ ID NO:—64)	FLAG-tag
2073	-	GATCCTTTGTCATCGTCATCCTTGTAGT CT (SEQ ID NO:—65)	FLAG-tag

CLAIMS

What is claimed is:

1. A method for at least in part inhibiting anti-parallel coiled coil formation of a coronavirus spike protein of a coronavirus, said method comprising:

decreasing contact between heptad repeat regions of said coronavirus spike protein.

2. The method according to claim 1 wherein a peptide and/or a functional fragment and/or an equivalent thereof decreases contact between heptad repeat regions of said coronavirus spike protein.

3. The method according to claim 2 wherein the peptide and/or a functional fragment and/or an equivalent thereof comprises a heptad repeat region of a coronavirus spike protein.

4. The method according to claim 1, claim 2, or claim 3, wherein said heptad repeat region comprises an amino acid sequence of SARS HR2 and/or HR1 according to FIG. 1 (SEQ ID NOS: 23 & 118, respectively), and/or a functional fragment and/or a derivative thereof.

5. The method according to claim 1, wherein an antibody and/or a functional fragment and/or an equivalent thereof decreases contact between heptad repeat regions of said coronavirus spike protein.

6. The method according to claim 1, claim 2, claim 3, claim 4, or claim 5, wherein the coronavirus comprises a group 1 coronavirus.

7. The method according to claim 6, wherein the coronavirus comprises a feline corona virus.

8. The method according to claim 7, wherein the coronavirus comprises a feline infectious peritonitis (FIP) virus.

9. The method according to claim 6, wherein the coronavirus comprises a human corona virus.

10. The method according to claim 1, claim 2, claim 3, claim 4, or claim 5, wherein the coronavirus comprises a group 2 coronavirus.

11. The method according to claim 10, wherein said coronavirus comprises a mouse hepatitis virus (MHV).

12. A method according to claim 1, claim 2, claim 3, claim 4, or claim 5, wherein the coronavirus causes Severe Acute Respiratory Syndrome (SARS).

13. A method for inhibiting of coronavirus spike protein mediated cell to cell fusion, said method comprising:

decreasing contact between heptad repeat regions of said coronavirus spike protein.

14. A method of selecting a compound that binds to a heptad repeat region of a coronavirus spike protein, said method comprising:

contacting *in vitro* at least one heptad region of a coronavirus spike protein with a collection of compounds, and

measuring the formation of an anti-parallel coiled coil in said coronavirus spike protein.

15. A compound selected by the method of claim 14.

16. An antibody, functional fragment, and/or derivative thereof, said antibody, functional fragment, and/or derivative thereof capable of decreasing the contact between heptad repeat regions of a coronavirus spike protein.

17. A composition comprising:

the compound of claim 15, and/or

an antibody and/or a functional fragment and/or a derivative thereof, capable of decreasing the contact between heptad repeat regions of a coronavirus spike protein, and

a suitable diluent and/ or carrier.

18. A method of treating coronavirus infections in a subject, said method comprising:

providing to the subject the composition of claim 17.

19. A diagnostic kit for detecting coronavirus infection in a sample of a subject, said diagnostic kit comprising:

the compound of claim 15 or an antibody, functional fragment, and/or derivative thereof, said antibody, functional fragment, and/or derivative thereof capable of decreasing the contact between heptad repeat regions of a coronavirus spike protein, together with

means of detecting binding of said compound or antibody functional fragment, and/or derivative thereof to the coronavirus.

20. A diagnostic kit for detecting antibodies directed against coronavirus in a sample from a subject, said diagnostic kit comprising:

the compound according to claim 15, and

means for detecting binding of said compound to said antibodies.

21. A method of attenuating a coronavirus, said method comprising:

decreasing the contact between heptad repeat regions of the spike protein of said coronavirus.

22. An attenuated coronavirus having decreased contact between heptad repeat regions of the spike protein of said attenuated coronavirus.

23. The method according to claim 3 wherein said peptide comprises an amino acid sequence according to peptide sHR2-1, and/or sHR2-2, and/or sHR2-8, and/or sHR2-9 as depicted in FIG. ~~11 B,~~ 11B, and/or a functional fragment and/or an equivalent thereof.

24. A method for at least in part inhibiting a fusion of a coronavirus with a cell membrane, said method comprising decreasing binding of a fusion peptide with said cell membrane.

25. The method according to claim 24, wherein said fusion peptide comprises the amino acid sequence of SARS-CoV as depicted in FIG. 17.

26. The method according to claim 24, wherein a specific binding molecule for said fusion peptide decreases binding of a fusion peptide with said cell membrane.

27. The method according to claim 26, wherein said specific binding molecule is an antibody, functional fragment thereof, and/or derivative thereof.

ABSTRACT

The invention relates to the field of coronaviruses and diagnosis, therapeutic use, and vaccines therefor. Methods are shown for at least in part inhibiting anti-parallel coiled coil formation of a coronavirus spike protein which methods include decreasing the contact between heptad repeat regions of the coronavirus spike protein. The invention provides a peptide comprising a heptad repeat region of a ~~corona~~ coronaviral spike protein and/or a functional fragment and/or a derivative thereof. The invention also provides antibodies and compounds inhibiting ~~corona~~ coronaviral infection of cells, and/or cell-to-cell fusion. The invention also includes heptad repeat regions and a fusion peptide of SARS-CoV.

APPENDIX C

(STATEMENT UNDER 37 C.F.R. §§ 1.821 THROUGH 1.825)

(Serial No. 10/750,411)

PATENT

IN THE UNITED STATES PATENT AND TRADEMARK OFFICE

In re Application of:

Rottier et al.

Serial No.: 10/750,411

Filed: December 30, 2003

For: CORONA-VIRUS-LIKE PARTICLES COMPRISING FUNCTIONALLY DELETED GENOMES

Confirmation No.: 4659

Examiner: M. Mosher

Group Art Unit: 1648

Attorney Docket No.: 2183-6265US

CERTIFICATE OF MAILING

I hereby certify that this correspondence along with any attachments referred to or identified as being attached or enclosed is being deposited with the United States Postal Service as First Class Mail on the date of deposit shown below with sufficient postage and in an envelope addressed to the Commissioner for Patents, P.O. Box 1450, Alexandria, VA 22313-1450.

February 7, 2005
Date

Betty Vowles
Signature

Betty Vowles
Name (Type/Print)

STATEMENT UNDER 37 C.F.R. §§ 1.821 THROUGH 1.825

Commissioner for Patents
P.O. Box 1450
Alexandria, VA 22313-1450

Sir:

I, Daniel J. Morath, Ph.D., an agent registered to practice before the United States Patent & Trademark Office and agentp of record for this application, state that:

1. The enclosed paper copy of the substitute SEQUENCE LISTING, as well as the enclosed copy of the substitute SEQUENCE LISTING in computer readable form (CRF), are included herewith to comply with the requirements of 37 C.F.R. §§ 1.821 and/or 1.825 as requested by the Examiner.

2. The enclosed copy of the substitute SEQUENCE LISTING in computer readable form (CRF) is believed to be the same as the paper copy of the substitute SEQUENCE LISTING.

3. The SEQUENCE LISTINGS submitted herewith are believed to contain no "new matter" with regard to the referenced patent application.

Respectfully submitted,

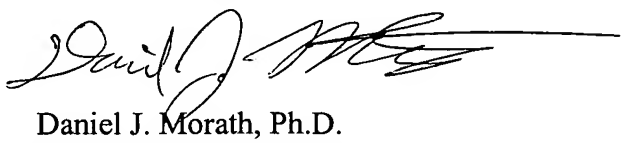

Daniel J. Morath, Ph.D.
Registration No. 55,896
Agent for Applicants
TRASKBRITT, P.C.
P.O. Box 2550
Salt Lake City, Utah 84110-2550
Telephone: 801-532-1922

Date: February 4, 2005

APPENDIX D

(SUBSTITUTE SEQUENCE LISTING)

(Serial No. 10/750,411)

SEQUENCE LISTING

<110> Rottier, Petrus J.M.
de Haan, Cornelis A.M.
Haijema, Bert J.
Bosch, Berend J.

<120> Coronavirus-like particles comprising functionally deleted genomes

<130> 2183-6265US

<140> To Be Assigned
<141> 2003-12-03

<150> US 10/714,534
<151> 2003-11-14

<150> US 10/414,256
<151> 2003-04-14

<150> PCT/NL02/00318
<151> 2002-05-17

<160> 65

<170> PatentIn version 3.2

<210> 1
<211> 64
<212> PRT
<213> Artificial

<220>
<223> sHR2-1

<400> 1

Glu Leu Asp Ser Phe Lys Glu Glu Leu Asp Lys Tyr Phe Lys Asn His
1 5 10 15

Thr Ser Pro Asp Val Asp Leu Gly Asp Ile Ser Gly Ile Asn Ala Ser
20 25 30

Val Val Asn Ile Gln Lys Glu Ile Asp Arg Leu Asn Glu Val Ala Lys
35 40 45

Asn Leu Asn Glu Ser Leu Ile Asp Leu Gln Glu Leu Gly Lys Tyr Glu
50 55 60

<210> 2
<211> 60
<212> PRT

<213> Artificial

<220>
<223> sHR2-2

<400> 2

Phe Lys Glu Glu Leu Asp Lys Tyr Phe Lys Asn His Thr Ser Pro Asp
1 5 10 15

Val Asp Leu Gly Asp Ile Ser Gly Ile Asn Ala Ser Val Val Asn Ile
20 25 30

Gln Lys Glu Ile Asp Arg Leu Asn Glu Val Ala Lys Asn Leu Asn Glu
35 40 45

Ser Leu Ile Asp Leu Gln Glu Leu Gly Lys Tyr Glu
50 55 60

<210> 3
<211> 68
<212> PRT
<213> Artificial

<220>
<223> sHR2-8

<400> 3

Glu Leu Asp Ser Phe Lys Glu Glu Leu Asp Lys Tyr Phe Lys Asn His
1 5 10 15

Thr Ser Pro Asp Val Asp Leu Gly Asp Ile Ser Gly Ile Asn Ala Ser
20 25 30

Val Val Asn Ile Gln Lys Glu Ile Asp Arg Leu Asn Glu Val Ala Lys
35 40 45

Asn Leu Asn Glu Ser Leu Ile Asp Leu Gln Glu Leu Gly Lys Tyr Glu
50 55 60

Gln Tyr Ile Lys
65

<210> 4
<211> 60
<212> PRT
<213> Artificial

<220>
<223> sHR2-9

<400> 4

Glu Leu Asp Ser Phe Lys Glu Glu Leu Asp Lys Tyr Phe Lys Asn His
1 5 10 15

Thr Ser Pro Asp Val Asp Leu Gly Asp Ile Ser Gly Ile Asn Ala Ser
20 25 30

Val Val Asn Ile Gln Lys Glu Ile Asp Arg Leu Asn Glu Val Ala Lys
35 40 45

Asn Leu Asn Glu Ser Leu Ile Asp Leu Gln Glu Leu
50 55 60

<210> 5
<211> 41
<212> PRT
<213> Severe Acute Respiratory Syndrome Cononavirus

<400> 5

Ala Ala Tyr Thr Ala Ala Leu Val Ser Gly Thr Ala Thr Ala Gly Trp
1 5 10 15

Thr Phe Gly Ala Gly Ala Ala Leu Gln Ile Pro Phe Ala Met Gln Met
20 25 30

Ala Tyr Arg Phe Asn Gly Ile Gly Val
35 40

<210> 6
<211> 102
<212> PRT
<213> Severe Acute Respiratory Syndrome Cononavirus

<400> 6

Pro Phe Ala Met Gln Met Ala Tyr Arg Phe Asn Gly Ile Gly Val Thr
1 5 10 15

Gln Asn Val Leu Tyr Glu Asn Gln Lys Gln Ile Ala Asn Gln Phe Asn
20 25 30

Lys Ala Ile Ser Gln Ile Gln Glu Ser Leu Thr Thr Thr Ser Thr Ala

35 40 45

Leu Gly Lys Leu Gln Asp Val Val Asn Gln Asn Ala Gln Ala Leu Asn
50 55 60

Thr Leu Val Lys Gln Leu Ser Ser Asn Phe Gly Ala Ile Ser Ser Val
65 70 75 80

Leu Asn Asp Ile Leu Ser Arg Leu Asp Lys Val Glu Ala Glu Val Gln
85 90 95

Ile Asp Arg Leu Ile Thr
100

<210> 7
<211> 78
<212> PRT
<213> Severe Acute Respiratory Syndrome Cononavirus

<400> 7

Pro Glu Leu Asp Ser Phe Lys Glu Glu Leu Asp Lys Tyr Phe Lys Asn
1 5 10 15

His Thr Ser Pro Asp Val Asp Leu Gly Asp Ile Ser Gly Ile Asn Ala
20 25 30

Ser Val Val Asn Ile Gln Lys Glu Ile Asp Arg Leu Asn Glu Val Ala
35 40 45

Lys Asn Leu Asn Glu Ser Leu Ile Asp Leu Gln Glu Leu Gly Lys Tyr
50 55 60

Glu Gln Tyr Ile Lys Trp Pro Trp Tyr Val Trp Leu Gly Phe
65 70 75

<210> 8
<211> 116
<212> PRT
<213> Feline Infectious Peritonitis Virus

<400> 8

Pro Phe Ala Val Ala Val Gln Ala Arg Leu Asn Tyr Val Ala Leu Gln
1 5 10 15

Thr Asp Val Leu Asn Lys Asn Gln Gln Ile Leu Ala Asn Ala Phe Asn
20 25 30

Gln Ala Ile Gly Asn Ile Thr Gln Ala Phe Gly Lys Val Asn Asp Ala
35 40 45

Ile His Gln Thr Ser Gln Gly Leu Ala Thr Val Ala Lys Ala Leu Ala
50 55 60

Lys Val Gln Asp Val Val Asn Thr Gln Gly Gln Ala Leu Ser His Leu
65 70 75 80

Thr Val Gln Leu Gln Asn Asn Phe Gln Ala Ile Ser Ser Ser Ile Ser
85 90 95

Asp Ile Tyr Asn Arg Leu Asp Glu Ile Ser Ala Asp Ala Gln Val Asp
100 105 110

Arg Leu Ile Thr
115

<210> 9
<211> 93
<212> PRT
<213> Feline Infectious Peritonitis Virus

<400> 9

Pro Asp Tyr Ile Asp Ile Asn Gln Thr Val Gln Asp Ile Leu Glu Asn
1 5 10 15

Tyr Arg Pro Asn Trp Thr Val Pro Glu Phe Thr Leu Asp Ile Phe Asn
20 25 30

Ala Thr Tyr Leu Asn Leu Thr Gly Glu Ile Asp Asp Leu Glu Phe Arg
35 40 45

Ser Glu Lys Leu His Asn Thr Thr Val Glu Leu Ala Ile Leu Ile Asp
50 55 60

Asn Ile Asn Asn Thr Leu Val Asn Leu Glu Trp Leu Asn Arg Ile Glu
65 70 75 80

Thr Tyr Val Lys Trp Pro Trp Tyr Val Trp Leu Leu Ile
85 90

<210> 10
<211> 116
<212> PRT
<213> Human Cornavirus Strain 229E

<400> 10

Pro Phe Ser Lys Ala Ile Gln Ala Arg Leu Asn Tyr Val Ala Leu Gln
1 5 10 15

Thr Asp Val Leu Gln Glu Asn Gln Lys Ile Leu Ala Ala Ser Phe Asn
20 25 30

Lys Ala Met Thr Asn Ile Val Asp Ala Phe Thr Gly Val Asn Asp Ala
35 40 45

Ile Thr Gln Thr Ser Gln Ala Leu Gln Thr Val Ala Thr Ala Leu Asn
50 55 60

Lys Ile Gln Asp Val Val Asn Gln Gln Gly Asn Ser Leu Asn His Leu
65 70 75 80

Thr Ser Gln Leu Arg Gln Asn Phe Gln Ala Ile Ser Ser Ser Ile Gln
85 90 95

Ala Ile Tyr Asp Arg Leu Asp Thr Ile Gln Ala Asp Gln Gln Val Asp
100 105 110

Arg Leu Ile Thr
115

<210> 11
<211> 92
<212> PRT
<213> Human Cornavirus Strain 229E

<400> 11

Pro Glu Tyr Ile Asp Val Asn Lys Thr Leu Gln Glu Leu Ser Tyr Lys
1 5 10 15

Leu Pro Asn Tyr Thr Val Pro Asp Leu Val Val Glu Gln Tyr Asn Gln
20 25 30

Thr Ile Leu Asn Leu Thr Ser Glu Ile Ser Thr Leu Glu Asn Lys Ser

35 40 45

Ala Glu Leu Asn Tyr Thr Val Gln Lys Leu Gln Thr Leu Ile Asp Asn
50 55 60

Ile Asn Ser Thr Leu Val Asp Leu Lys Trp Leu Asn Arg Val Glu Thr
65 70 75 80

Tyr Ile Lys Trp Pro Trp Trp Val Trp Leu Cys Ile
85 90

<210> 12
<211> 102
<212> PRT
<213> Mouse Hepatitis Virus

<400> 12

Pro Phe Ser Leu Ser Val Gln Tyr Arg Ile Asn Gly Leu Gly Val Thr
1 5 10 15

Met Asn Val Leu Ser Glu Asn Gln Lys Met Ile Ala Ser Ala Phe Asn
20 25 30

Asn Ala Leu Gly Ala Ile Gln Asp Gly Phe Asp Ala Thr Asn Ser Ala
35 40 45

Leu Gly Lys Ile Gln Ser Val Val Asn Ala Asn Ala Glu Ala Leu Asn
50 55 60

Asn Leu Leu Asn Gln Leu Ser Asn Arg Phe Gly Ala Ile Ser Ala Ser
65 70 75 80

Leu Gln Glu Ile Leu Thr Arg Leu Glu Ala Val Glu Ala Lys Ala Gln
85 90 95

Ile Asp Arg Leu Ile Asn
100

<210> 13
<211> 79
<212> PRT
<213> Mouse Hepatitis Virus

<400> 13

Pro Asn Pro Pro Asp Phe Lys Glu Glu Leu Asp Lys Trp Phe Lys Asn
1 5 10 15

Gln Thr Ser Ile Ala Pro Asp Leu Ser Leu Asp Phe Glu Lys Ile Asn
20 25 30

Val Thr Leu Leu Asp Leu Thr Tyr Glu Met Asn Arg Ile Gln Asp Ala
35 40 45

Ile Lys Lys Leu Asn Glu Ser Tyr Ile Asn Leu Lys Glu Val Gly Thr
50 55 60

Tyr Glu Met Tyr Val Lys Trp Pro Trp Tyr Val Trp Leu Leu Ile
65 70 75

<210> 14
<211> 102
<212> PRT
<213> Human Cornavirus Strain OC43

<400> 14

Pro Phe Tyr Leu Asn Val Gln Tyr Arg Ile Asn Gly Leu Gly Val Thr
1 5 10 15

Met Asp Val Leu Ser Gln Asn Gln Lys Leu Ile Ala Asn Ala Phe Asn
20 25 30

Asn Ala Leu Tyr Ala Ile Gln Glu Gly Phe Asp Ala Thr Asn Ser Ala
35 40 45

Leu Val Lys Ile Gln Ala Val Val Asn Ala Asn Ala Glu Ala Leu Asn
50 55 60

Asn Leu Leu Gln Gln Leu Ser Asn Arg Phe Gly Ala Ile Ser Ala Ser
65 70 75 80

Leu Gln Glu Ile Leu Ser Arg Leu Asp Ala Ile Glu Ala Glu Ala Gln
85 90 95

Ile Asp Arg Leu Ile Asn
100

<210> 15
<211> 77

<212> PRT
<213> Human Cornavirus Strain OC43

<400> 15

Pro Asn Leu Pro Asp Phe Lys Glu Glu Leu Asp Gln Trp Phe Lys Asn
1 5 10 15

Gln Thr Ser Val Ala Pro Asp Leu Ser Leu Asp Tyr Ile Asn Val Thr
20 25 30

Phe Leu Asp Leu Gln Val Glu Met Asn Arg Leu Gln Glu Ala Ile Lys
35 40 45

Val Leu Asn Gln Ser Tyr Ile Asn Leu Lys Asp Ile Gly Thr Tyr Glu
50 55 60

Tyr Tyr Val Lys Trp Pro Trp Tyr Val Trp Leu Leu Ile
65 70 75

<210> 16
<211> 102
<212> PRT
<213> Infectious Bronchitis Virus

<400> 16

Pro Phe Ala Thr Gln Leu Gln Ala Arg Ile Asn His Leu Gly Ile Thr
1 5 10 15

Gln Ser Leu Leu Leu Lys Asn Gln Glu Lys Ile Ala Ala Ser Phe Asn
20 25 30

Lys Ala Ile Gly His Met Gln Glu Gly Phe Arg Ser Thr Ser Leu Ala
35 40 45

Leu Gln Gln Ile Gln Asp Val Val Ser Lys Gln Ser Ala Ile Leu Thr
50 55 60

Glu Thr Met Ala Ser Leu Asn Lys Asn Phe Gly Ala Ile Ser Ser Val
65 70 75 80

Ile Gln Glu Ile Tyr Gln Gln Phe Asp Ala Ile Gln Ala Asn Ala Gln
85 90 95

Val Asp Arg Leu Ile Thr

100

<210> 17
<211> 78
<212> PRT
<213> Infectious Bronchitis Virus

<400> 17

Asp Asn Asp Asp Phe Asp Phe Asn Asp Glu Leu Ser Lys Trp Trp Asn
1 5 10 15

Asp Thr Lys His Glu Leu Pro Asp Phe Asp Lys Phe Asn Tyr Thr Val
20 25 30

Pro Ile Leu Asp Ile Asp Ser Glu Ile Asp Arg Ile Gln Gly Val Ile
35 40 45

Gln Gly Leu Asn Asp Ser Leu Ile Asp Leu Glu Lys Leu Ser Ile Leu
50 55 60

Lys Thr Tyr Ile Lys Trp Pro Trp Tyr Val Trp Leu Ala Ile
65 70 75

<210> 18
<211> 98
<212> PRT
<213> Artificial

<220>
<223> HR1 derived peptide

<400> 18

Gly Ser Ala Tyr Arg Phe Asn Gly Ile Gly Val Thr Gln Asn Val Leu
1 5 10 15

Tyr Glu Asn Gln Lys Gln Ile Ala Asn Gln Phe Asn Lys Ala Ile Ser
20 25 30

Gln Ile Gln Glu Ser Leu Thr Thr Thr Ser Thr Ala Leu Gly Lys Leu
35 40 45

Gln Asp Val Val Asn Gln Asn Ala Gln Ala Leu Asn Thr Leu Val Lys
50 55 60

Gln Leu Ser Ser Asn Phe Gly Ala Ile Ser Ser Val Leu Asn Asp Ile

65 70 75 80

Leu Ser Arg Leu Asp Lys Val Glu Ala Glu Val Gln Ile Asp Arg Leu
85 90 95

Ile Thr

<210> 19
<211> 82
<212> PRT
<213> Artificial

<220>
<223> HR1a derived peptide

<400> 19

Gly Ser Asn Gln Lys Gln Ile Ala Asn Gln Phe Asn Lys Ala Ile Ser
1 5 10 15

Gln Ile Gln Glu Ser Leu Thr Thr Thr Ser Thr Ala Leu Gly Lys Leu
20 25 30

Gln Asp Val Val Asn Gln Asn Ala Gln Ala Leu Asn Thr Leu Val Lys
35 40 45

Gln Leu Ser Ser Asn Phe Gly Ala Ile Ser Ser Val Leu Asn Asp Ile
50 55 60

Leu Ser Arg Leu Asp Lys Val Glu Ala Glu Val Gln Ile Asp Arg Leu
65 70 75 80

Ile Thr

<210> 20
<211> 48
<212> PRT
<213> Artificial

<220>
<223> HR1b derived peptide

<400> 20

Gly Ser Asn Gln Asn Ala Gln Ala Leu Asn Thr Leu Val Lys Gln Leu
1 5 10 15

Ser Ser Asn Phe Gly Ala Ile Ser Ser Val Leu Asn Asp Ile Leu Ser
20 25 30

Arg Leu Asp Lys Val Glu Ala Glu Val Gln Ile Asp Arg Leu Ile Thr
35 40 45

<210> 21
<211> 49
<212> PRT
<213> Artificial

<220>
<223> HR1c derived peptide

<400> 21

Gly Ser Asn Gln Lys Gln Ile Ala Asn Gln Phe Asn Lys Ala Ile Ser
1 5 10 15

Gln Ile Gln Glu Ser Leu Thr Thr Thr Ser Thr Ala Leu Gly Lys Leu
20 25 30

Gln Asp Val Val Asn Gln Asn Ala Gln Ala Leu Asn Thr Leu Val Lys
35 40 45

Gln

<210> 22
<211> 106
<212> PRT
<213> Artificial

<220>
<223> Flag tagged HR1

<400> 22

Asp Tyr Lys Asp Asp Asp Asp Lys Gly Ser Ala Tyr Arg Phe Asn Gly
1 5 10 15

Ile Gly Val Thr Gln Asn Val Leu Tyr Glu Asn Gln Lys Gln Ile Ala
20 25 30

Asn Gln Phe Asn Lys Ala Ile Ser Gln Ile Gln Glu Ser Leu Thr Thr
35 40 45

Thr Ser Thr Ala Leu Gly Lys Leu Gln Asp Val Val Asn Gln Asn Ala
50 55 60

Gln Ala Leu Asn Thr Leu Val Lys Gln Leu Ser Ser Asn Phe Gly Ala
65 70 75 80

Ile Ser Ser Val Leu Asn Asp Ile Leu Ser Arg Leu Asp Lys Val Glu
85 90 95

Ala Glu Val Gln Ile Asp Arg Leu Ile Thr
100 105

<210> 23
<211> 47
<212> PRT
<213> Artificial

<220>
<223> HR2 derived peptide

<400> 23

Gly Ser Asp Val Asp Leu Gly Asp Ile Ser Gly Ile Asn Ala Ser Val
1 5 10 15

Val Asn Ile Gln Lys Glu Ile Asp Arg Leu Asn Glu Val Ala Lys Asn
20 25 30

Leu Asn Glu Ser Leu Ile Asp Leu Gln Glu Leu Gly Lys Tyr Glu
35 40 45

<210> 24
<211> 66
<212> PRT
<213> Artificial

<220>
<223> HR2-1 derived peptide

<400> 24

Gly Ser Glu Leu Asp Ser Phe Lys Glu Glu Leu Asp Lys Tyr Phe Lys
1 5 10 15

Asn His Thr Ser Pro Asp Val Asp Leu Gly Asp Ile Ser Gly Ile Asn
20 25 30

Ala Ser Val Val Asn Ile Gln Lys Glu Ile Asp Arg Leu Asn Glu Val
35 40 45

Ala Lys Asn Leu Asn Glu Ser Leu Ile Asp Leu Gln Glu Leu Gly Lys
50 55 60

Tyr Glu
65

<210> 25
<211> 55
<212> PRT
<213> Artificial

<220>
<223> Flag tagged HR2

<400> 25

Asp Tyr Lys Asp Asp Asp Asp Lys Gly Ser Asp Val Asp Leu Gly Asp
1 5 10 15

Ile Ser Gly Ile Asn Ala Ser Val Val Asn Ile Gln Lys Glu Ile Asp
20 25 30

Arg Leu Asn Glu Val Ala Lys Asn Leu Asn Glu Ser Leu Ile Asp Leu
35 40 45

Gln Glu Leu Gly Lys Tyr Glu
50 55

<210> 26
<211> 336
<212> PRT
<213> Artificial

<220>
<223> GST-HR1

<400> 26

Met Ser Pro Ile Leu Gly Tyr Trp Lys Ile Lys Gly Leu Val Gln Pro
1 5 10 15

Thr Arg Leu Leu Leu Glu Tyr Leu Glu Glu Lys Tyr Glu Glu His Leu
20 25 30

Tyr Glu Arg Asp Glu Gly Asp Lys Trp Arg Asn Lys Lys Phe Glu Leu

```
        35                  40                  45

Gly Leu Glu Phe Pro Asn Leu Pro Tyr Tyr Ile Asp Gly Asp Val Lys
    50                  55                  60

Leu Thr Gln Ser Met Ala Ile Ile Arg Tyr Ile Ala Asp Lys His Asn
65                  70                  75                  80

Met Leu Gly Gly Cys Pro Lys Glu Arg Ala Glu Ile Ser Met Leu Glu
                85                  90                  95

Gly Ala Val Leu Asp Ile Arg Tyr Gly Val Ser Arg Ile Ala Tyr Ser
            100                 105                 110

Lys Asp Phe Glu Thr Leu Lys Val Asp Phe Leu Ser Lys Leu Pro Glu
        115                 120                 125

Met Leu Lys Met Phe Glu Asp Arg Leu Cys His Lys Thr Tyr Leu Asn
    130                 135                 140

Gly Asp His Val Thr His Pro Asp Phe Met Leu Tyr Asp Ala Leu Asp
145                 150                 155                 160

Val Val Leu Tyr Met Asp Pro Met Cys Leu Asp Ala Phe Pro Lys Leu
                165                 170                 175

Val Cys Phe Lys Lys Arg Ile Glu Ala Ile Pro Gln Ile Asp Lys Tyr
            180                 185                 190

Leu Lys Ser Ser Lys Tyr Ile Ala Trp Pro Leu Gln Gly Trp Gln Ala
        195                 200                 205

Thr Phe Gly Gly Gly Asp His Pro Pro Lys Ser Asp Leu Val Pro Arg
    210                 215                 220

Gly Ser Gln Ala Arg Leu Asn Tyr Val Ala Leu Gln Thr Asp Val Leu
225                 230                 235                 240

Asn Lys Asn Gln Gln Ile Leu Ala Asn Ala Phe Asn Gln Ala Ile Gly
                245                 250                 255

Asn Ile Thr Gln Ala Phe Gly Lys Val Asn Asp Ala Ile His Gln Thr
            260                 265                 270
```

Ser Gln Gly Leu Ala Thr Val Ala Lys Ala Leu Ala Lys Val Gln Asp
275 280 285

Val Val Asn Thr Gln Gly Gln Ala Leu Ser His Leu Thr Val Gln Leu
290 295 300

Gln Asn Asn Phe Gln Ala Ile Ser Ser Ser Ile Ser Asp Ile Tyr Asn
305 310 315 320

Arg Leu Asp Glu Leu Ser Ala Asp Ala Gln Val Asp Arg Leu Ile Thr
325 330 335

<210> 27
<211> 277
<212> PRT
<213> Artificial

<220>
<223> GST-HR2

<400> 27

Met Ser Pro Ile Leu Gly Tyr Trp Lys Ile Lys Gly Leu Val Gln Pro
1 5 10 15

Thr Arg Leu Leu Leu Glu Tyr Leu Glu Glu Lys Tyr Glu Glu His Leu
20 25 30

Tyr Glu Arg Asp Glu Gly Asp Lys Trp Arg Asn Lys Lys Phe Glu Leu
35 40 45

Gly Leu Glu Phe Pro Asn Leu Pro Tyr Tyr Ile Asp Gly Asp Val Lys
50 55 60

Leu Thr Gln Ser Met Ala Ile Ile Arg Tyr Ile Ala Asp Lys His Asn
65 70 75 80

Met Leu Gly Gly Cys Pro Lys Glu Arg Ala Glu Ile Ser Met Leu Glu
85 90 95

Gly Ala Val Leu Asp Ile Arg Tyr Gly Val Ser Arg Ile Ala Tyr Ser
100 105 110

Lys Asp Phe Glu Thr Leu Lys Val Asp Phe Leu Ser Lys Leu Pro Glu

```
        115                 120                 125

Met Leu Lys Met Phe Glu Asp Arg Leu Cys His Lys Thr Tyr Leu Asn
    130                 135                 140

Gly Asp His Val Thr His Pro Asp Phe Met Leu Tyr Asp Ala Leu Asp
145                 150                 155                 160

Val Val Leu Tyr Met Asp Pro Met Cys Leu Asp Ala Phe Pro Lys Leu
                165                 170                 175

Val Cys Phe Lys Lys Arg Ile Glu Ala Ile Pro Gln Ile Asp Lys Tyr
            180                 185                 190

Leu Lys Ser Ser Lys Tyr Ile Ala Trp Pro Leu Gln Gly Trp Gln Ala
        195                 200                 205

Thr Phe Gly Gly Gly Asp His Pro Pro Lys Ser Asp Leu Val Pro Arg
    210                 215                 220

Gly Ser Glu Phe Thr Leu Asp Ile Phe Asn Ala Thr Tyr Leu Asn Leu
225                 230                 235                 240

Thr Gly Glu Ile Asp Asp Leu Glu Phe Arg Ser Glu Lys Leu His Asn
                245                 250                 255

Thr Thr Val Glu Leu Ala Ile Leu Ile Asp Asn Ile Asn Asn Thr Leu
            260                 265                 270

Val Asn Leu Glu Trp
        275
```

<210> 28
<211> 582
<212> DNA
<213> Artificial

<220>
<223> SARS nucleotide and deduced protein sequence derived from an RT-PCR fragment

220>
<221> misc_feature
<222> (3)..(4)
<223> The 'Xaa' at amino acids 3 and 4 stands for an unknown amino acid.

<220>
<221> CDS
<222> (1)..(582)

<400> 28

```
gaa atc hcg sct tct gct aat ctt gct gct act aaa atg tct gag tgt       48
Glu Ile Xaa Xaa Ser Ala Asn Leu Ala Ala Thr Lys Met Ser Glu Cys
1               5                  10                  15

gtt ctt gga caa tca aaa aga gtt gac ttt tgt gga aag ggc tac cac       96
Val Leu Gly Gln Ser Lys Arg Val Asp Phe Cys Gly Lys Gly Tyr His
            20                  25                  30

ctt atg tcc ttc cca caa gca gcc ccg cat ggt gtt gtc ttc cta cat      144
Leu Met Ser Phe Pro Gln Ala Ala Pro His Gly Val Val Phe Leu His
        35                  40                  45

gtc acg tat gtg cca tcc cag gag agg aac ttc acc aca gcg cca gca      192
Val Thr Tyr Val Pro Ser Gln Glu Arg Asn Phe Thr Thr Ala Pro Ala
    50                  55                  60

att tgt cat gaa ggc aaa gca tac ttc cct cgt gaa ggt gtt ttt gtg      240
Ile Cys His Glu Gly Lys Ala Tyr Phe Pro Arg Glu Gly Val Phe Val
65                  70                  75                  80

ttt aat ggc act tct tgg ttt att aca cag agg aac ttc ttt tct cca      288
Phe Asn Gly Thr Ser Trp Phe Ile Thr Gln Arg Asn Phe Phe Ser Pro
                85                  90                  95

caa ata att act aca gac aat aca ttt gtc tca gga aat tgt gat gtc      336
Gln Ile Ile Thr Thr Asp Asn Thr Phe Val Ser Gly Asn Cys Asp Val
            100                 105                 110

gtt att ggc atc att aac aac aca gtt tat gat cct ctg caa cct gag      384
Val Ile Gly Ile Ile Asn Asn Thr Val Tyr Asp Pro Leu Gln Pro Glu
        115                 120                 125

ctt gac tca ttc aaa gaa gag ctg gac aag tac ttc aaa aat cat aca      432
Leu Asp Ser Phe Lys Glu Glu Leu Asp Lys Tyr Phe Lys Asn His Thr
    130                 135                 140

tca cca gat gtt gat ctt ggc gac att tca ggc att aac gct tct gtc      480
Ser Pro Asp Val Asp Leu Gly Asp Ile Ser Gly Ile Asn Ala Ser Val
145                 150                 155                 160

gtc aac att caa aaa gaa att gac cgc ctc aat gag gtc gct aaa aat      528
Val Asn Ile Gln Lys Glu Ile Asp Arg Leu Asn Glu Val Ala Lys Asn
                165                 170                 175

tta aat gaa tca ctc att gac ctt caa gaa ttg gga aaa tat gag caa      576
Leu Asn Glu Ser Leu Ile Asp Leu Gln Glu Leu Gly Lys Tyr Glu Gln
            180                 185                 190

tat att                                                             582
Tyr Ile
```

<210> 29
<211> 194
<212> PRT
<213> Artificial

<220>
<221> misc_feature
<222> (3)..(3)
<223> The 'Xaa' at location 3 stands for Thr, Pro, or Ser.

<220>
<221> misc_feature
<222> (4)..(4)
<223> The 'Xaa' at location 4 stands for Ala, or Pro.

<220>
<223> Synthetic Construct

<400> 29

Glu Ile Xaa Xaa Ser Ala Asn Leu Ala Ala Thr Lys Met Ser Glu Cys
1 5 10 15

Val Leu Gly Gln Ser Lys Arg Val Asp Phe Cys Gly Lys Gly Tyr His
20 25 30

Leu Met Ser Phe Pro Gln Ala Ala Pro His Gly Val Val Phe Leu His
35 40 45

Val Thr Tyr Val Pro Ser Gln Glu Arg Asn Phe Thr Thr Ala Pro Ala
50 55 60

Ile Cys His Glu Gly Lys Ala Tyr Phe Pro Arg Glu Gly Val Phe Val
65 70 75 80

Phe Asn Gly Thr Ser Trp Phe Ile Thr Gln Arg Asn Phe Phe Ser Pro
85 90 95

Gln Ile Ile Thr Thr Asp Asn Thr Phe Val Ser Gly Asn Cys Asp Val
100 105 110

Val Ile Gly Ile Ile Asn Asn Thr Val Tyr Asp Pro Leu Gln Pro Glu
115 120 125

Leu Asp Ser Phe Lys Glu Glu Leu Asp Lys Tyr Phe Lys Asn His Thr
130 135 140

Ser Pro Asp Val Asp Leu Gly Asp Ile Ser Gly Ile Asn Ala Ser Val
145 150 155 160

Val Asn Ile Gln Lys Glu Ile Asp Arg Leu Asn Glu Val Ala Lys Asn
165 170 175

Leu Asn Glu Ser Leu Ile Asp Leu Gln Glu Leu Gly Lys Tyr Glu Gln
180 185 190

Tyr Ile

<210> 30
<211> 56
<212> PRT
<213> Artificial

<220>
<223> sHR2-3

<400> 30

Leu Asp Lys Tyr Phe Lys Asn His Thr Ser Pro Asp Val Asp Leu Gly
1 5 10 15

Asp Ile Ser Gly Ile Asn Ala Ser Val Val Asn Ile Gln Lys Glu Ile
20 25 30

Asp Arg Leu Asn Glu Val Ala Lys Asn Leu Asn Glu Ser Leu Ile Asp
35 40 45

Leu Gln Glu Leu Gly Lys Tyr Glu
50 55

<210> 31
<211> 52
<212> PRT
<213> Artificial

<220>
<223> sHR2-4

<400> 31

Phe Lys Asn His Thr Ser Pro Asp Val Asp Leu Gly Asp Ile Ser Gly
1 5 10 15

Ile Asn Ala Ser Val Val Asn Ile Gln Lys Glu Ile Asp Arg Leu Asn

20 25 30

Glu Val Ala Lys Asn Leu Asn Glu Ser Leu Ile Asp Leu Gln Glu Leu
35 40 45

Gly Lys Tyr Glu
50

<210> 32
<211> 48
<212> PRT
<213> Artificial

<220>
<223> sHR2-5

<400> 32

Thr Ser Pro Asp Val Asp Leu Gly Asp Ile Ser Gly Ile Asn Ala Ser
1 5 10 15

Val Val Asn Ile Gln Lys Glu Ile Asp Arg Leu Asn Glu Val Ala Lys
20 25 30

Asn Leu Asn Glu Ser Leu Ile Asp Leu Gln Glu Leu Gly Lys Tyr Glu
35 40 45

<210> 33
<211> 44
<212> PRT
<213> Artificial

<220>
<223> sHR2-6

<400> 33

Val Asp Leu Gly Asp Ile Ser Gly Ile Asn Ala Ser Val Val Asn Ile
1 5 10 15

Gln Lys Glu Ile Asp Arg Leu Asn Glu Val Ala Lys Asn Leu Asn Glu
20 25 30

Ser Leu Ile Asp Leu Gln Glu Leu Gly Lys Tyr Glu
35 40

<210> 34
<211> 40

<212> PRT
<213> Artificial

<220>
<223> SHR2-7

<400> 34

Asp Ile Ser Gly Ile Asn Ala Ser Val Val Asn Ile Gln Lys Glu Ile
1 5 10 15

Asp Arg Leu Asn Glu Val Ala Lys Asn Leu Asn Glu Ser Leu Ile Asp
20 25 30

Leu Gln Glu Leu Gly Lys Tyr Glu
35 40

<210> 35
<211> 56
<212> PRT
<213> Artificial

<220>
<223> sHR2-10

<400> 35

Glu Leu Asp Ser Phe Lys Glu Glu Leu Asp Lys Tyr Phe Lys Asn His
1 5 10 15

Thr Ser Pro Asp Val Asp Leu Gly Asp Ile Ser Gly Ile Asn Ala Ser
20 25 30

Val Val Asn Ile Gln Lys Glu Ile Asp Arg Leu Asn Glu Val Ala Lys
35 40 45

Asn Leu Asn Glu Ser Leu Ile Asp
50 55

<210> 36
<211> 39
<212> PRT
<213> Artificial

<220>
<223> mHR2

<400> 36

Asp Leu Ser Leu Asp Phe Glu Lys Leu Asn Val Thr Leu Leu Asp Leu

1 5 10 15

Thr Tyr Glu Met Asn Arg Ile Gln Asp Ala Ile Lys Lys Leu Asn Glu
20 25 30

Ser Tyr Ile Asn Leu Lys Glu
35

<210> 37
<211> 96
<212> PRT
<213> Artificial

<220>
<223> sHR1

<400> 37

Ala Tyr Arg Phe Asn Gly Ile Gly Val Thr Gln Asn Val Leu Tyr Glu
1 5 10 15

Asn Gln Lys Gln Ile Ala Asn Gln Phe Asn Lys Ala Ile Ser Gln Ile
20 25 30

Gln Glu Ser Leu Thr Thr Thr Ser Thr Ala Leu Gly Lys Leu Gln Asp
35 40 45

Val Val Asn Gln Asn Ala Gln Ala Leu Asn Thr Leu Val Lys Gln Leu
50 55 60

Ser Ser Asn Phe Gly Ala Ile Ser Ser Val Leu Asn Asp Ile Leu Ser
65 70 75 80

Arg Leu Asp Lys Val Glu Ala Glu Val Gln Ile Asp Arg Leu Ile Thr
85 90 95

<210> 38
<211> 80
<212> PRT
<213> Artificial

<220>
<223> sHR1a

<400> 38

Asn Gln Lys Gln Ile Ala Asn Gln Phe Asn Lys Ala Ile Ser Gln Ile
1 5 10 15

Gln Glu Ser Leu Thr Thr Thr Ser Thr Ala Leu Gly Lys Leu Gln Asp
20 25 30

Val Val Asn Gln Asn Ala Gln Ala Leu Asn Thr Leu Val Lys Gln Leu
35 40 45

Ser Ser Asn Phe Gly Ala Ile Ser Ser Val Leu Asn Asp Ile Leu Ser
50 55 60

Arg Leu Asp Lys Val Glu Ala Glu Val Gln Ile Asp Arg Leu Ile Thr
65 70 75 80

<210> 39
<211> 46
<212> PRT
<213> Artificial

<220>
<223> sHR1b

<400> 39

Asn Gln Asn Ala Gln Ala Leu Asn Thr Leu Val Lys Gln Leu Ser Ser
1 5 10 15

Asn Phe Gly Ala Ile Ser Ser Val Leu Asn Asp Ile Leu Ser Arg Leu
20 25 30

Asp Lys Val Glu Ala Glu Val Gln Ile Asp Arg Leu Ile Thr
35 40 45

<210> 40
<211> 47
<212> PRT
<213> Artificial

<220>
<223> sHR1c

<400> 40

Asn Gln Lys Gln Ile Ala Asn Gln Phe Asn Lys Ala Ile Ser Gln Ile
1 5 10 15

Gln Glu Ser Leu Thr Thr Thr Ser Thr Ala Leu Gly Lys Leu Gln Asp
20 25 30

Val Val Asn Gln Asn Ala Gln Ala Leu Asn Thr Leu Val Lys Gln
35 40 45

<210> 41
<211> 42
<212> DNA
<213> Artificial

<220>
<223> Primer 973

<400> 41
gtggatccat cgaaggtcgt caatatagaa ttaatggttt ag 42

<210> 42
<211> 37
<212> DNA
<213> Artificial

<220>
<223> Primer 974

<400> 42
gtggatccat cgaaggtcgt aatgcaaatg ctgaagc 37

<210> 43
<211> 29
<212> DNA
<213> Artificial

<220>
<223> Primer 975

<400> 43
ggaattcaat taataagacg atctatctg 29

<210> 44
<211> 27
<212> DNA
<213> Artificial

<220>
<223> Primer 976

<400> 44
cgaattcatt ccttgaggtt gatgtag 27

<210> 45
<211> 38
<212> DNA
<213> Artificial

<220>
<223> Primer 990

<400> 45
gcggatccat cgaaggtcgt gatttatctc tcgatttc 38

<210> 46
<211> 25
<212> DNA
<213> Artificial

<220>
<223> Primer 1151

<400> 46
gtggatccaa ccaaaagatg attgc 25

<210> 47
<211> 28
<212> DNA
<213> Artificial

<220>
<223> Primer 1152

<400> 47
ggaattcaat tgagtgcttc agcatttg 28

<210> 48
<211> 25
<212> DNA
<213> Artificial

<220>
<223> Primer 2006

<400> 48
gcggatccgc atataggttc aatgg 25

<210> 49
<211> 25
<212> DNA
<213> Artificial

<220>
<223> Primer 2007

<400> 49
cgaattcatg taattaacct gtcaa 25

<210> 50

<211> 25
<212> DNA
<213> Artificial

<220>
<223> Primer 2008

<400> 50
gcggatccaa ccaaaaacaa atcgc 25

<210> 51
<211> 25
<212> DNA
<213> Artificial

<220>
<223> Primer 2009

<400> 51
gcggatccaa ccagaatgct caagc 25

<210> 52
<211> 25
<212> DNA
<213> Artificial

<220>
<223> Primer 2010

<400> 52
cgaattcatt gtttaacaag tgtgt 25

<210> 53
<211> 25
<212> DNA
<213> Artificial

<220>
<223> Primer 1998

<400> 53
cgaattcact catattttcc caatt 25

<210> 54
<211> 25
<212> DNA
<213> Artificial

<220>
<223> Primer 1999

<400> 54
gcggatccga gcttgactca ttcaa 25

<210> 55
<211> 25
<212> DNA
<213> Artificial

<220>
<223> Primer 2064

<400> 55
gcggatcctt caaagaagag ctgga 25

<210> 56
<211> 25
<212> DNA
<213> Artificial

<220>
<223> Primer 2065

<400> 56
gcggatccct ggacaagtac ttcaa 25

<210> 57
<211> 25
<212> DNA
<213> Artificial

<220>
<223> Primer 2066

<400> 57
gcggatcctt caaaaatcat acatc 25

<210> 58
<211> 25
<212> DNA
<213> Artificial

<220>
<223> Primer 2067

<400> 58
gcggatccac atcaccagat gttga 25

<210> 59
<211> 25
<212> DNA
<213> Artificial

<220>
<223> Primer 2068

<400> 59
gcggatccgt tgatcttggc gacat 25

<210> 60
<211> 25
<212> DNA
<213> Artificial

<220>
<223> Primer 2069

<400> 60
gcggatccga catttcaggc attaa 25

<210> 61
<211> 25
<212> DNA
<213> Artificial

<220>
<223> Primer 2034

<400> 61
cgaattcatt taatatattg ctcat 25

<210> 62
<211> 25
<212> DNA
<213> Artificial

<220>
<223> Primer 2070

<400> 62
cgaattcaca attcttgaag gtcaa 25

<210> 63
<211> 25
<212> DNA
<213> Artificial

<220>
<223> Primer 2071

<400> 63
cgaattcagt caatgagtga ttcat 25

<210> 64
<211> 30
<212> DNA
<213> Artificial

<220>
<223> Primer 2072

<400> 64
gatcagacta caaggatgac gatgacaaag 30

<210> 65
<211> 30
<212> DNA
<213> Artificial

<220>
<223> Primer 2073

<400> 65
gatcctttgt catcgtcatc cttgtagtct 30